

Accelerating Roundabout Implementation in the United States - Volume II of VII

Assessment of Roundabout Capacity Models for the Highway Capacity Manual

SEPTEMBER 2015

Updated October 2020

PUBLICATION NO. FHWA-SA-15-070



U.S. Department of Transportation
Federal Highway Administration

Safe Roads for a Safer Future
Investment in roadway safety saves lives

SI* (MODERN METRIC) CONVERSION FACTORS

APPROXIMATE CONVERSIONS TO SI UNITS

Symbol	When You Know	Multiply By	To Find	Symbol
LENGTH				
in	inches	25.4	millimeters	mm
ft	feet	0.305	meters	m
yd	yards	0.914	meters	m
mi	miles	1.61	kilometers	km
AREA				
in ²	square inches	645.2	square millimeters	mm ²
ft ²	square feet	0.093	square meters	m ²
yd ²	square yard	0.836	square meters	m ²
ac	acres	0.405	hectares	ha
mi ²	square miles	2.59	square kilometers	km ²
VOLUME				
fl oz	fluid ounces	29.57	milliliters	mL
gal	gallons	3.785	liters	L
ft ³	cubic feet	0.028	cubic meters	m ³
yd ³	cubic yards	0.765	cubic meters	m ³
NOTE: volumes greater than 1000 L shall be shown in m ³				
MASS				
oz	ounces	28.35	grams	g
lb	pounds	0.454	kilograms	kg
T	short tons (2000 lb)	0.907	megagrams (or "metric ton")	Mg (or "t")
TEMPERATURE (exact degrees)				
°F	Fahrenheit	5 (F-32)/9 or (F-32)/1.8	Celsius	°C
ILLUMINATION				
fc	foot-candles	10.76	lux	lx
fl	foot-Lamberts	3.426	candela/m ²	cd/m ²
FORCE and PRESSURE or STRESS				
lbf	poundforce	4.45	newtons	N
lbf/in ²	poundforce per square inch	6.89	kilopascals	kPa
APPROXIMATE CONVERSIONS FROM SI UNITS				
Symbol	When You Know	Multiply By	To Find	Symbol
LENGTH				
mm	millimeters	0.039	inches	in
m	meters	3.28	feet	ft
m	meters	1.09	yards	yd
km	kilometers	0.621	miles	mi
AREA				
mm ²	square millimeters	0.0016	square inches	in ²
m ²	square meters	10.764	square feet	ft ²
m ²	square meters	1.195	square yards	yd ²
ha	hectares	2.47	acres	ac
km ²	square kilometers	0.386	square miles	mi ²
VOLUME				
mL	milliliters	0.034	fluid ounces	fl oz
L	liters	0.264	gallons	gal
m ³	cubic meters	35.314	cubic feet	ft ³
m ³	cubic meters	1.307	cubic yards	yd ³
MASS				
g	grams	0.035	ounces	oz
kg	kilograms	2.202	pounds	lb
Mg (or "t")	megagrams (or "metric ton")	1.103	short tons (2000 lb)	T
TEMPERATURE (exact degrees)				
°C	Celsius	1.8C+32	Fahrenheit	°F
ILLUMINATION				
lx	lux	0.0929	foot-candles	fc
cd/m ²	candela/m ²	0.2919	foot-Lamberts	fl
FORCE and PRESSURE or STRESS				
N	newtons	0.225	poundforce	lbf
kPa	kilopascals	0.145	poundforce per square inch	lbf/in ²


*SI is the symbol for the International System of Units. Appropriate rounding should be made to comply with Section 4 of ASTM E380.
(Revised March 2003)

FOREWORD

Since the Federal Highway Administration (FHWA) published the first *Roundabouts Informational Guide* in 2000, the estimated number of roundabouts in the United States has grown from fewer than one hundred to several thousand. Roundabouts remain a high priority for FHWA due to their proven ability to reduce severe crashes by an average of 80 percent. They are featured as one of the Office of Safety *Proven Safety Countermeasures* and were included in the *Every Day Counts 2* campaign for Intersection & Interchange Geometrics.

As roundabouts became more common across a wide range of traffic conditions, specific questions emerged on how to further tailor certain aspects of their design to better meet the needs of a growing number and diversity of stakeholders. The substantial work performed for this project – *Accelerating Roundabout Implementation in the United States* – sought to address several of the most pressing issues of National significance, including enhancing safety, improving operational efficiency, considering environmental effects, accommodating freight movement and providing pedestrian accessibility. This work represents yet another notable step forward in advancing roundabouts in the United States.

The electronic versions of each of the seven report volumes that document this project are available on the Office of Safety website at <http://safety.fhwa.dot.gov/>.



Michael S. Griffith
Director
Office of Safety Technologies

NOTICE

This document is disseminated under the sponsorship of the U.S. Department of Transportation in the interest of information exchange. The U.S. Government assumes no liability for the use of the information contained in this document. This report does not constitute a standard, specification, or regulation.

The U.S. Government does not endorse products or manufacturers. Trademarks or manufacturers' names appear in this report only because they are considered essential to the objective of the document.

QUALITY ASSURANCE STATEMENT

The Federal Highway Administration (FHWA) provides high-quality information to serve Government, industry, and the public in a manner that promotes public understanding. Standards and policies are used to ensure and maximize the quality, objectivity, utility, and integrity of its information. FHWA periodically reviews quality issues and adjusts its programs and processes to ensure continuous quality improvement.

TECHNICAL REPORT DOCUMENTATION PAGE

1. Report No. FHWA-SA-15-070		2. Government Accession No.		3. Recipient's Catalog No.	
4. Title and Subtitle Accelerating Roundabouts in the United States: Volume II of VII - Assessment of Roundabout Capacity Models for the Highway Capacity Manual			5. Report Date September 2015		
			6. Performing Organization Code:		
7. Author(s) Lee A. Rodegerdts, Anais Malinge, Patrick S. Marnell, Scott G. Beaird, Matt J. Kittelson, and Yuri S. Mereszczak			8. Performing Organization Report No. 11861 Task 3		
9. Performing Organization Name and Address Kittelson & Associates, Inc. 610 SW Alder St., Suite 700 Portland, OR 97205			10. Work Unit No. (TRAIS)		
			11. Contract or Grant No. DTFH61-10-D-00023-T-11002		
12. Sponsoring Agency Name and Address Office of Safety Federal Highway Administration United States Department of Transportation 1200 New Jersey Avenue SE Washington, DC 20590			13. Type of Report and Period Covered Technical Report August 2011 through September 2015		
			14. Sponsoring Agency Code FHWA HSA		
15. Supplementary Notes The Contracting Officer's Technical Manager (COTM) was Jeffrey Shaw, HSST Safety Design Team					
16. Abstract <p>This volume is second in a series of seven. The other volumes in the series are: Volume I - Evaluation of Rectangular Rapid-Flashing Beacons (RRFB) at Multilane Roundabouts, Volume III – Assessment of the Environmental Characteristics of Roundabouts, Volume IV – A Review of Fatal and Severe Injury Crashes at Roundabouts, Volume V – Evaluation of Geometric Parameters that Affect Truck Maneuvering and Stability, Volume VI – Investigation of Crosswalk Design and Driver Behaviors, and Volume VII – Human Factor Assessment of Traffic Control Device Effectiveness. These reports document a Federal Highway Administration (FHWA) project to investigate and evaluate several important aspects of roundabout design and operation for the purpose of providing practitioners with better information, leading to more widespread and routine implementation of higher quality roundabouts.</p> <p>This report presents an assessment and development of updated roundabout capacity models for implementation in the major update of the HCM 2010. The roundabout capacity models in the HCM 2010 are based on data collected in 2003 as part of NCHRP Report 572; this task is based on a new set of capacity data collected in 2012. A total of 819 usable minutes of data at single-lane roundabouts, 711 minutes of usable data were obtained for the multilane case for two entry lanes conflicting with two circulating lanes, and 519 minutes of usable data were obtained for the multilane case for two entry lanes conflicting with one circulating lane. Parametric analyses were conducted to extract and review critical headway, follow-up time, and key geometric parameters. The new data confirmed that the HCM 2010 generally underestimates capacity. The most promising models involve recalibrating the HCM 2010 models with an intercept that is calibrated to follow-up time and a slope parameter based on regression of the data. Additional calibration factors such as critical headway or geometric parameters beyond number of lanes were not found to add significant improvement.</p>					
17. Key Words Roundabouts, capacity, operational performance, calibration, HCM			18. Distribution Statement No restrictions. This document is available to the public at http://safety.fhwa.dot.gov/		
19. Security Classif. (of this report) Unclassified		20. Security Classif. (of this page) Unclassified		21. No. of Pages 94	22. Price
Form DOT F 1700.7 (8-72)			Reproduction of completed page authorized		

TABLE OF CONTENTS

FOREWORD	i
NOTICE	i
QUALITY ASSURANCE STATEMENT	i
TABLE OF CONTENTS	iii
LIST OF FIGURES	v
LIST OF TABLES	viii
CHAPTER 1. INTRODUCTION	1
SCOPE OF STUDY	2
RESEARCH APPROACH	2
Summarize Existing Relationships	2
Site Inventory and Data Collection	2
Operational Model Development	3
CHAPTER 2. LITERATURE REVIEW	5
NCHRP REPORT 572 METHOD	5
HCM 2010 METHOD	6
HCM 2010 ROUNDABOUT MODEL CALIBRATION	7
Bend, OR	9
California	9
Carmel, IN	10
Wisconsin	11
Kansas	11
OTHER CAPACITY INFLUENCES	12
ALTERNATIVE ROUNDABOUT CAPACITY MODELS	12
CHAPTER 3. DATA CHARACTERISTICS	15
SITE INVENTORY	15
Single-Lane Sites	21
Multilane Sites	23
DATA COLLECTION AND REDUCTION	26
CHAPTER 4. PARAMETRIC ANALYSES	31
CRITICAL HEADWAY	31
Single-Lane Critical Headway	31

Multilane Critical Headway	32
FOLLOW-UP TIME.....	35
Single-Lane Follow-Up Times	35
Multilane Follow-Up Time.....	36
GEOMETRIC PARAMETRIC ANALYSIS	38
CHAPTER 5. MODEL DEVELOPMENT.....	45
ASSESSMENT OF HCM 2010 MODEL	45
Single-Lane Model.....	45
Multilane Models	46
DEVELOPMENT OF SINGLE-LANE MODELS.....	50
Regression	50
Calibration	51
Localized Regression	53
Regression Model Form	55
DEVELOPMENT OF MULTILANE MODELS	61
Regression	62
Calibration	65
INFLUENCE OF EXITING VEHICLES	69
ANALYSIS OF CAPACITY TRENDS OVER TIME	75
SUMMARY OF MODEL DEVELOPMENT	79
CHAPTER 6. CONCLUSIONS AND RECOMMENDATIONS	83
REFERENCES.....	85

LIST OF FIGURES

Figure 1. Equation. Capacity model for single lane roundabouts from NCHRP Report 572.....	5
Figure 2. Equation. Capacity model for critical lane of multilane roundabouts from NCHRP Report 572.	5
Figure 3. Equation. Sieglloch capacity model.....	6
Figure 4. Equation. HCM 2010 capacity model for one-lane entry conflicting with one circulating lane.	6
Figure 5. Equation. HCM 2010 capacity model for right lane of two-lane entry conflicting with two circulating lanes.....	7
Figure 6. Equation. HCM 2010 capacity model for left lane of two-lane entry conflicting with two circulating lanes.....	7
Figure 7. Equation. HCM 2010 capacity model for each lane of a two-lane entry conflicting with one circulating lane.	7
Figure 8. Equation. HCM 2010 capacity model for one-lane entry conflicting with two circulating lanes.	7
Figure 9. Equation. Capacity model for single-lane roundabouts in Bend, OR.⁽⁵⁾	9
Figure 10. Equation. Capacity model for multilane roundabouts in Bend, OR.⁽⁵⁾	9
Figure 11. Equation. Capacity model for single-lane roundabouts in California.⁽⁶⁾.....	9
Figure 12. Equation. Capacity model for multilane roundabouts in California.⁽⁶⁾	10
Figure 13. Equation. Capacity model for single-lane roundabouts in Carmel, IN.⁽⁷⁾	10
Figure 14. Image. Example of nonvisible back of queue.	26
Figure 15. Image. Example of rolling queues.	27
Figure 16. Scatter Plot. Follow-up time vs. inscribed circle diameter.	39
Figure 17. Scatter Plot. Follow-up time vs. entry lane width.....	40
Figure 18. Scatter Plot. Follow-up time vs. entry angle.	41
Figure 19. Scatter Plot. Follow-up time vs. splitter island width.	42
Figure 20. Scatter Plot. Assessment of HCM 2010 model for single-lane roundabout sites.	46
Figure 21. Scatter Plot. Assessment of HCM 2010 model for 2x2 multilane roundabout sites and right entry lane.	47
Figure 22. Scatter Plot. Assessment of HCM 2010 model for 2x2 multilane roundabout sites and left entry lane.	48
Figure 23. Scatter Plot. Assessment of HCM 2010 model for 2x1 multilane roundabout sites and right entry lane.	49
Figure 24. Scatter Plot. Assessment of HCM 2010 model for 2x1 multilane roundabout sites and left entry lane.	50

Figure 25. Scatter Plot. Regression models for single-lane roundabout sites.....	51
Figure 26. Equation. Follow-up headway as a field-observable parameter to calibrate the y-intercept.....	51
Figure 27. Scatter Plot. Regression models for single-lane roundabout sites with calibration to follow-up time.	52
Figure 28. Scatter Plot. Regression models for single-lane roundabout sites, normalized by follow-up time.....	53
Figure 31. Scatter Plot. Regression models for Carmel, IN data.	55
Figure 32. Scatter Plot. Regression of group means for single-lane sites.	56
Figure 33. Scatter Plot. Exponential regression of group means, predicted vs. measured entering flow, for single-lane sites.	57
Figure 34. Scatter Plot. Linear regression of group means, predicted vs. measured entering flow for single-lane sites.....	58
Figure 35. Scatter Plot. Regression of group means for Carmel-only single-lane roundabout sites.....	59
Figure 36. Scatter Plot. Regression of group means for non-Carmel single-lane roundabout sites.	60
Figure 37. Scatter Plot. Regression models for two approaches at a single roundabout in Carmel, IN.	61
Figure 38. Scatter Plot. Regression models for multilane, 2x2 roundabout sites, right entry lane.	62
Figure 39. Scatter Plot. Regression models for multilane, 2x2 roundabout sites, left entry lane.	63
Figure 40. Scatter Plot. Regression models for multilane, 2x1 roundabout sites, right entry lane.	64
Figure 41. Scatter Plot. Regression models for multilane, 2x1 roundabout sites, left entry lane.	65
Figure 42. Scatter Plot. Regression models for multilane 2x2 roundabout sites, right entry lane with calibration to follow-up time.	66
Figure 43. Scatter Plot. Regression models for multilane 2x2 roundabout sites, left entry lane with calibration to follow-up time.	67
Figure 44. Scatter Plot. Regression models for multilane 2x1 roundabout sites with calibration matching the y-intercept to the 2x2 roundabout, right entry lane.	68
Figure 45. Scatter Plot. Regression models for multilane 2x1 roundabout sites, combined right and left entry lanes with calibration to combined follow-up time.	69
Figure 46. Equation. Equation incorporating constant exiting vehicles flow to calculate effective conflicting flow.....	70

Figure 47. Scatter Plot. Regression models for single-lane sites with calibration to follow-up time and constant effects of exiting vehicles. 71

Figure 48. Equation. Equation incorporating variable exiting vehicle flow to calculate effective conflicting flow. 72

Figure 49. Scatter Plot. Regression models for single-lane sites with calibration to follow-up time and variable effects of exiting vehicles. 73

Figure 50. Scatter Plot. Regression models for 2x2 multilane roundabout sites and left entry lane with calibration to follow-up time and constant effects of exiting vehicles. 74

Figure 51. Scatter Plot. Regression models for 2x2 multilane roundabout sites and left entry lane with calibration to follow-up time and variable effects of exiting vehicles. 75

Figure 52. Scatter Plot. Comparison of 2003 and 2012 flow data for single-lane roundabout site (WA04 North Leg)..... 76

Figure 53. Scatter Plot. Comparison of 2003 and 2012 flow data for multilane roundabout site VT03 east leg, right lane. 77

Figure 54. Scatter Plot. Comparison of 2003 and 2012 flow data for multilane roundabout site VT03 south leg, right lane. 78

Figure 55. Scatter Plot. Comparison of 2003 and 2012 flow data for multilane roundabout site VT03 west leg, right lane. 79

Figure 56. Equation. Model Summary, Exponential Model Form..... 80

Figure 57. Equation. Model Summary, Linear Model Form..... 80

LIST OF TABLES

Table 1. Critical headway and follow-up headways for single-lane roundabouts.	8
Table 2. Critical headway and follow-up headways for multilane roundabouts.	8
Table 3. Roundabout sites where video data were collected.	16
Table 4. Summary of single-lane roundabout data.	22
Table 5. Summary of multilane 2x2 roundabout configuration data.	24
Table 6. Summary of multilane 2x1 roundabout configuration data.	25
Table 7. Summary of multilane 1x2 roundabout configuration data.	25
Table 8. Example of data binning, where shaded rows representing arrival times of 12:01:46 to 12:02:47 are a valid one-minute data point.	28
Table 9. Example of coded events, where coded events (5, 6, 13-16) are shaded.	29
Table 10. Critical headway estimates for single-lane sites.	32
Table 11. Results for critical headways in multilane roundabouts.	33
Table 12. Summary of results for critical headway in multilane roundabouts.	34
Table 13. Follow-up time estimates for single-lane roundabout sites.	36
Table 14. Follow-up time estimates for multilane roundabout sites.	37
Table 15. Results of the geometric parameter correlation analysis	39
Table 16. RMSE for data sets applied to the HCM 2010 model for single-lane roundabout sites.	45
Table 17. RMSE for data sets applied to the HCM 2010 model for multilane roundabout sites.	46
Figure 29. Equation. Revised exponential model based on single-lane data from Carmel, IN.	54
Figure 30. Equation. Revised linear model based on single-lane data from Carmel, IN.	54
Table 18. Regression analysis of the Carmel-based model.	54
Table 19. Comparison of single-lane roundabout models.	80
Table 20. Comparison of multilane roundabout models.	81
Table 21. Recommended models for roundabout types, configuration, and entry lanes.	83

CHAPTER 1. INTRODUCTION

The debate over the best way to model the operational performance of roundabouts in the United States has had a colorful history over the past twenty years. In the early days of practice in the United States, there were no models available that were developed and/or calibrated to conditions found in the United States. Practitioners used models from other countries, primarily Australia (i.e., SIDRA) and the United Kingdom (i.e., RODEL or ARCADY), to analyze roundabouts and make design decisions.

In 2002, the National Cooperative Highway Research Program (NCHRP) initiated NCHRP Project 03-65, of which one objective was to collect operational data (collected during 2003) and develop performance models based on observed conditions in the United States. The outcomes of this study were published in NCHRP Report 572,⁽¹⁾ which included an early draft chapter intended for the Highway Capacity Manual (HCM) on the analysis of roundabouts. The Transportation Research Board (TRB) Committee on Highway Capacity and Quality of Service evaluated the results of the NCHRP Report 572 work, made modifications based on committee and subcommittee member input, and adopted two new chapters on roundabouts into the Highway Capacity Manual 2010.⁽²⁾ These chapters, Chapter 21 and Chapter 33, form the main chapters and supplemental information on roundabout operational analysis, respectively. The adoption of this methodology into the HCM was significant in that it established a model in an industry-accepted document that can be applied consistently alongside methodologies for conventional intersection forms.

The NCHRP Report 572 study was significant in being the first major study of roundabout operational performance in the United States. However, it uncovered significant differences between observed operational performance of roundabouts in the United States and what had been observed in other countries. Some of the key observations from that study are directly applicable to the development of updated capacity models performed for this project. Those observations include:

Driver-to-driver variation within a given site. The data observed showed considerable variation from minute to minute for a given site (in this document, “site” refers to a single approach within a roundabout), and this variation when aggregated across all sites creates a variance in capacity that appears to be intrinsic to the operation of the roundabout. From a practical standpoint, this means that any capacity estimates have an uncertainty associated with them that is inherently part of estimating the performance of an unsignalized intersection where capacity is a function of individual driver decisions. This led to the recommendation of a simple model where only aggregate geometric parameters in terms of number of lanes were found to be statistically significant.

Perception that capacity will increase over time. The number and diversity of sites available to the researchers in 2003 was constrained to approximately 300 roundabouts known to exist at that time. Most of these were recently constructed and thus were not necessarily operating to their design condition, or under saturated conditions. An underlying hypothesis in this study is that an increase in capacity would be realized over time as drivers become more familiar with roundabouts.

Use of turn signals on exit. This factor, looked at in the more general context of the effect of exiting vehicles on entry capacity, has been evaluated in previous research and is worth examining in this study (for example, Mereszczak et al. 2005).

Suboptimal design. Some have speculated that sites operating with some degree of queuing may have had design features which caused them to operate less optimally than would be desired, particularly for multilane roundabouts. Example design features included poor entry path alignment (path overlap) that caused poor lane utilization. Under these design conditions, while the right lane of the entry was operating under queued conditions and thus could be measured, the left lane often would have either intermittent or no queues.

Other factors that may influence capacity but are not likely to be of significance for this study. These include a fleet of larger vehicles relative to other countries, which affects acceleration and following distance, and the general dominance of stop control versus yield control in the United States, which is believed to contribute to a tendency to stop or nearly stop even when faced with yield control and no conflicting vehicles.

SCOPE OF STUDY

The scope of this study includes the following activities and products:

- Develop an updated site inventory of selected roundabouts accessible to the transportation profession.
- Update and expand on a comprehensive database of operational data of selected roundabouts for use in the research.
- Develop an updated operational analysis procedure for the HCM, including capacity estimates for single-lane and multilane roundabouts.

RESEARCH APPROACH

The detailed approaches for each of the major components of this study are described in the following sections.

Summarize Existing Relationships

A literature review, presented in chapter 2, focuses on efforts to analyze the capacity of roundabouts in the United States, building upon the research and methodologies in NCHRP Report 572 and HCM 2010. This review is targeted on identifying calibration or new modeling efforts within the U.S. For a more holistic review of roundabout capacity models used throughout the world, refer to NCHRP Report 572.

Site Inventory and Data Collection

A major element of the study included updating and expanding the inventory of U.S. roundabouts compiled for NCHRP Report 572. At selected sites, the research team collected and summarized data on operational performance and geometric parameters. Specific data collection

methods included extensive video recording during peak and off-peak periods. These methods are described in detail in chapter 3.

Operational Model Development

Operational model development included the following tasks:

- Estimate critical headway and follow-up headway for each site and for the population of sites studied.
- Examine geometric parameters.
- Compare field data to the HCM 2010 model and regression.
- Perform an empirical regression of observed capacity as a function of circulating flow.
- Develop a draft revised HCM procedure that incorporates the findings from this study.

These are discussed in detail in chapters 4 and 5, with conclusions and recommendations presented in chapter 6.

CHAPTER 2. LITERATURE REVIEW

To support the research approach documented herein, an extensive literature review was completed to identify calibration or new modeling efforts within the United States, building upon the research and methodologies in NCHRP Report 572⁽¹⁾ and the HCM 2010.⁽²⁾ The following section provides a summary of the literature review and documents key findings

NCHRP REPORT 572 METHOD

The NCHRP Report 572 models show less capacity than many international models, because data has suggested that U.S. drivers do not use roundabouts as aggressively as other countries, including many European countries and Australia. Further, NCHRP Report 572 found that while aggregate geometric details such as number and assignment of lanes was significant in determining capacity, the fine details of geometric design, such as lane width, could not be distinguished due to considerable variation within driver behavior at a given location.

From the research conducted in NCHRP Report 572, the following capacity models were developed for U.S. roundabouts. For single-lane roundabouts, the equation in figure 1 applies.

$$c = 1130 * \exp(-0.0010 * v_c)$$

Figure 1. Equation. Capacity model for single lane roundabouts from NCHRP Report 572.

Where c = entry capacity (pc/h) and v_c = conflicting flow (pc/h).

For multilane roundabouts, the equation in figure 2 applies.

$$c_{crit} = 1130 * \exp(-0.0007 * v_c)$$

Figure 2. Equation. Capacity model for critical lane of multilane roundabouts from NCHRP Report 572.

Where c_{crit} = entry capacity of critical lane (pc/h) and v_c = conflicting flow (pc/h).

In the case of multilane roundabouts, per NCHRP Report 572, the capacity is calculated for the critical lane.

The NCHRP Report 572 researchers developed the analysis methodologies such that the capacity models could be updated to reflect local conditions or changing national conditions. This allows the assumed capacity to be increased or decreased depending upon two key parameters related to driver behavior: critical headway and follow-up headway. The analytical model form that most closely matches the regression model form is the Siegloch model. (See reference 3, as presented in 4.) As such, the exponential model parameters can be calibrated using locally measured parameters in the Siegloch model as shown in figure 3.

$$C = A * \exp(-B * v_c)$$

$$A = 3600/t_f$$

$$B = (t_c - t_f/2)/3600$$

Figure 3. Equation. Sieglöch capacity model.

Where C = entry capacity (pcu/h), v_c = conflicting flow (pcu/h), t_f = follow-up headway (s), and t_c = critical headway (s).

The calibration factors may differ between geographical areas based on driver familiarity with roundabouts and/or overall aggressiveness. In addition, calibration factors may change within a geographical area over time after roundabouts are introduced and drivers become more familiar with roundabout operations.

HCM 2010 METHOD

The roundabout procedure included in the HCM 2010 is based on the method described in NCHRP Report 572, but with a number of modifications. For example, in HCM 2010, circulating flow is converted to passenger-car-equivalents (PCEs) to determine capacity and is then converted back to vehicles for use in volume-to-capacity, control delay, and queue calculations. The control delay equation presented in NCHRP Report 572 is modified in the HCM 2010 to adapt the stop-controlled control delay equation for two-way stop-controlled (TWSC) intersections for use in the yield-controlled environment at a roundabout. The final term of the control delay equation for roundabouts includes a “+ 5 * min[v/c, 1]” term. At v/c=0, the term is zero (reflecting a low likelihood of coming to a complete stop); at v/c>=1, the term is five (reflecting a high likelihood of coming to a complete stop); and it is linear between v/c=0 and one. Additionally, in the HCM 2010, on multilane approaches, a lane utilization factor of 0.53 was assumed for the lane deemed to be dominant. Level of Service (LOS) is determined for the intersection as a whole, all approaches, and all lanes, not just the critical lane as in NCHRP Report 572. The control delay thresholds to determine LOS are based on what is currently used for other unsignalized intersections. For consistency with other methods in HCM 2010, LOS F includes the condition where v/c exceeds 1.0. These modifications result in minor differences from the original procedure proposed by NCHRP Report 572.

As a result of these modifications, the HCM 2010 presents a larger set of capacity models to cover a variety of lane configurations, including hybrid combinations of one-lane and two-lane entries and circulatory roadways. For a one-lane entry conflicting with one circulating lane (such as at single-lane roundabouts), the equation in figure 4 applies.

$$C_{e,pce} = 1130 * \exp(-0.0010 * v_{c,pce})$$

Figure 4. Equation. HCM 2010 capacity model for one-lane entry conflicting with one circulating lane.

Where $c_{e,pce}$ = entry capacity (pc/h) and $v_{c,pce}$ = conflicting flow (pc/h).

For multilane roundabouts, the choice of equation depends on the number of entry lanes and the number of conflicting circulating lanes. For a two-lane entry conflicting with two circulating lanes, the equation in figure 5 applies to the right entry lane, and the equation in figure 6 applies to the left entry lane. For a two-lane entry conflicting with one circulating lane, the equation in figure 7 applies to each entry lane. For a one-lane entry conflicting with two circulating lanes, the equation in figure 8 applies.

$$c_{e,pce} = 1130 * \exp (-0.0007 * v_{c,pce})$$

Figure 5. Equation. HCM 2010 capacity model for right lane of two-lane entry conflicting with two circulating lanes.

$$c_{e,pce} = 1130 * \exp (-0.00075 * v_{c,pce})$$

Figure 6. Equation. HCM 2010 capacity model for left lane of two-lane entry conflicting with two circulating lanes.

$$c_{e,pce} = 1130 * \exp (-0.0010 * v_{c,pce})$$

Figure 7. Equation. HCM 2010 capacity model for each lane of a two-lane entry conflicting with one circulating lane.

$$c_{e,pce} = 1130 * \exp (-0.0010 * v_{c,pce})$$

Figure 8. Equation. HCM 2010 capacity model for one-lane entry conflicting with two circulating lanes.

Where $c_{e,pce}$ = entry capacity (pc/h) and $v_{c,pce}$ = conflicting flow (pc/h).

HCM 2010 ROUNDABOUT MODEL CALIBRATION

Based on the recommendations outlined in NCHRP Report 572 and HCM 2010, several jurisdictions have developed and documented local calibration efforts of the capacity models in NCHRP Report 572 and HCM 2010. These efforts provide an opportunity to distinguish local driving conditions from a more generalized national model. Most notably, the following studies were found: Bend, OR;⁽⁵⁾ California;⁽⁶⁾ Carmel, IN;⁽⁷⁾ Wisconsin;⁽⁸⁾ Maryland;⁽⁹⁾ and Kansas.⁽¹⁰⁾ Table 1 and table 2 below show the critical headways and follow-up headways reported in the studies discussed for single-lane and multilane roundabouts, respectively. The table suggests a wide range of potential observations. Further commentary on some of these studies, included recommended models, is provided below.

Table 1. Critical headway and follow-up headways for single-lane roundabouts.

Gap Acceptance Parameters	NCHRP Report 572⁽¹⁾ (s)	Bend, OR⁽⁵⁾ (s)	California⁽⁶⁾ (s)	Carmel, IN⁽⁷⁾ (s)	Wisconsin⁽⁸⁾ (s)	Maryland⁽⁹⁾ (s)	Kansas⁽¹⁰⁾ (s)
Critical Headway	5.1	4.1	4.5-5.3	3.4-3.8	4.8-5.5	2.5-2.6	No change from NCHRP Report 572
Follow-up Headway	3.2	2.7	2.3-2.8	2.1-2.4	2.6-3.8	Not studied	No change from NCHRP Report 572

Table 2. Critical headway and follow-up headways for multilane roundabouts.

Gap Acceptance Parameters	NCHRP Report 572⁽¹⁾ (s)	Bend, OR⁽⁵⁾ (s)	California⁽⁶⁾ (s)	Carmel, IN⁽⁷⁾ (s)	Wisconsin⁽⁸⁾ (s)	Maryland⁽⁹⁾ (s)	Kansas⁽¹⁰⁾ (s)
Critical Headway, Right Lane	4.2	Not studied	4.0-4.8	Not studied	3.4-4.4	Not studied	Not studied
Critical Headway, Left Lane	4.5	Not studied	4.4-5.1	Not studied	4.1-4.8	Not studied	Not studied
Follow-up Headway, Right Lane	3.1	Not studied	2.1-2.3	Not studied	2.2-3.0	Not studied	Not studied
Follow-up Headway, Left Lane	3.4	Not studied	1.8-2.7	Not studied	2.5-3.1	Not studied	Not studied

Bend, OR

The effort conducted for Bend, OR, specifies a variety of analysis parameters, including LOS thresholds, queuing analysis procedures, and other such considerations.⁽⁵⁾ In addition, data were collected at existing roundabouts within Bend to determine local driver characteristics. Based on that effort, the capacity model in figure 9 was recommended for use for single-lane roundabout analyses within the city, and the capacity model in figure 10 was recommended for use in multilane roundabout analyses.

$$c_{pe} = 1333 * \exp(-0.0008 * v_{c,pce})$$

Figure 9. Equation. Capacity model for single-lane roundabouts in Bend, OR.⁽⁵⁾

$$c_{pe} = 1333 * \exp(-0.0007 * v_{c,pce})$$

Figure 10. Equation. Capacity model for multilane roundabouts in Bend, OR.⁽⁵⁾

Where c_{pe} = capacity, adjusted for heavy vehicles (pc/h), and $v_{c,pce}$ = conflicting circulating flow rate, adjusted for heavy vehicles (pc/h).

In this case, the single-lane model was calibrated to produce a higher capacity than the national average. However, no multilane roundabouts existed within the city limits at the time of the calibration study. As such, the national model was included in an unmodified form.

It should be noted that Bend has a large number of roundabouts and, as a result, a driver population that is likely more familiar with roundabouts than the average U.S. citizen. Based on this, Bend, OR's finding that the roundabouts within Bend operate at a higher capacity than what was shown in NCHRP Report 572 suggests the possibility that driver population familiarity with roundabouts can increase the observed capacity.

California

Tian et al. developed a set of calibrated roundabout analysis equations for use by Caltrans throughout the state of California.⁽⁶⁾ These analyses were based on data collected at nine representative roundabouts locations throughout the state. Based on the data collected, the calibrated equation in figure 11 was developed for single-lane roundabouts, and the equations in figure 12 was developed for multilane roundabouts.

$$c_{pe} = 1400 * \exp(-0.0010 * v_{c,pce})$$

Figure 11. Equation. Capacity model for single-lane roundabouts in California.⁽⁶⁾

$$\text{Right Lane: } c_{pe} = 1640 * \exp(-0.0009 * v_{c,pce})$$

$$\text{Left Lane: } c_{pe} = 1640 * \exp(-0.0010 * v_{c,pce})$$

Figure 12. Equation. Capacity model for multilane roundabouts in California.⁽⁶⁾

Where C_{pe} = capacity, adjusted for heavy vehicles (pc/h), and $v_{c,pce}$ = conflicting circulating flow rate, adjusted for heavy vehicles (pc/h).

California results were able to make predictions about the capacity of multilane roundabouts by lane. As such, the resultant capacity equations are more consistent with the procedures outlined in HCM 2010.

Of particular note, the critical headways observed by the Caltrans calibration effort were not found to be statistically different from what was developed for NCHRP Report 572. However, the follow-up headways, which were found to be considerably lower than what was produced by NCHRP Report 572, were determined to be statistically different.

Further, conflicting flow rate and speed were found to have moderate to low negative correlation with both critical headway and follow-up headway. With an increase in conflicting flow and/or speed, the critical headway and follow-up headway tend to decrease. The results from the correlation analyses indicate that the correlation between speed and follow-up headway is the strongest, and the correlation between conflicting flow and follow-up headway is the weakest.

Carmel, IN

While some jurisdictions have focused on calibrating the existing NCHRP Report 572 model, others have developed new models altogether due to poor fit with a calibrated HCM 2010 model. This approach was taken in Carmel, IN, which is known to have one of the largest concentrations of roundabouts in the United States. Wei, Grenard and Shah⁽⁷⁾ developed a method to derive a simplified and calibrated linear equation based on observations made at three single-lane roundabouts within Carmel. The developed method is shown in figure 13.

$$c = -0.8698 * v_c + 1503$$

Figure 13. Equation. Capacity model for single-lane roundabouts in Carmel, IN.⁽⁷⁾

Where c = capacity of the approach (veh/h), and v_c = conflicting flow (veh/h).

Based on this procedure, the research team found that roundabouts in Carmel operate with a higher capacity than what was predicted by NCHRP Report 572.

In the case of Carmel, the developed model cannot easily be calibrated to other jurisdictions. Rather, the developers of this model suggest that other locations develop similar local models by enacting a similar process. While this approach likely produces reasonable results for the local area, producing a similar model for other jurisdictions would require that the area have

roundabouts at which to collect data. Until that time, national models would likely have to be relied upon.

Wisconsin

The Wisconsin DOT analysis of roundabouts within the state of Wisconsin collected data for 14 roundabouts including both single and multilane varieties.⁽⁸⁾ Of these, two single-lane and two multilane roundabouts were analyzed in depth to determine operational characteristics of roundabouts specifically related to Wisconsin drivers.

The findings of this analysis showed that the critical and follow-up headways observed were within the data ranges reported by NCHRP Report 572. Also, consistent with current thinking, the critical and follow-up headways were observed to decrease as congestion increased. In addition, larger vehicles, such as trucks, were found to have higher critical and follow-up headways while smaller vehicles, such as motorcycles, were found to have lower critical and follow-up headways than was observed for traditional passenger cars.

Kansas

The Kansas DOT commissioned a study to look at calibrating the HCM 2010 equations for use in Kansas. The roundabout calibration effort collected data for 10 roundabouts within the state.⁽¹⁰⁾ Of those, three were analyzed in more detail. Specifically, critical headway and follow-up headway were calculated for the purpose of producing calibrated roundabout analysis models for single-lane roundabouts.

During the calculation of critical headway, the researchers identified an issue when using the critical headway calculation method used by NCHRP Report 572 (which is based on the two-way stop-controlled model included in the HCM). Specifically, they attempted to calculate critical headway by statistically estimating the minimum headway between circulating vehicles that an entering driver would most likely accept based on the gap or gaps the entering driver was observed to reject and the gap the entering driver actually accepted.

This method averages all accepted gap times as recorded, which is well suited for high volume sites where there is a somewhat consistent stream of circulating traffic. However, as circulating volume decreases and headways between circulating vehicles increase, this method tends to produce large estimate critical headway values. For example, if a series of circulating vehicles pass and there is a full minute gap before the next circulating vehicle arrives, this method would produce an accepted gap time of 60 s. A driver clearly would not require a 60 s gap under normal conditions. As such, this method can produce results that higher critical headway values than one would expect.

To address this issue, the Kansas researchers also used the method employed by the researchers of the California roundabout calibration effort described earlier. Specifically, this modified approach caps all accepted gap values at 8.0 s, meaning any recorded gap longer than 8.0 s is modified and a value of 8.0 s is used for critical headway calculations.

Based on using the modified method originally used by the California researchers, the Kansas research team produced critical headway and follow-up headway results that were not

statistically different than NCHRP Report 572 results. As such, the team concluded that the national models produced by NCHRP Report 572 were adequate for roundabout analysis in Kansas without further modification.

OTHER CAPACITY INFLUENCES

Recent research has shown that roundabout characteristics not currently accounted for in analysis models may have a positive impact on the ability to calculate capacities. Specifically, the Wisconsin DOT report⁽¹⁰⁾ and Mereszczak, et al.⁽¹¹⁾ each quantified the effects of exiting vehicles on overall roundabout capacity. For example, if a vehicle is exiting, a driver might be more willing to enter the roundabout than if the roundabout were not exiting. Mereszczak, et al.⁽¹¹⁾ expanded on Hagrings' research⁽¹²⁾ that showed the capacity of a given approach will increase when the proportion of exiting vehicles increases even when the major street flow remains the same. Wisconsin researchers evaluated the effect that exiting vehicles have on the calculation of critical and follow-up headway calculations, which also directly affect the calculation of capacities at roundabouts, as described previously. As shown, the consideration of exiting vehicles reduced the calculated critical headway and follow-up headway in all scenarios presented. The researchers attribute this to the observation that when entering drivers rejected long headways in the circulating stream, there usually was a vehicle exiting during that period. By accounting for exiting vehicles, those long headways were able to be reduced.

ALTERNATIVE ROUNDABOUT CAPACITY MODELS

Although HCM 2010 uses the research in NCHRP Report 572 as the basis of the procedure included in the manual, other methods are identified in the manual as alternatives where the HCM method might not be applicable. In reality, the application of HCM 2010 appears to be uneven around the United States, likely because software programs are in the process of incorporating the new or updated methodologies into their respective platforms, and because other software packages implementing international methods^(13,14) have been in use for many years.

Evaluations of HCM 2010 methods to other roundabout capacity models may yield strikingly different results for certain movements. The discrepancies highlighted a key concern facing roundabout analysis procedures in the United States today: with the number of analysis procedures being applied to roundabout analyses, results may indicate both favorable and unfavorable operational results for the same analysis scenario depending upon what methodology is used. Further, favorable or unfavorable results may be dictated by the availability of local calibration factors. For the case of roundabouts where a number of deterministic models can be applied, analysts may be expected to interpret the reasonableness of very technical models and their applicability to a specific project.

Methods other than traditional gap acceptance or empirical regression techniques have been used outside the United States. Specifically, the additive conflict flow (ACF) method was evaluated in Germany for use in estimating the performance of mini-roundabouts.⁽¹⁵⁾ The ACF method was developed as a new technique for TWSC intersection analysis as an alternative to the theory of gap acceptance, on which the current TWSC and roundabout methodologies in HCM 2010 are based. Researchers argue that this method is more intuitive than the priority system currently

applied to TWSC because movement priority rankings do not always make sense when considering pedestrian interactions. A distinct advantage of the ACF method is the ability to calculate in a single step the capacity for any stream of traffic as a function of traffic volumes of other streams. This reality highlights the ACF methods as a substitute to gap acceptance theory, especially when pedestrian movements have an effect on normal intersection operations. In the case of mini-roundabouts, the ACF method makes it possible to calculate the capacities of mini-roundabout entries and exits while taking crossing pedestrian streams into account.⁽¹⁶⁾

CHAPTER 3. DATA CHARACTERISTICS

The following section describes the process by which an updated inventory of roundabouts in the United States was developed, including site selection, data collection, and data reduction.

SITE INVENTORY

One of the products of this research is an updated site inventory that contains information on selected roundabouts. A range of site characteristics is vital to the successful development of models with sensitivity to a range of influencing factors. These characteristics are that the sites:

- Have a high likelihood of queued conditions for some portion of the day, preferably at least fifteen minutes, on at least one approach.
- Have a range of approach versus circulatory roadway lane configurations (e.g., single-lane approach vs. two-lane circulatory roadway, etc.).
- Include multiple sites within approximately one hour drive time to maximize data collection resources.
- Include diversity in geography and driver type.
- Have a range of geometric conditions, such as splitter island widths.
- Include overlapping sites with those in NCHRP Report 572 to demonstrate potential change in performance over time.
- Are overlapped with or in close proximity to NCHRP Project 03-100 sites for data collection efficiency.

Table 3 displays a summary of sites observed as part of this study.

Table 3. Roundabout sites where video data were collected.

Community	Intersection	Intersection Code	Leg	No. of Entering Lanes	No. of Circulating Lanes	No. of Exiting Lanes
Eagle, CO	Eby Creek Road/US 6 (Grand Avenue)	CO01	S	1	1	1
Eagle, CO	Eby Creek Road/US 6 (Grand Avenue)	CO02	W	1	1	1
Eagle, CO	Eby Creek Road/US 6 (Grand Avenue)	CO03	N	2	1	1
Eagle, CO	Eby Creek Road/US 6 (Grand Avenue)	CO04	E	1	1	2
Golden, CO	Golden Road/Johnson Road/16th Street	CO02	N	1	2	1
Golden, CO	Golden Road/Johnson Road/16th Street	CO03	W	2	2	2
Golden, CO	Golden Road/Johnson Road/16th Street	CO04	E	2	2	2
Golden, CO	Golden Road/Johnson Road/16th Street	CO05	S	2	2	2
Golden, CO	Golden Road/Ulysses Street	CO38	N	1	1	1
Golden, CO	Golden Road/Ulysses Street	CO39	E	1	1	1
Golden, CO	Golden Road/Ulysses Street	CO40	S	1	1	1
Golden, CO	Golden Road/Ulysses Street	CO41	W	1	1	1
Avon, CO	Beaver Creek Boulevard/Avon Road	CO06	N	3	2	2
Avon, CO	Beaver Creek Boulevard/Avon Road	CO07	E	3	2	1
Avon, CO	Beaver Creek Boulevard/Avon Road	CO08	S	3	2	2
Avon, CO	Beaver Creek Boulevard/Avon Road	CO09	W	3	2	1
Avon, CO	Benchmark Road/Avon Road	CO07	N	2	2	2
Avon, CO	Benchmark Road/Avon Road	CO08	E	2	2	1
Avon, CO	Benchmark Road/Avon Road	CO09	S	2	2	2
Avon, CO	Benchmark Road/Avon Road	CO10	W	1	2	1
Avon, CO	I-70 EB/Avon Road	CO08	S	2	2	2
Avon, CO	I-70 EB/Avon Road	CO08	W	2	2	0
Avon, CO	I-70 WB/Avon Road	CO09	N	2	2	1
Avon, CO	I-70 WB/Avon Road	CO09	E	3	1	0
Avon, CO	US 6/Avon Road/Village Road	CO10	N	2	2	2
Avon, CO	US 6/Avon Road/Village Road	CO10	E	2	2	1
Avon, CO	US 6/Avon Road/Village Road	CO10	S	2	2	2
Avon, CO	US 6/Avon Road/Village Road	CO10	W	2	2	1

Community	Intersection	Intersection Code	Leg	No. of Entering Lanes	No. of Circulating Lanes	No. of Exiting Lanes
Vail, CO	I-70 EB/Chamonix Road	CO49	SW	2	1	0
Vail, CO	I-70 EB/Chamonix Road	CO49	NW	1	1	1
Vail, CO	I-70 EB/Chamonix Road	CO49	S	1	1	1
Vail, CO	I-70 EB/Chamonix Road	CO49	N	1	1	1
Vail, CO	I-70 EB/Chamonix Road	CO49	E	1	1	1
Vail, CO	I-70 WB/Chamonix Road	CO50	W	2	2	1
Vail, CO	I-70 WB/Chamonix Road	CO50	S	2	2	1
Vail, CO	I-70 WB/Chamonix Road	CO50	N		2	1
Vail, CO	I-70 WB/Chamonix Road	CO50	NE	2	2	0
Vail, CO	I-70 WB/Chamonix Road	CO50	SE	2	2	1
Vail, CO	I-70 EB/Vail Road	CO51	N	2	2	1
Vail, CO	I-70 EB/Vail Road	CO51	E	3	2	2
Vail, CO	I-70 EB/Vail Road	CO51	S	2	2	1
Vail, CO	I-70 EB/Vail Road	CO51	NW	2	2	0
Vail, CO	I-70 EB/Vail Road	CO51	SW	3	2	1
Vail, CO	I-70 WB/Vail Road	CO52	SE	2	1	0
Vail, CO	I-70 WB/Vail Road	CO52	NE	2	1	1
Vail, CO	I-70 WB/Vail Road	CO52	W	2	1	1
Edwards, CO	Miller Ranch Road/Edwards Access Road	CO54	N	2	1	2
Edwards, CO	Miller Ranch Road/Edwards Access Road	CO54	W	1	2	1
Edwards, CO	Miller Ranch Road/Edwards Access Road	CO54	E	2	2	1
Edwards, CO	Miller Ranch Road/Edwards Access Road	CO54	S	2	1	2
Edwards, CO	I-70 EB On-Ramp/Edwards Access Road	CO55	S	2	1	1
Edwards, CO	I-70 EB On-Ramp/Edwards Access Road	CO55	N	1	1	2
Edwards, CO	I-70 EB On-Ramp/Edwards Access Road	CO55	W	2	2	0
Edwards, CO	I-70 WB On-Ramp/Edwards Access Road	CO56	N	2	2	1
Edwards, CO	I-70 WB On-Ramp/Edwards Access Road	CO56	E	2	2	0
Edwards, CO	I-70 WB On-Ramp/Edwards Access Road	CO56	S	2	1	2
Carmel, IN	126th Street/Hazel Dell Parkway	IN02	N	2	2	2

Community	Intersection	Intersection Code	Leg	No. of Entering Lanes	No. of Circulating Lanes	No. of Exiting Lanes
Carmel, IN	126th Street/Hazel Dell Parkway	IN02	S	2	1	2
Carmel, IN	126th Street/Hazel Dell Parkway	IN02	E	2	2	1
Carmel, IN	126th Street/Hazel Dell Parkway	IN02	W	2	2	1
Carmel, IN	116th Street/Illinois Street	IN06	S	2	2	2
Carmel, IN	116th Street/Illinois Street	IN06	N	2	2	2
Carmel, IN	116th Street/Illinois Street	IN06	E	2	2	2
Carmel, IN	116th Street/Illinois Street	IN06	W	2	2	2
Carmel, IN	96th Street/Ditch Road	IN07	S	1	1	1
Carmel, IN	96th Street/Ditch Road	IN07	N	1	1	1
Carmel, IN	96th Street/Ditch Road	IN07	E	1	1	1
Carmel, IN	96th Street/Ditch Road	IN07	W	1	1	1
Carmel, IN	96th Street/Westfield Boulevard	IN08	S	2	1	1
Carmel, IN	96th Street/Westfield Boulevard	IN08	N	1	1	1
Carmel, IN	96th Street/Westfield Boulevard	IN08	E	1	1	1
Carmel, IN	116th Street/Spring Mill Road	IN09	S	1	1	1
Carmel, IN	116th Street/Spring Mill Road	IN09	N	1	1	2
Carmel, IN	116th Street/Spring Mill Road	IN09	E	2	1	1
Carmel, IN	116th Street/Spring Mill Road	IN09	W	1	1	1
Carmel, IN	106th Street/Spring Mill Road	IN10	N	1	1	1
Carmel, IN	106th Street/Spring Mill Road	IN10	S	1	1	1
Carmel, IN	106th Street/Spring Mill Road	IN10	E	1	1	1
Carmel, IN	106th Street/Spring Mill Road	IN10	W	1	1	1
Carmel, IN	136th Street/Keystone Parkway SB	IN11	S	0	1	1
Carmel, IN	136th Street/Keystone Parkway SB	IN11	N	1	1	0
Carmel, IN	136th Street/Keystone Parkway SB	IN11	W	2	1	1
Carmel, IN	136th Street/Keystone Parkway NB	IN12	S	1	1	0
Carmel, IN	136th Street/Keystone Parkway NB	IN12	N	0	1	1
Carmel, IN	136th Street/Keystone Parkway NB	IN12	E	1	1	1
Malta, NY	SR 67 (Dunning Street)/US 9	NY06	N	2	2	2

Community	Intersection	Intersection Code	Leg	No. of Entering Lanes	No. of Circulating Lanes	No. of Exiting Lanes
Malta, NY	SR 67 (Dunning Street)/US 9	NY06	E	2	2	1
Malta, NY	SR 67 (Dunning Street)/US 9	NY06	S	2	2	2
Malta, NY	SR 67 (Dunning Street)/US 9	NY06	W	2	2	1
Glens Falls, NY	US 9/Warren Street/Hudson Avenue/Glen Street	NY07	W	1	1	1
Glens Falls, NY	US 9/Warren Street/Hudson Avenue/Glen Street	NY07	S	1	1	1
Glens Falls, NY	US 9/Warren Street/Hudson Avenue/Glen Street	NY07	NE	1	1	1
Glens Falls, NY	US 9/Warren Street/Hudson Avenue/Glen Street	NY07	NW	1	1	1
Glens Falls, NY	US 9/Warren Street/Hudson Avenue/Glen Street	NY07	E	1	1	1
Rotterdam, NY	Curry Road (SR 7)/Hamburg Street (SR 146)	NY08	W	1	1	1
Rotterdam, NY	Curry Road (SR 7)/Hamburg Street (SR 146)	NY08	S	1	1	1
Rotterdam, NY	Curry Road (SR 7)/Hamburg Street (SR 146)	NY08	N	1	1	1
Rotterdam, NY	Curry Road (SR 7)/Hamburg Street (SR 146)	NY08	E	1	1	1
Slingerlands, NY	Lagrange Road (SR 85)/New Scotland Road	NY09	N	2	1	2
Slingerlands, NY	Lagrange Road (SR 85)/New Scotland Road	NY09	E	2	2	2
Slingerlands, NY	Lagrange Road (SR 85)/New Scotland Road	NY09	S	2	1	2
Slingerlands, NY	Lagrange Road (SR 85)/New Scotland Road	NY09	W	2	2	2
Gilbert's Corner, VA	US 50/ US 15	VA01	N	2	1	1
Gilbert's Corner, VA	US 50/ US 15	VA01	E	1	2	1
Gilbert's Corner, VA	US 50/ US 15	VA01	S	2	1	1
Gilbert's Corner, VA	US 50/ US 15	VA01	W	1	2	1
Brattleboro, VT	SR 9/US 5	VT03	W	2	2	1
Brattleboro, VT	SR 9/US 5	VT03	E	2	2	1
Brattleboro, VT	SR 9/US 5	VT03	N	2	2	1
Port Orchard, WA	SR 166/Mile Hill Drive/Bethel Avenue	WA04	N	1	1	1
Port Orchard, WA	SR 166/Mile Hill Drive/Bethel Avenue	WA04	E	1	1	1
Monroe, WA	164th Street/SR 522 NB Ramp/Tester Road	WA06	E	2	1	2
Monroe, WA	164th Street/SR 522 NB Ramp/Tester Road	WA06	SW	2	2	0
Monroe, WA	164th Street/SR 522 NB Ramp/Tester Road	WA06	S	1	2	1
Gig Harbor, WA	SR 16 NB/Burnham Drive NW/Borgen Boulevard	WA09	N	2	2	1

Community	Intersection	Intersection Code	Leg	No. of Entering Lanes	No. of Circulating Lanes	No. of Exiting Lanes
Gig Harbor, WA	SR 16 NB/Burnham Drive NW/Borgen Boulevard	WA09	SE	2	2	1
Gig Harbor, WA	SR 16 NB/Burnham Drive NW/Borgen Boulevard	WA09	SW	2	2	0
Gig Harbor, WA	SR 16 NB/Burnham Drive NW/Borgen Boulevard	WA09	E	2	1	2
Gig Harbor, WA	4th Avenue/Olympic Street	WA31	N	2	1	2
Gig Harbor, WA	4th Avenue/Olympic Street	WA31	S	2	1	1
Gig Harbor, WA	4th Avenue/Olympic Street	WA31	E	2	2	1
Gig Harbor, WA	SR 16 SB/Burnham Drive NW	WA32	N	2	2	0
Gig Harbor, WA	SR 16 SB/Burnham Drive NW	WA32	W	2	2	1
Olympia, WA	14th Avenue/Jefferson Street	WA30	N	2	2	1
Olympia, WA	14th Avenue/Jefferson Street	WA30	S	2	2	1
Olympia, WA	14th Avenue/Jefferson Street	WA30	E	2	1	2
Olympia, WA	14th Avenue/Jefferson Street	WA30	W	2	2	2
Lake Stevens, WA	Lundeen Park Way/Callow Road	WA33	E	1	1	1
Lake Stevens, WA	Lundeen Park Way/Callow Road	WA33	W	1	1	1
Anacortes, WA	SR 20 Spur/Commercial Avenue	WA34	N	1	1	1
Anacortes, WA	SR 20 Spur/Commercial Avenue	WA34	E	1	1	1
Bellingham, WA	Pole Road/SR 539	WA35	N	2	2	2
Bellingham, WA	Pole Road/SR 539	WA35	S	2	2	2
Bellingham, WA	Pole Road/SR 539	WA35	E	1	1	1
Bellingham, WA	Pole Road/SR 539	WA35	W	1	1	1

Single-Lane Sites

This section summarizes the sites for each roundabout that yielded single-lane data sets. The data are summarized in table 4. A total of 819 usable minutes of data were usable for the capacity modeling exercise after excluding minutes without queuing and minutes with pedestrian events. This is nearly three times as much data as was available in the NCHRP Report 572 study (318 minutes).

Table 4. Summary of single-lane roundabout data.

Subarea	Site	Site Code	Usable Data Points
Carmel, IN	136th Street/Keystone Parkway NB	IN12-E	4
Carmel, IN	136th Street/Keystone Parkway NB	IN12-S	71
Carmel, IN	96th Street/Ditch Road	IN07-E	31
Carmel, IN	96th Street/Ditch Road	IN07-S	10
Carmel, IN	96th Street/Westfield Boulevard	IN08-N	13
Carmel, IN	116th Street/Spring Mill Road	IN09-S	54
Carmel, IN	116th Street/Spring Mill Road	IN09-W	139
Carmel, IN	106th Street/Spring Mill Road	IN10-E	51
Carmel, IN	106th Street/Spring Mill Road	IN10-N	32
Carmel, IN	106th Street/Spring Mill Road	IN10-W	32
Carmel, IN	Subtotal	n/a	437
New York State	US 9/Warren Street/Hudson Avenue/Glen Street	NY07-S	71
New York State	US 9/Warren Street/Hudson Avenue/Glen Street	NY07-W	92
New York State	US 9/Warren Street/Hudson Avenue/Glen Street	NY07-E	65
New York State	US 9/Warren Street/Hudson Avenue/Glen Street	NY07-NW	13
New York State	US 9/Warren Street/Hudson Avenue/Glen Street	NY07-NE	1
New York State	Curry Road (SR 7)/Hamburg Street (SR14)	NY08-N	9
New York State	Curry Road (SR 7)/Hamburg Street (SR14)	NY08-W	21
New York State	Subtotal	n/a	272
Washington State	SR 166/Mile Hill Drive/Bethel Avenue	WA04-E	26
Washington State	SR 166/Mile Hill Drive/Bethel Avenue	WA04-N	16
Washington State	Lundeen Park Way/Callow Road	WA33-E	4
Washington State	Lundeen Park Way/Callow Road	WA33-W	13
Washington State	SR 20 Spur/Commercial Avenue	WA34-E	7
Washington State	SR 20 Spur/Commercial Avenue	WA34-N	5
Washington State	Subtotal	n/a	71
Colorado	Eby Creek Road/US 6 (Grand Avenue)	CO01-W	39
All Sites	Total Data Points	n/a	952
All Sites	Data Points with One or More Pedestrian Events	n/a	133
All Sites	Total Usable Data Points	n/a	819

Multilane Sites

This section summarizes the sites that yielded multilane data set for different multilane roundabout configurations. The data from sites with two entering lanes and two circulating lanes (hereafter 2x2 sites) are summarized in table 5; data from sites with two entering lanes and one circulating lane (hereafter 2x1 sites) are summarized in table 6; and data from sites with one entering lane and two circulating lanes (hereafter referred to as 1x2 site) are summarized in table 7. The data sample for the 1x2 sites is too small to use for model development. However, 711 minutes of usable data were obtained for the 2x2 case, representing 366 minutes of right-lane data and 345 minutes of left-lane data, and 519 minutes of usable data were obtained for the 2x1 case, representing 231 minutes of right-lane data and 288 minutes of left-lane data. This total of 1,230 minutes of lane-specific data compares favorably to the NCHRP Report 572 study, where a total of 383 minutes of approach data and 473 minutes of lane-specific data were collected.

Table 5. Summary of multilane 2x2 roundabout configuration data.

Subarea	Site	Site Code	Usable Data Points - Right Lane	Usable Data Points - Left Lane
Colorado	Golden Road/Johnson Road/16th Street	CO02-E	n/a	1
Colorado	Golden Road/Johnson Road/16th Street	CO02-S	1	1
Colorado	US 6/Avon Road/Village Road	CO10-W	n/a	4
Colorado	US 6/Avon Road/Village Road	CO10-E	0	15
Colorado	I-70 EB/Chamonix Road	CO49-E	2	n/a
Colorado	I-70 WB/Chamonix Road	CO50-S	1	n/a
Colorado	I-70 EB/Vail Road	CO51-N	70	73
Carmel, IN	126th Street/Hazel Dell Parkway	IN02-N	9	n/a
Carmel, IN	116th Street/Illinois Street	IN06-E	0	0
Carmel, IN	116th Street/Illinois Street	IN06-N	7	2
New York	SR 67 (Dunning Street)/US 9	NY06-S	23	20
New York	SR 67 (Dunning Street)/US 9	NY06-W	15	2
New York	SR 67 (Dunning Street)/US 9	NY06-E	5	0
New York	Lagrange Road (SR 85)/New Scotland Road	NY09-N	n/a	5
New York	Lagrange Road (SR 85)/New Scotland Road	NY09-E	23	0
New York	Lagrange Road (SR 85)/New Scotland Road	NY09-W	21	3
Vermont	SR 9/US 5	VT03-E	11	5
Vermont	SR 9/US 5	VT03-S	35	4
Vermont	SR 9/US 5	VT03-W	66	4
Washington State	164th Street/SR 522 NB Ramp/Tester Road	WA06-SW	4	2
Washington State	SR 16 NB/Burnham Drive NW/Borgen Blvd	WA09-SE	n/a	20
Washington State	14th Avenue/Jefferson Street	WA30-N	4	4
Washington State	14th Avenue/Jefferson Street	WA30-S	12	7
Washington State	14th Avenue/Jefferson Street	WA30-W	7	16
Washington State	4th Avenue/Olympic Street	WA31-E	48	21
Washington State	SR 16 SB/Burnham Drive NW	WA32-W	n/a	6
Washington State	SR 16 SB/Burnham Drive NW	WA32-N	2	130
All 2x2 Sites	Total Data Points	n/a	366	345

Table 6. Summary of multilane 2x1 roundabout configuration data.

Subarea	Site	Site Code	Usable Data Points - Right Lane	Usable Data Points - Left Lane
Colorado	Eby Creek Road/US 6 (Grand Avenue)	CO01-N	1	0
Carmel, IN	126th Street/Hazel Dell Parkway	IN02-S	75	106
Carmel, IN	136th Street/Keystone Parkway SB	IN11-W	8	26
Washington State	SR 16 NB/Burnham Drive NW/Borgen Blvd	WA09-E	87	86
Washington State	14th Avenue/Jefferson Street	WA30-E	12	n/a
Washington State	4th Avenue/Olympic Street	WA31-S	29	60
Washington State	4th Avenue/Olympic Street	WA31-N	0	10
Virginia	SR 50/SR 15	VA01-S	19	n/a
All 2x1 Sites	Total Data Points	n/a	231	288

Table 7. Summary of multilane 1x2 roundabout configuration data.

Subarea	Site	Site Code	Usable Data Points
Virginia	SR 50/SR 15	VA01-W	37
Virginia	SR 50/SR 15	VA01-E	7
All 1x2 Sites	Total Data Points	n/a	44

DATA COLLECTION AND REDUCTION

The data set consists of one-minute bins, as described in the following section, of data defined by one of two criteria: a minimum queue or a maximum move-up time. The minimum queue criterion requires an observed standing queue for a full minute. A standing queue is defined as at least two vehicles in queue (i.e., at least one vehicle behind the vehicle at the yield line). Because the back of queue is not always visible in the video and therefore was not coded for some sites, a second criterion, maximum move-up time, was used to identify data points that most likely represented queued conditions (including rolling queues).

Figure 14 displays an example of a camera angle where the back of the queue is not clearly visible and could not be accurately recorded. Figure 15 displays two images of a rolling vehicle queue take eight seconds apart (note the red sport utility vehicle as a common element in both images). No conflicting vehicles are present during this time period and no vehicles in the rolling queue stop before entering the roundabout. The rolling queues clearly represent conditions near saturation but would not be captured using a minimum queue criterion. These represent an important set of data for low conflicting flows.



Figure 14. Image. Example of nonvisible back of queue.

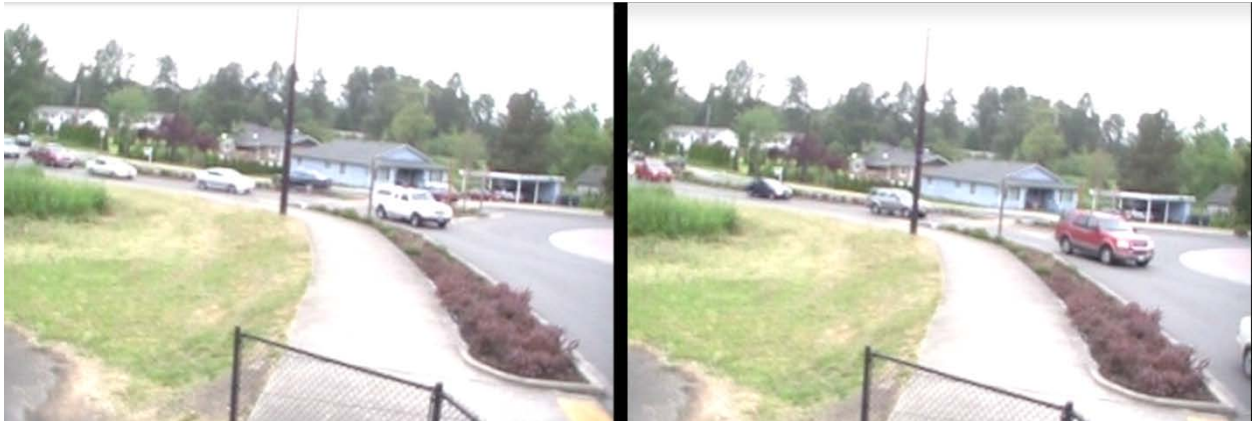


Figure 15. Image. Example of rolling queues.

A maximum move-up time of six seconds was used to identify valid data points. If the time interval between each vehicle departing from and the next vehicle arriving at the yield line was six seconds or less for a full minute, the data point was considered valid for the maximum move-up time data set.

Table 8 shows an example of the one-minute data bins that were developed from a single lane site. The data binning was executed by importing the raw, time-stamped event codes into a spreadsheet. A macro routine within the spreadsheet evaluated each arrival time code to determine if one of the two criteria (i.e., a queue of at least two vehicles or a move-up time of six seconds or less) was met. The spreadsheet considered each of the two criteria independently. If one of the criteria was met, the routine continued to look down the data set until a full minute had elapsed between the original arrival event and the last arrival event that constituted a full minute of valid data.

Once a full minute had elapsed, a bin of data was created. The number of entering and circulating events associated with this bin, inclusive of those circulating and entering events associated with the last arrival event, was counted. For example, in table 8, the departure time of 12:02:56 is associated with the last arrival event of 12:02:47 and was therefore included in the entering vehicle count.

As shown in table 8, this method results in data bins that are at least a minute but vary in duration based on the actual arrival and departure times. The data bins were normalized by using the actual duration (e.g., 1.17 minutes) to calculate entering and circulating flow rates for the individual data bins.

Table 8. Example of data binning, where shaded rows representing arrival times of 12:01:46 to 12:02:47 are a valid one-minute data point.

Arrival Time	Departure Time	Move-up Time (s)
12:01:41	12:01:44	0.25
12:01:46	12:01:48	1.56
12:01:49	12:01:51	0.39
12:01:51	12:01:53	0.375
12:01:54	12:01:56	0.749
12:01:58	12:01:58	2.148
12:01:58	12:02:02	0.468
12:02:03	12:02:08	0.406
12:02:08	12:02:11	0.64
12:02:11	12:02:18	0.061
12:02:18	12:02:20	0.437
12:02:20	12:02:22	0.358
12:02:22	12:02:26	0.39
12:02:26	12:02:38	0.327
12:02:38	12:02:40	0.39
12:02:41	12:02:47	0.64
12:02:47	12:02:56	0.6
12:02:56	12:03:01	0.312

Multilane data was extracted in the same manner as above using a macro routine within a spreadsheet to first separate multilane data into left and right lane data sets.

Upon completing the two-day video collection for all sites, the research team pre-screened all video segments to ensure reduction of time periods with saturated conditions. The screened time periods were then reduced to extract time stamps. Table 9 lists the events and respective codes used to reduce single-lane roundabout data. The shaded rows (5, 6, 13, 14, 15 and 16) represent those codes that have a direct input in calculating the maximum move-up times. The codes for multilane roundabout data accounts for multiple entry and circulating lanes, but is otherwise consistent with single-lane roundabout codes.

For all sites, pedestrian events were recorded for the purpose of identifying minutes of data that might be influenced by pedestrian activity. Any minutes of data that included pedestrian events were excluded from the analysis.

Table 9. Example of coded events, where coded events (5, 6, 13-16) are shaded.

Code	Event Name
1	Entry Leg: Pedestrian Arrival
2	Entry Leg: Pedestrian Enters Crosswalk
3	Entry Leg: Pedestrian Completes Crossing
4	Exit Leg: Pedestrian Enters Crossing
5	Right Lane: Circulating Vehicle
6	Right Lane: Exiting Vehicle
7	Bypass Lane: Entering Vehicle Position 1
8	Bypass Lane: Entering Vehicle Departure
9	Exit Leg: Pedestrian Arrival
10	Exit Leg: Pedestrian Completes Crossing
11	Next vehicle is a heavy (1 press indicates that a Position 1 + Departure are both heavy movements)
12	Next vehicle is a bicycle (1 press indicates that a Position 1 + Departure are both bike movements)
13	Right Lane: Entering Vehicle Departure (Right Turn) - Indicates most recent right lane departure was a right turn
14	Right Lane: Entering Vehicle Back of Queue
15	Right Lane: Entering Vehicle Departure (Through)
16	Right Lane: Entering Vehicle Position 1

CHAPTER 4. PARAMETRIC ANALYSES

The model development for this project examined two key sets of potential parameters for use in model descriptions: driver behavior parameters, including critical headway and follow-up headway, and geometric parameters. These are discussed further in the following sections.

CRITICAL HEADWAY

Per the HCM 2010, the critical headway, t_c , is defined as “The minimum headway in the major traffic stream that will allow the entry of one minor-street vehicle.”⁽²⁾ In theory, the driver rejects any headway within the circulating stream that is less than the critical headway and accepts any such headway greater than the critical headway. As such, the largest rejected headway will be less than the critical headway, and all accepted headways will be greater than the critical headway. Such theory assumes that drivers’ behaviors are consistent and rational.

The critical headway was evaluated using the Maximum Likelihood Technique as was documented in NCHRP Report 572. In accordance with the critical headway methodology tested and recommended in NCHRP Report 572, only observations that contained a rejected gap were evaluated. The probabilistic distribution for the critical headways is assumed to be log-normal. Critical headway data were reduced only during periods of known or estimated queuing (based on a maximum move-up time of six seconds), making the data collection effort similar to that described as Method 3 in NCHRP Report 572.

Single-Lane Critical Headway

Table 10 lists the critical headways for single-lane sites. The critical headways vary between 3.3 s and 6.5 s with a weighted average of 4.7 s and a standard deviation of 1.6 s. Some sites have fewer than 100 critical headway observations. While the average critical headway of these sites may change with a larger sample size, the result is indicative of the average behavior of the site during those minutes when queuing was observed.

Table 10. Critical headway estimates for single-lane sites.

Site	Number of Observations, n	Mean	Std. Dev.
CO01-W	15	6.5	3.4
IN07-E	52	4.5	2
IN07-S	5	4	1.5
IN08-N	50	4.3	1.3
IN09-S	93	3.5	1.5
IN09-W	203	3.6	1
IN10-E	10	3.7	2.3
IN10-N	85	3.8	1
IN10-W	51	3.3	1.8
IN12-E	67	4	1
NY07-E	272	4.8	1.4
NY07-N	263	5	1.4
NY07-S	273	5.1	1.5
NY07-W	768	4.6	1.7
NY08-N	51	5.5	1.9
NY08-W	102	4.9	1
WA04-E	65	5.1	1.9
WA04-N	299	5.6	2.2
WA34-E	18	5.6	2
Total	2,742	n/a	n/a
Average	n/a	4.7	1.6

Multilane Critical Headway

For a multilane roundabout, the critical headway was calculated in a similar way to single-lane roundabouts, and is consistent with the NCHRP Report 572 methodology. For multilane roundabouts, this method combines circulating volumes into a single conflicting stream. For each entry lane, this methodology assumes that all conflicting vehicles have an influence on the entering driver's behavior, which will be true in some cases and generally conservative.

Table 11 lists the critical headways for multilane sites by roundabout lane configuration and entry lane, with a summary provided in table 12. Some sites have fewer than 50 critical headway observations. While the average critical headway of these sites may change with a larger sample size, the result is indicative of the average behavior of the site during those minutes when queuing was observed.

Table 11. Results for critical headways in multilane roundabouts.

Site	Configuration	Entry Lane	Number of Observations, n	Mean	Std. Dev.
IN02-N	2x2	right	174	5.5	2.1
IN06-N	2x2	right	23	4.1	1.4
NY06-N	2x2	right	99	4.9	1.3
NY06-W	2x2	right	408	4.5	1.6
NY09-W	2x2	right	157	4.3	1.2
VT03-E	2x2	right	153	5	1.6
VT03-S	2x2	right	251	4.6	1.6
VT03-W	2x2	right	573	5.4	2.3
WA06-SW	2x2	right	72	4.1	1.4
WA09-N	2x2	right	59	4.2	1.4
WA09-SE	2x2	right	228	4.5	2
WA09-SW	2x2	right	78	4.4	1.2
WA30-S	2x2	right	214	3.8	1.6
WA30-W	2x2	right	130	5	1.4
WA31-E	2x2	right	227	4.5	1.1
WA32-N	2x2	right	184	4	1.8
CO10-S	2x2	right	66	5.1	1.5
CO49-E	2x2	right	76	8.6	4.4
CO50-E2	2x2	right	56	6	1.1
CO51-N	2x2	right	12	12.9	6.5
CO51-S	2x2	right	88	5.6	2.5
CO51-W	2x2	right	72	5.1	2.1
Total	2x2	right	3,400	n/a	n/a
Average	2x2	right	n/a	4.9	1.8
IN02-N	2x2	left	207	5.2	1
IN06-E	2x2	left	2	4	0.4
IN06-N	2x2	left	79	11.1	12
NY09-W	2x2	left	121	4.4	0.9
VT03-E	2x2	left	118	5.8	1.8
VT03-S	2x2	left	125	6.1	1.7
VT03-W	2x2	left	437	5.1	2.1
WA06-SW	2x2	left	53	4.8	2.2
WA09-N	2x2	left	88	4.4	1.4
WA09-SE	2x2	left	143	4.7	2.3
WA09-SW	2x2	left	113	4.6	1.1
WA30-S	2x2	left	35	4.5	1.4
WA30-W	2x2	left	142	5.2	1.3
WA31-E	2x2	left	181	5.3	2
WA32-N	2x2	left	309	4.9	2.6
CO01-N	2x2	left	65	4.9	2.5
CO10-S	2x2	left	50	5.6	1.9

Site	Configuration	Entry Lane	Number of Observations, n	Mean	Std. Dev.
CO10-W	2x2	left	53	6.5	2.5
CO49-E	2x2	left	87	8.3	3
CO51-N	2x2	left	12	13.2	3.8
CO51-S	2x2	left	51	6.3	2.1
C051-W	2x2	left	32	4.8	1.7
Total	2x2	left	2,503	n/a	n/a
Average	2x2	left	n/a	5.5	2.2
VA01-S	2x1	right	193	5	1.2
IN02-S	2x1	right	327	4.4	1.2
IN11-W	2x1	right	74	3.8	1
WA09-E	2x1	right	505	4.2	1.3
WA30-E	2x1	right	11	4.9	2.8
WA31-N	2x1	right	42	6.1	0.6
WA31-S	2x1	right	168	4	0.9
CO01-N	2x1	right	128	4.2	4.2
Total	2x1	right	1,448	n/a	n/a
Average	2x1	right	n/a	4.3	1.5
VA01-S	2x1	left	53	4.6	0.9
IN02-S	2x1	left	366	4.6	1.1
IN11-W	2x1	left	77	4.2	1.1
WA09-E	2x1	left	448	4.5	1.1
WA31-N	2x1	left	85	6.6	2.2
WA31-S	2x1	left	99	4.1	0.8
Total	2x1	left	1,128	n/a	n/a
Average	2x1	left	n/a	4.6	1.1
VA01-W	1x2	n/a	260	5.3	1.8
VA01-E	1x2	n/a	185	4.9	1
Total	1x2	n/a	445	n/a	n/a
Average	1x2	n/a	n/a	5.2	1.5

Table 12. Summary of results for critical headway in multilane roundabouts.

Lane configuration and entry lane	Range (s)	Weighted Average (s)
2x2, right lane	3.8-12.9	4.9
2x2, left lane	4.0-13.2	5.5
2x1, right lane	3.8-6.1	4.3
2x1, left lane	4.1-6.6	4.6
1x2	4.9-5.3	5.2

FOLLOW-UP TIME

Per the HCM 2010, the follow-up time, or follow-up headway, t_f , is defined as “the time between the departure of one vehicle from the minor street and the departure of the next vehicle using the same major-street headway, under a condition of continuous queuing on the minor street”.⁽²⁾ In addition, the follow-up headway methodology was further refined from the technique used for NCHRP Report 572 to exclude the effect of exiting vehicles. This was done by identifying and excluding any consecutive entering vehicle events with one or more intervening exiting vehicle events, even if there were no intervening conflicting vehicles. The resulting follow-up headway measurement is therefore a pure measurement of two consecutive entering vehicles with no intervening real or perceived conflicts.

Single-Lane Follow-Up Times

Table 13 lists the follow-up times for single-lane sites. The follow-up times vary between 1.7 s. and 3.0 s. with a weighted average of 2.6 s. and a standard deviation of 1.0 s.

Table 13. Follow-up time estimates for single-lane roundabout sites.

Site	Number of Observations, n	Mean	Std. Dev.
CO01-W	83	2.8	1
CO49-W2	4	2.9	0.9
IN07-E	40	2.5	1.1
IN07-S	38	2	0.8
IN08-N	69	1.7	0.7
IN09-E	433	2.9	1.3
IN09-S	136	2.2	1.1
IN09-W	192	2.3	0.7
IN10-E	189	2.1	0.8
IN10-N	26	2.2	0.9
IN10-W	49	2	0.6
IN12-E	45	1.9	0.9
NY07-E	243	2.9	1
NY07-NW	141	2.8	0.9
NY07-NE	115	3	1.1
NY07-S	271	2.9	1
NY07-W	327	2.7	1.1
NY08-N	37	2.4	0.6
NY08-W	296	2.5	0.8
WA04-E	251	2.4	0.9
WA04-N	369	2.9	1.1
WA33-E	71	2.2	0.8
WA33-W	14	2.2	0.7
WA34-E	140	2.4	0.8
WA34-N	20	2.8	0.8
WA35-E	23	2.4	1.1
Total	2,647	n/a	n/a
Average	n/a	2.6	1

Multilane Follow-Up Time

Table 14 lists the follow-up headways for multilane sites by roundabout lane configuration and entry lane.

Table 14. Follow-up time estimates for multilane roundabout sites.

Site	Configuration	Entry Lane	Number of Observations, n	Mean	Std. Dev.
CO02-E	2x2	right	8	2.7	0.8
CO10-S	2x2	right	27	2.5	0.9
CO10-W	2x2	right	5	4.1	1.7
CO49-E	2x2	right	26	3.1	0.9
CO50-E2	2x2	right	33	2.3	0.8
CO51-W1	2x2	right	33	3.1	1.4
CO51-N	2x2	right	20	2.6	1.5
CO51-S	2x2	right	22	2.7	1
NY06-E	2x2	right	44	2.6	1.2
NY06-N	2x2	right	72	2.6	1
NY06-W	2x2	right	235	2.5	1
NY09-W	2x2	right	114	2.2	0.8
VT03-E	2x2	right	51	2.8	1
VT03-S	2x2	right	346	2.3	1
VT03-W	2x2	right	324	2.8	1.2
WA06-SW	2x2	right	30	2.8	1.6
WA09-N	2x2	right	9	2.2	0.5
WA09-SE	2x2	right	4	2.3	0.5
WA09-SW	2x2	right	105	2.9	1.5
WA30-S	2x2	right	14	2.7	1.3
WA30-W	2x2	right	93	2.6	1.2
WA31-E	2x2	right	192	2.7	1
IN02-N	2x2	right	148	2	0.9
IN06-N	2x2	right	9	2	0.9
Total	2x2	right	1,964	n/a	n/a
Average	2x2	right	n/a	2.5	1
CO02-E	2x2	left	7	3.2	1.3
CO10-S	2x2	left	8	2.5	1
CO10-W	2x2	left	81	2.9	1.2
CO49-E	2x2	left	163	3	1.1
CO51-W1	2x2	left	8	2.5	0.8
CO51-N	2x2	left	2	1.6	0.9
CO51-S	2x2	left	13	2.7	1.1
NY06-E	2x2	left	10	3.7	2.3
NY06-N	2x2	left	57	3.3	1.6
NY06-W	2x2	left	279	3.4	1.7
NY09-W	2x2	left	71	2	0.7
VT03-E	2x2	left	33	2.6	1.3
VT03-S	2x2	left	110	2.1	0.9
VT03-W	2x2	left	57	2.4	0.8
WA06-SW	2x2	left	25	2.7	1.8

Site	Configuration	Entry Lane	Number of Observations, n	Mean	Std. Dev.
WA09-N	2x2	left	12	2.4	0.4
WA09-SE	2x2	left	28	2.5	1
WA09-SW	2x2	left	126	2.4	1
WA30-S	2x2	left	27	2.6	1
WA30-W	2x2	left	162	2.4	1
WA31-E	2x2	left	92	2.5	0.8
WA32-W	2x2	left	6	2.2	1
IN02-N	2x2	left	148	1.9	1
IN06-E	2x2	left	36	3.2	1.8
IN06-N	2x2	left	2	3.2	0.7
Total	2x2	left	1,563	n/a	n/a
Average	2x2	left	n/a	2.7	1.2
VA01-S	2x1	right	215	2.3	0.9
CO01-N	2x1	right	79	2.8	1.2
WA09-E	2x1	right	188	2.4	0.8
WA30-E	2x1	right	16	2.4	0.6
WA31-N	2x1	right	52	2.4	0.7
WA31-S	2x1	right	96	2.5	1.1
IN02-S	2x1	right	214	2	0.8
IN11-W	2x1	right	26	2.2	0.6
Total	2x1	right	886	n/a	n/a
Average	2x1	right	n/a	2.3	0.9
VA01-S	2x1	left	11	1.5	0.7
CO01-N	2x1	left	19	2.3	0.8
WA09-E	2x1	left	263	2.2	0.6
WA30-E	2x1	left	2	2.9	0.1
WA31-N	2x1	left	357	2.2	0.5
IN02-S	2x1	left	271	1.8	0.6
IN11-W	2x1	left	25	2.2	0.4
Total	2x1	left	948	n/a	n/a
Average	2x1	left	n/a	2.1	0.6
VA01-W	1x2	n/a	221	2.5	0.8
VA01-E	1x2	n/a	91	2.5	0.9
Total	1x2	n/a	318	n/a	n/a
Average	1x2	n/a	n/a	2.5	0.9

GEOMETRIC PARAMETRIC ANALYSIS

For predictive purposes, it would be desirable to determine whether follow-up time, in particular, can be predicted using geometric parameters. The following geometric parameters were examined for their relationship to follow-up time: inscribed circle diameter, entry lane width (equal to entry width divided by the number of lanes), entry angle, and splitter island width. The correlations between follow-up headway and each of these parameters is presented in table 15.

The correlations observed in table 15 are generally not significant, as can be seen in the correlation and coefficient of determination (R^2) calculations.

Table 15. Results of the geometric parameter correlation analysis

Geometric Parameter	Correlation to Follow-up Time t_f	Coefficient of Determination R^2
Inscribed Circle Diameter (ft)	-0.051	0.0026
Average Lane Width (ft)	-0.186	0.0345
Entry Angle (degree)	0.242	0.0586
Splitter Island Width (ft)	-0.158	0.025

Follow-up time is plotted against each of these geometric parameters in figure 16 through figure 19 in the order in which they are listed in table 15.

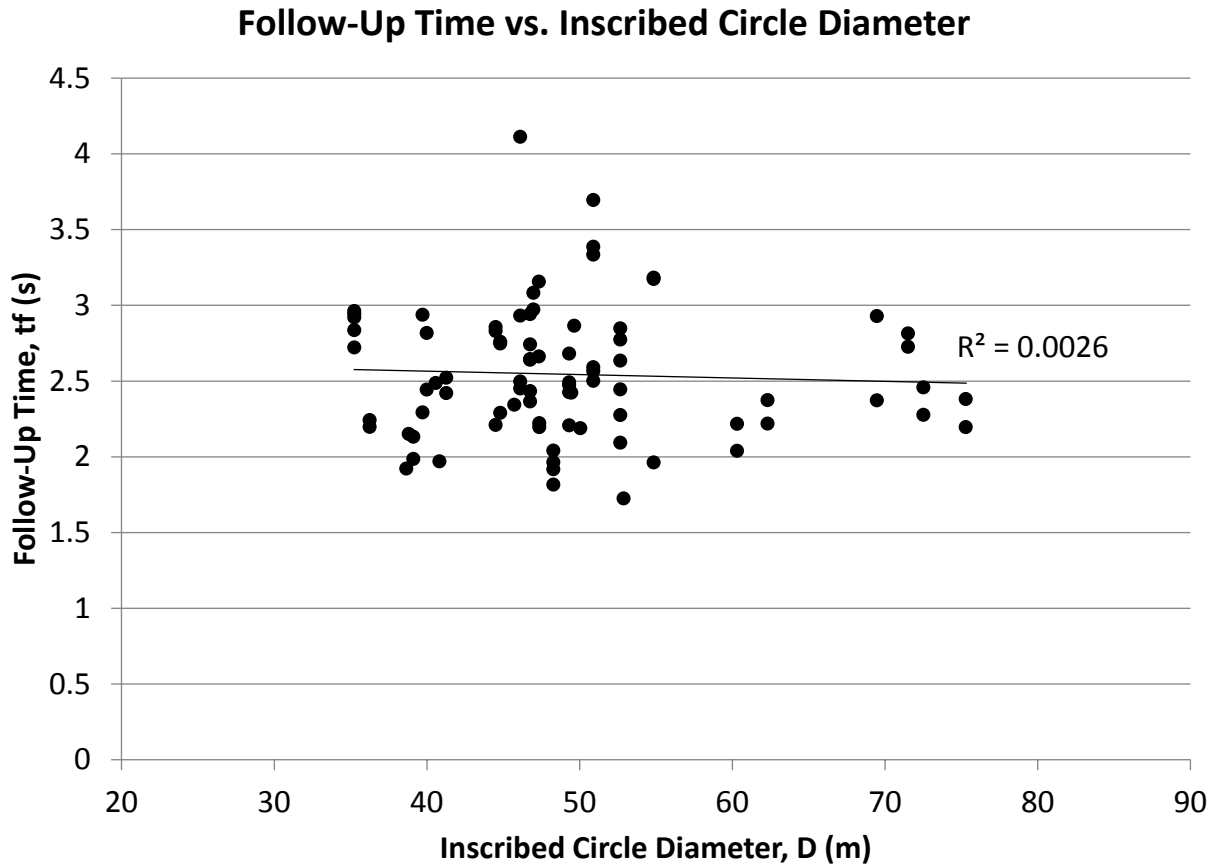
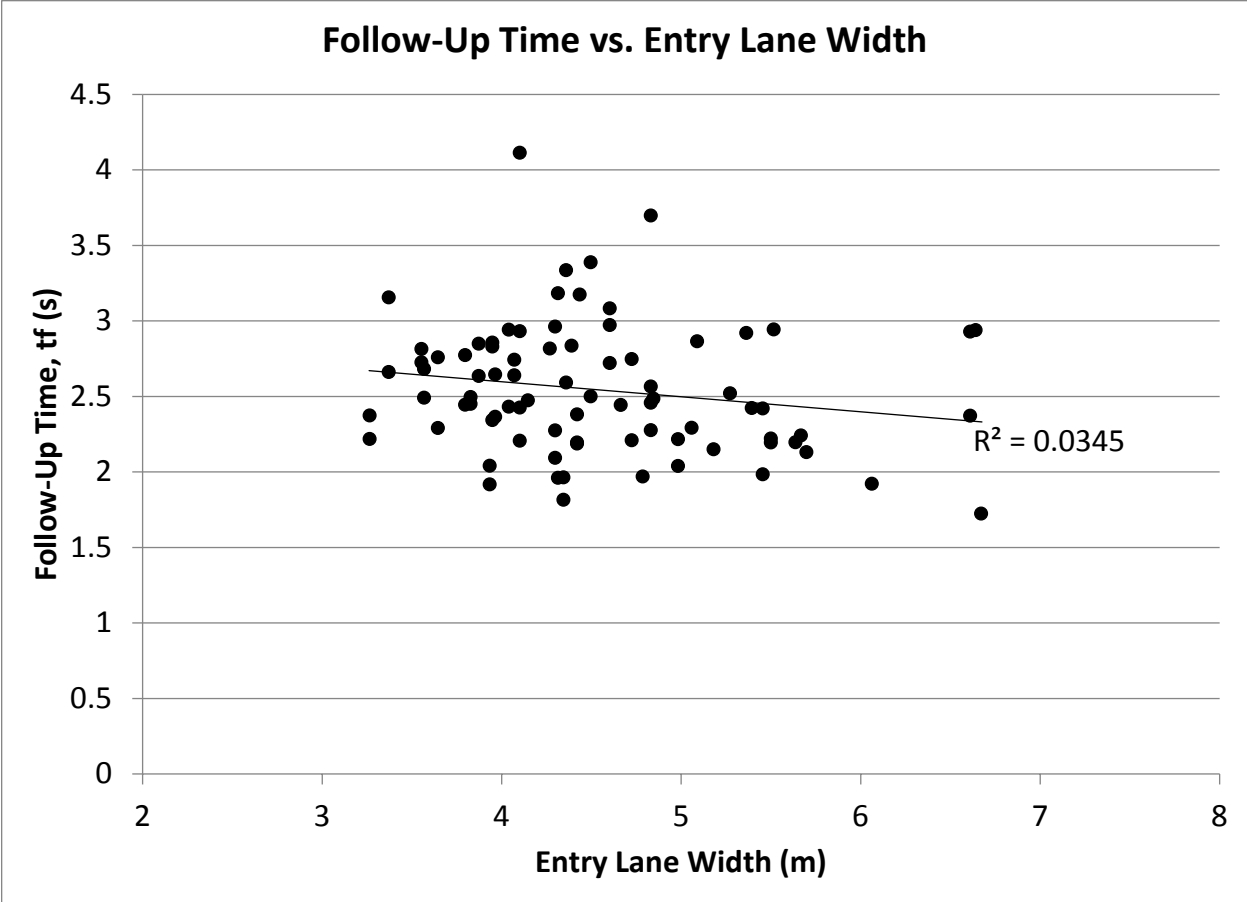


Figure 16. Scatter Plot. Follow-up time vs. inscribed circle diameter.



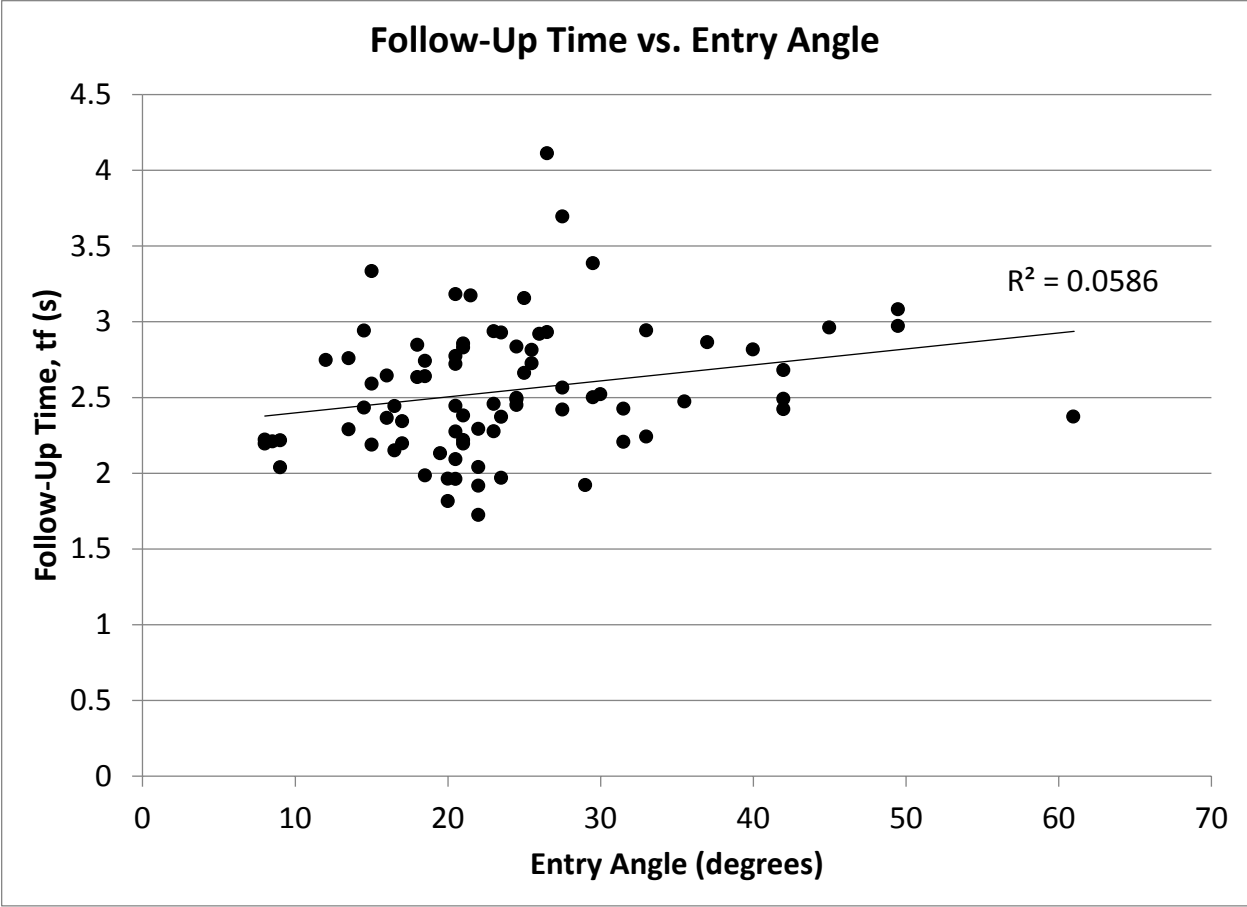


Figure 18. Scatter Plot. Follow-up time vs. entry angle.

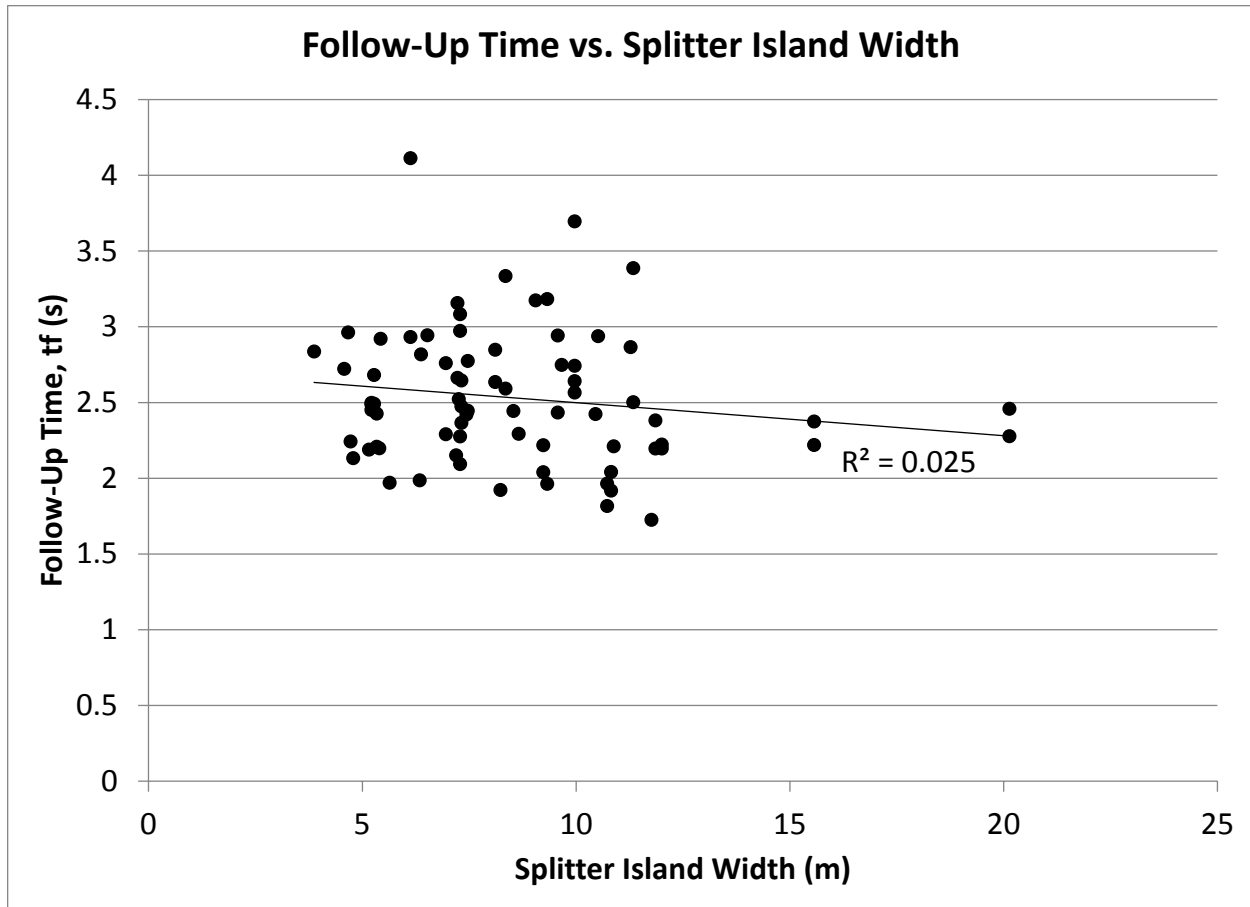


Figure 19. Scatter Plot. Follow-up time vs. splitter island width.

In reviewing the figures and correlation table, a number of observations can be made. First, each of the geometric parameters tested in this study trends in the direction that is intuitively expected. Increases in inscribed circle diameter, entry lane width, and splitter island width cause a decrease in follow-up time and thus an increase in capacity. Conversely, an increase in entry angle causes an increase in follow-up time and thus a decrease in capacity.

Second, entry angle shows the strongest correlation of any of the geometric parameters. However, the magnitude of the correlation is relatively weak (0.24), and the R^2 value is very small (<0.06). As can be seen visually, there is significantly more variation in the observed follow-up time for a given entry angle than there is in the mean follow-up time over the range of observed entry angles. This indicates that while entry angle may have some effect on follow-up time, the unexplained variation from site to site (presumed to be from driver behavior) is more dominant.

Last, it may be possible to derive geometric effects on capacity if a baseline value of follow-up time is known, as in through localized calibration. This level of detailed analysis was not explored further, however, because it does not appear to improve the quality of the fit of the model in predicting capacity across all sites. The variations from site to site appear to make it unlikely that the base value of follow-up time could be predicted accurately enough for the additional precision of geometric fine-tuning to be significant.

Based on these observations and given the constraints of budget and schedule, geometric parameters were not pursued further in this study. Further research in these areas is recommended to determine whether modeling power can be increased with their inclusion.

CHAPTER 5. MODEL DEVELOPMENT

To develop the model for this project, the team followed the below general steps:

- Assessed the fit of the HCM 2010 models to the new set of data.
- Developed new regression models fitted to the data.
- Explored calibration of models to localized driver behavior and/or geometric parameters.
- Verified the form of regression model—exponential or linear.
- Evaluated the effects of exiting vehicles on entry capacity.
- Analyzed capacity trends over time.

The following sections discuss these steps in more detail.

ASSESSMENT OF HCM 2010 MODEL

Single-Lane Model

The single-lane data were compared to the existing HCM 2010 capacity model using the root-mean-square error (RMSE) as the primary goodness-of-fit measurement, consistent with the methodology used in NCHRP Report 572. As seen in table 16, the RMSE for the HCM 2010 to the new data is 217, which is notably higher than the fit of the model reported in NCHRP Report 572 to the 2003 data.

Table 16. RMSE for data sets applied to the HCM 2010 model for single-lane roundabout sites.

HCM 2010 Model (from figure 14)	RMSE reported for NCHRP Report 572 Data Set	RMSE with TOPR 34 Data Set
$c_{e,pce} = 1130 \exp(-0.0010 * v_{c,pce})$	155	217

Figure 20 shows the HCM 2010 capacity model plotted against the data. Visual inspection of figure 20 demonstrates that the bulk of the observed data points lie above the HCM 2010 model, thus confirming that the HCM 2010 underpredicts observed capacity.

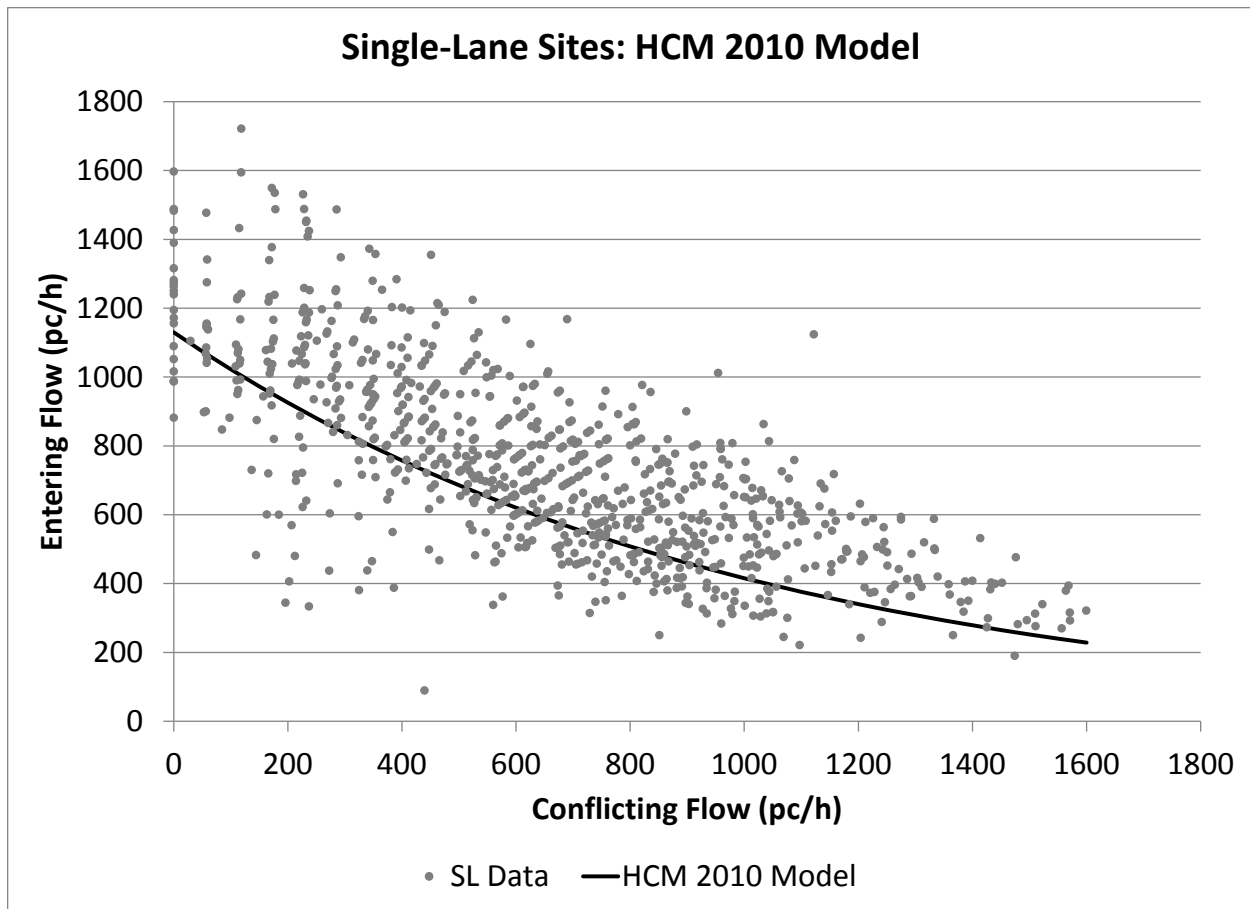


Figure 20. Scatter Plot. Assessment of HCM 2010 model for single-lane roundabout sites.

Multilane Models

Table 17 summarizes the RMSEs for each multilane configuration. Due to insufficient sample size, no comparison was made for the 1x2 configuration.

Table 17. RMSE for data sets applied to the HCM 2010 model for multilane roundabout sites.

HCM 2010 Model	RMSE reported for NCHRP Report 572 Data Set	RMSE with TOPR 34 Data Set
2x2 Right Lane: $v_e = 1130 \exp(-0.0007 v_c)$ (from figure 5)	145*	183
2x2 Left Lane: $v_e = 1130 \exp(-0.00075 v_c)$ (from figure 6)	N/A	218
2x1 Right Lane: $v_e = 1130 \exp(-0.0007 v_c)$ (from figure 5)	N/A	255
2x1 Left Lane: $v_e = 1130 \exp(-0.0007 v_c)$ (from figure 5)	N/A	224

Figure 21, figure 22, figure 23, and figure 24 show the HCM 2010 capacity models plotted against the data collected in this study for each roundabout configuration and entry lane in the order listed in table 17. The multilane capacity models in the HCM were developed using a combination of NCHRP Report 572 findings and post-NCHRP Report 572 analysis by the HCQS Committee in the development of HCM 2010. Note that the methodology used for NCHRP Report 572 focused on the critical lane of a two-lane approach, which in most cases was the right lane of a two-lane entry against two circulating lanes. The other cases included in the HCM 2010 were not directly reported in NCHRP Report 572.

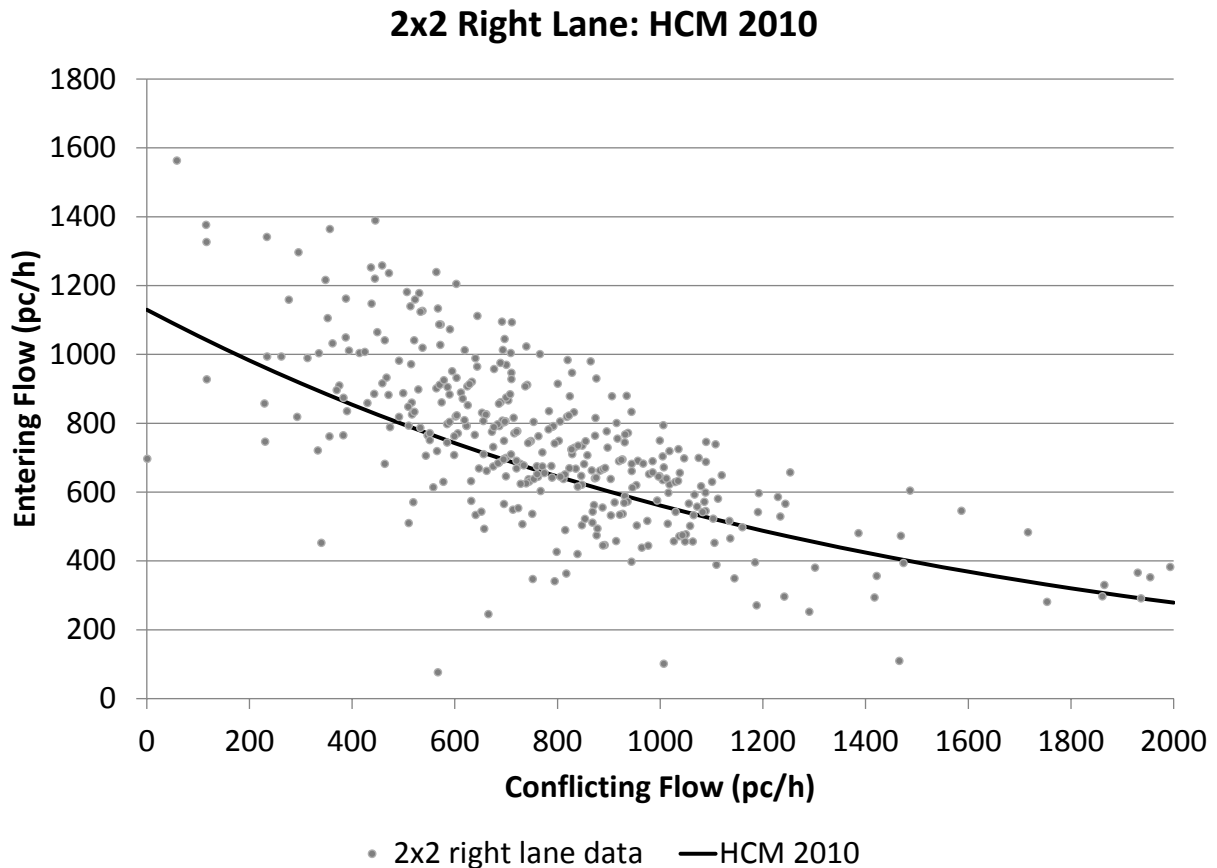


Figure 21. Scatter Plot. Assessment of HCM 2010 model for 2x2 multilane roundabout sites and right entry lane.

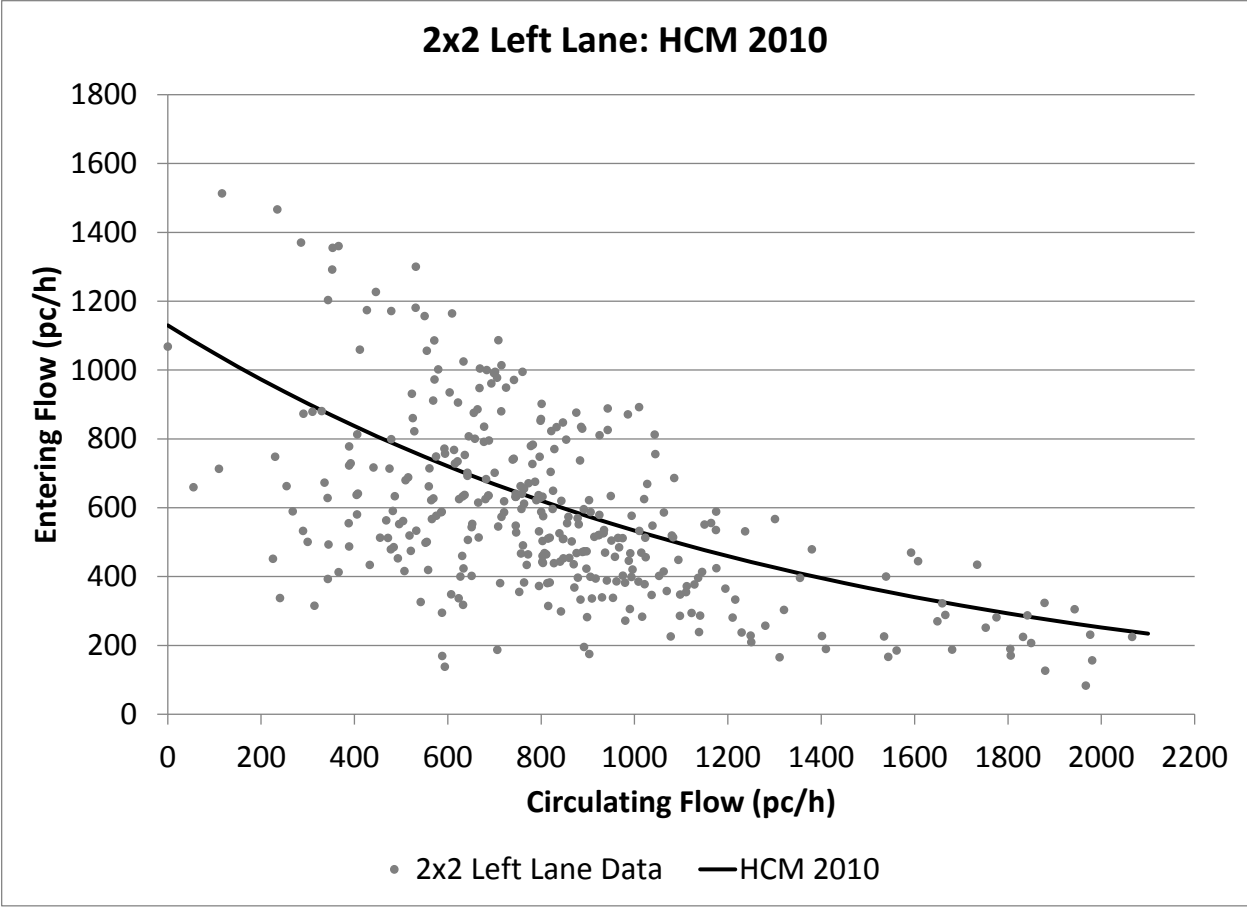


Figure 22. Scatter Plot. Assessment of HCM 2010 model for 2x2 multilane roundabout sites and left entry lane.

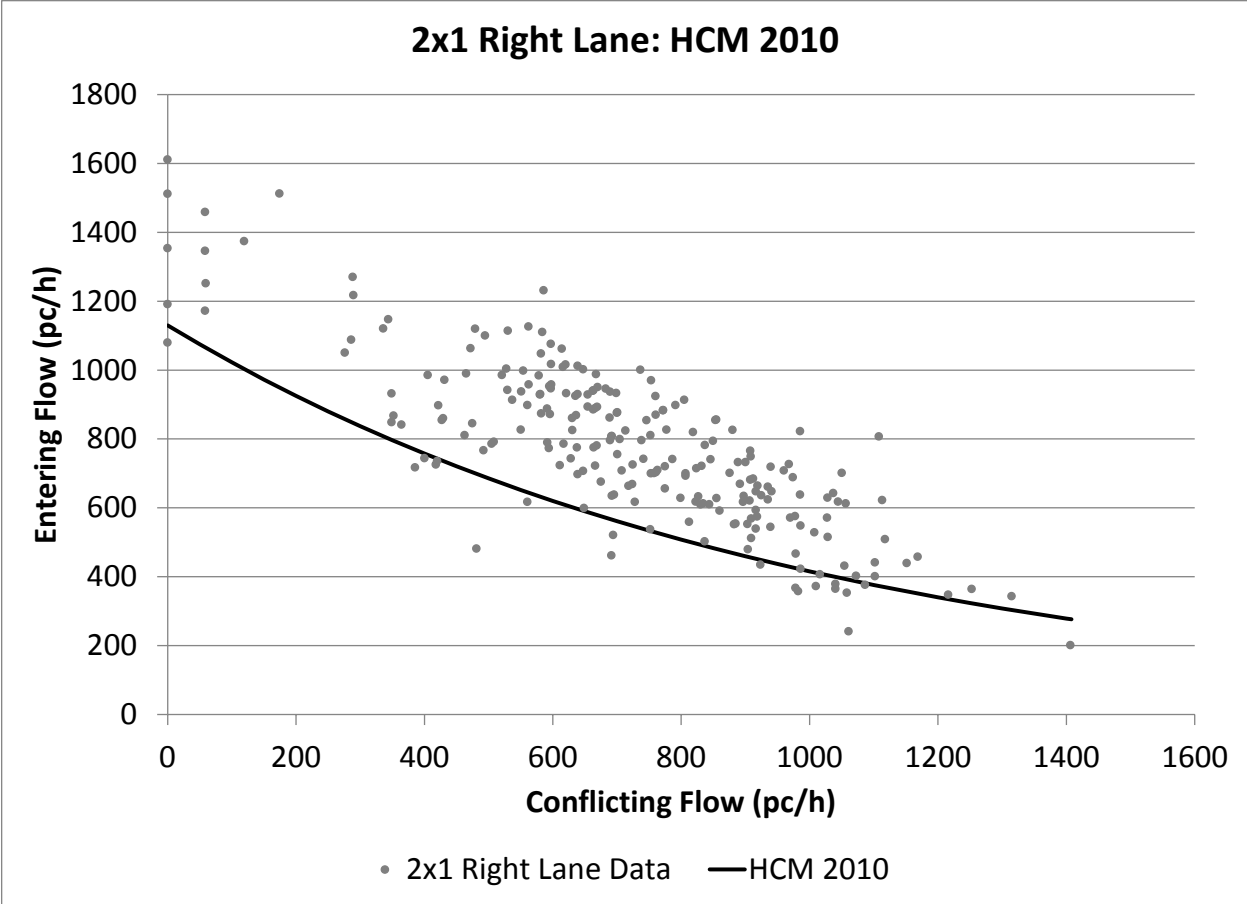


Figure 23. Scatter Plot. Assessment of HCM 2010 model for 2x1 multilane roundabout sites and right entry lane.

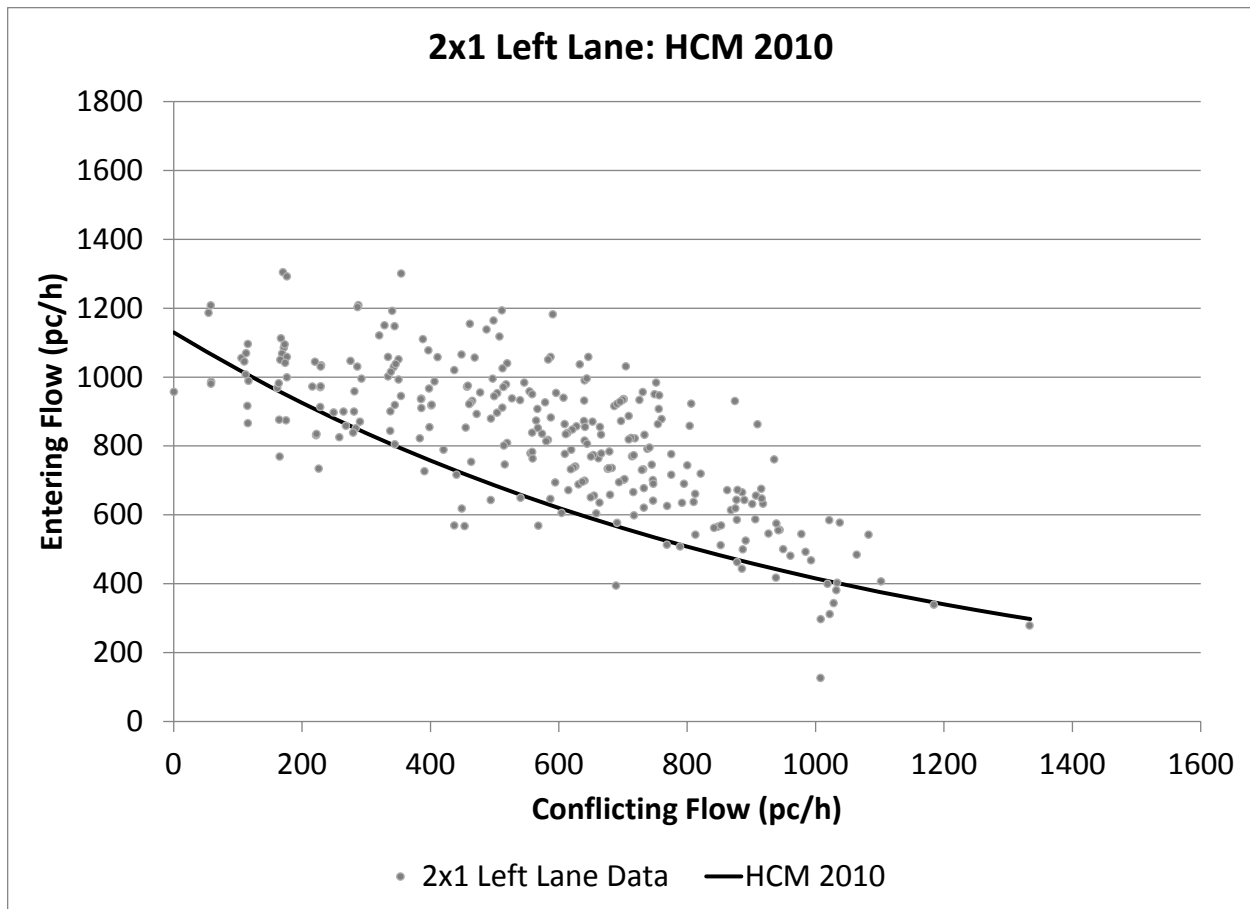


Figure 24. Scatter Plot. Assessment of HCM 2010 model for 2x1 multilane roundabout sites and left entry lane.

Visual inspection of the figures demonstrates that the HCM 2010 model for the right lane in the 2x2 case somewhat underpredicts the observed capacities and has the best RMSE of the four cases tested. Also, the HCM 2010 model for the left lane in the 2x2 case lies within the data, but the spread of data is considerable, leading to a higher RMSE. Finally, the HCM 2010 models for the 2x1 case significantly underpredict the observed capacities for both the right and left lanes, leading to the highest RMSEs of the cases tested.

DEVELOPMENT OF SINGLE-LANE MODELS

This section presents the development of single-lane models. The section presents regression, calibration, and localized modeling approaches, followed by a summary.

Regression

Linear and exponential regression models were developed using all single-lane data. Figure 25 shows these models plotted on the data. The regression analysis improves the fit of the capacity model considerably compared to the HCM 2010 model, with the exponential and linear models performing approximately the same (RMSE of 182 and 186, respectively). However, there is still considerable spread to the data, particularly for low circulatory flows.

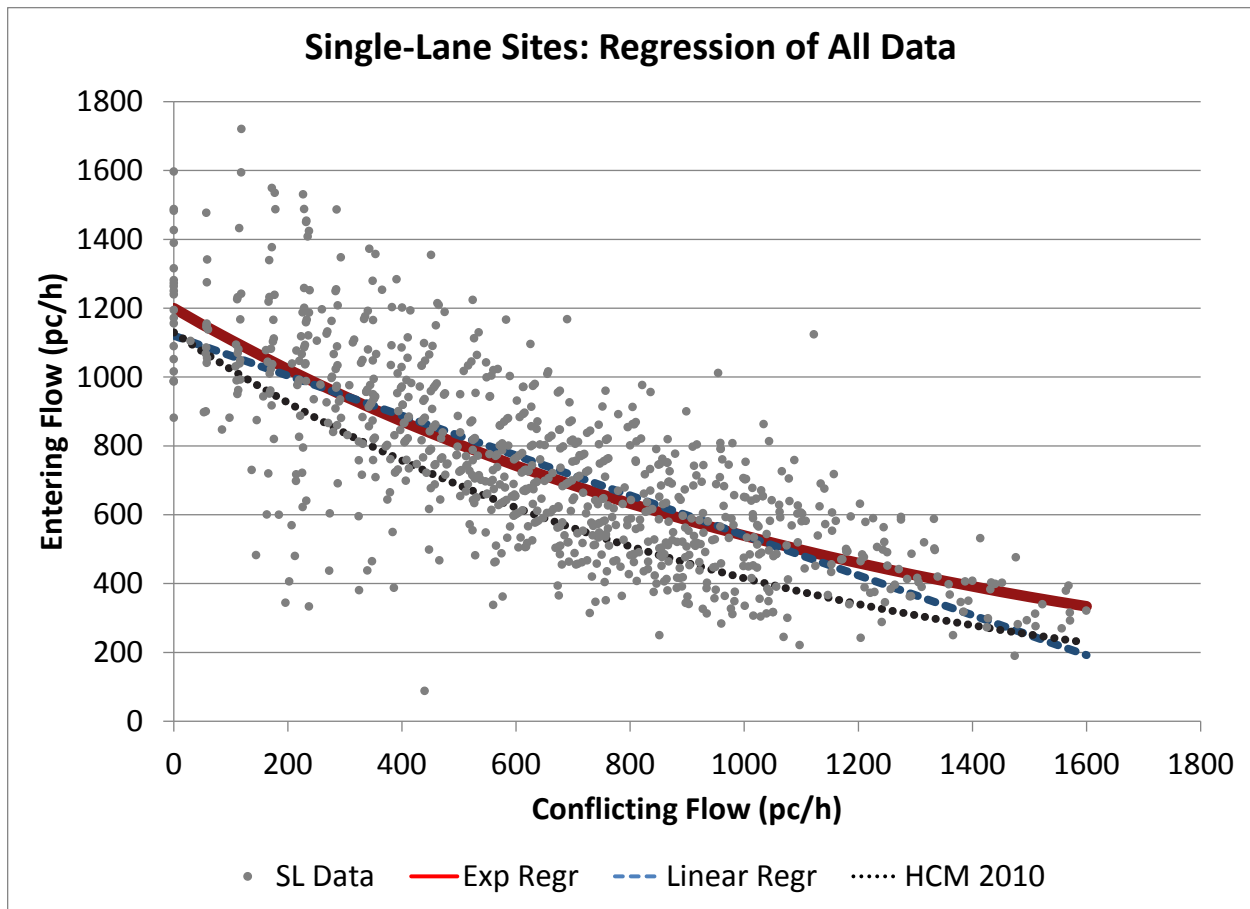


Figure 25. Scatter Plot. Regression models for single-lane roundabout sites.

Calibration

The generalized regression models shown previously are consistent in philosophy with those explored in NCHRP Report 572. However, it is desirable to determine whether a field-observable parameter can be used to anchor the regression models and thus enable their calibration to local conditions.

The primary field-observable parameter explored is the follow-up headway (t_f), which is directly related to the y-intercept as shown in figure 26.

$$A = 3600 / t_f$$

Figure 26. Equation. Follow-up headway as a field-observable parameter to calibrate the y-intercept.

Where $A = y\text{-intercept}$ and $t_f = \text{follow-up headway}$.

Using the data presented previously for follow-up time, a regression model was developed that fixes the y-intercept by the relationship above and allows the slope parameter to float to achieve the minimum RMSE. The resulting RMSE for the exponential model increases only slightly with

the fixed intercept, from 182 to 190; the resulting RMSE for the linear model increases more, from 186 to 223. As a result, the exponential model anchored to global follow-up time is a considerably better fit than its linear counterpart, as shown in figure 27.

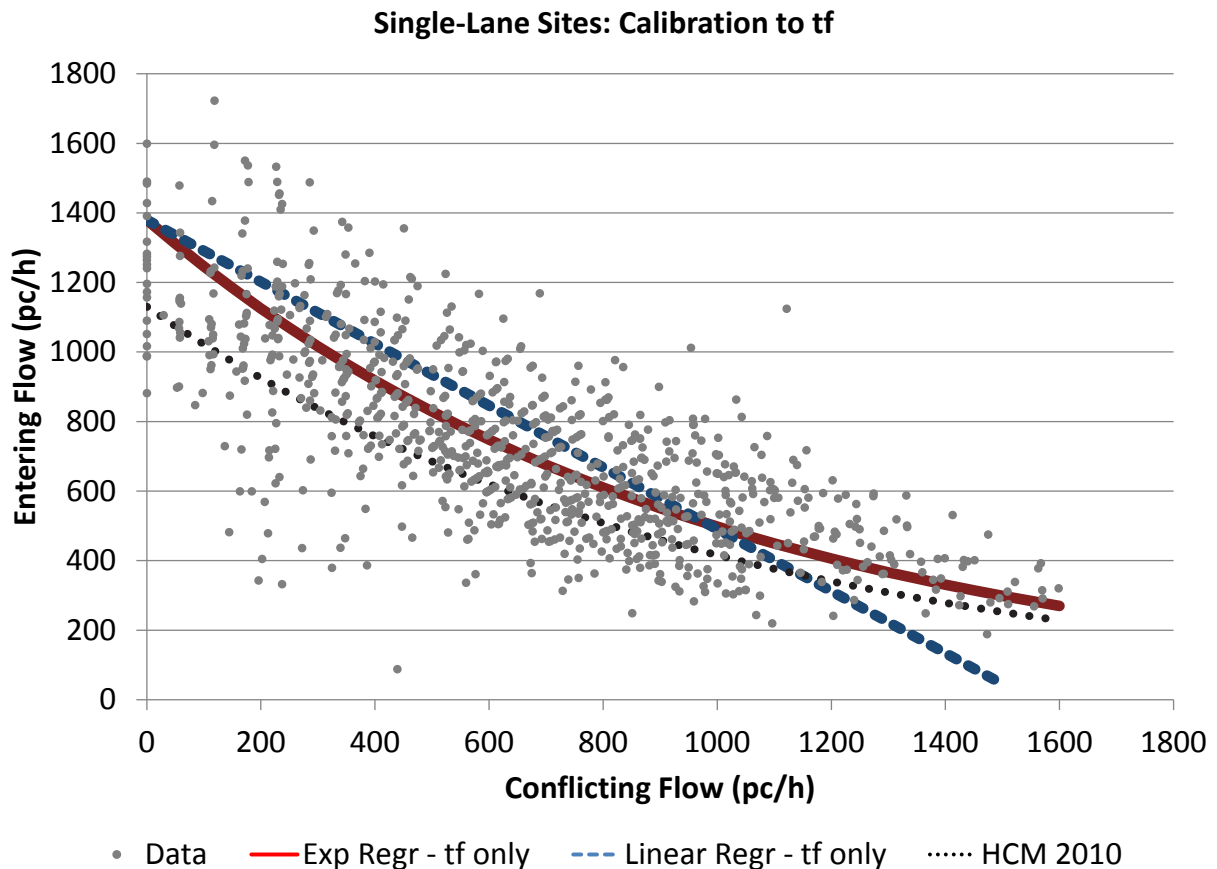


Figure 27. Scatter Plot. Regression models for single-lane roundabout sites with calibration to follow-up time.

In addition to using a global value of t_f to set the intercept, a second regression analysis was conducted using individual t_f values for each site. The best fit of the exponential model uses site-specific intercept values and a slope value of -0.00104 and results in a RMSE value of 171. This is shown graphically in figure 28, where the observed capacities are normalized by the calculated intercept for each site as the observed value of v_e divided by the result of 3600 divided by the measured t_f for that site.

As can be seen in figure 28, the normalization by follow-up time reduces the spread of the data around the model, with the data clustering more tightly around the model. This visually demonstrates that localized calibration to follow-up time improves the predictive fit of the model. The resulting RMSE of the normalized model is 0.115, which when multiplied by the mean follow-up time of 1380 results in an effective RMSE of 158. This numerically demonstrates a stronger fit when using localized calibration.

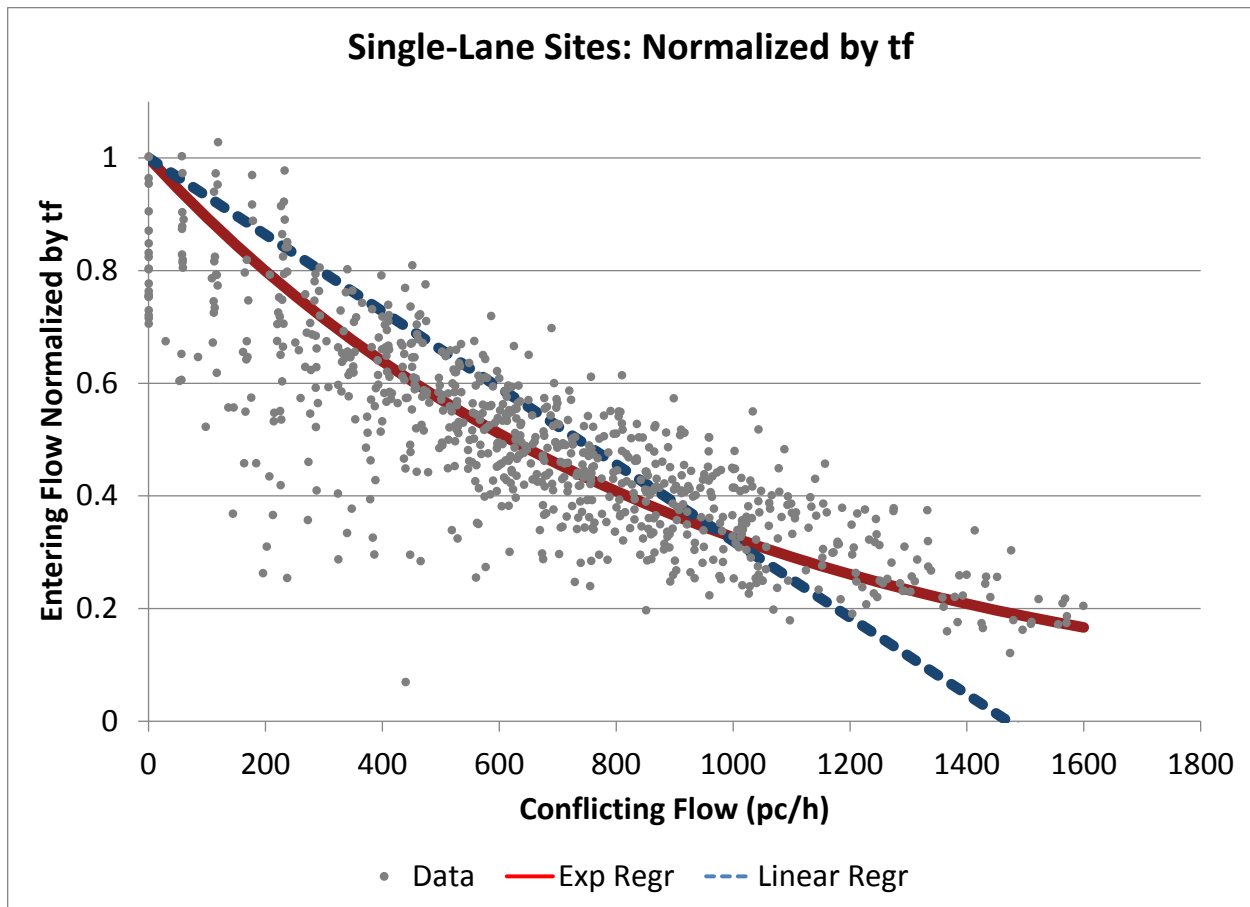


Figure 28. Scatter Plot. Regression models for single-lane roundabout sites, normalized by follow-up time.

A similar calibration was conducted using field-measured values for both follow-up time and critical headway, following the full procedure given in the HCM 2010, which applies only to the exponential model form (the Sieglösch model). The resulting model slightly increased the RMSE from 190 to 193. Due to these findings and prioritization of study resources, further use of critical headway for model calibration was not pursued further in this study.

Localized Regression

To further test the notion of localized modeling, a separate regression analysis was conducted for the subset of single-lane data from Carmel, IN. By inspection of the data by geographic area, it is evident that the Carmel sites exhibit a higher capacity than the other geographic subareas. Figure 29 and figure 30 are the equations for the revised exponential and linear models, respectively, and table 18 summarizes the results of these regression analyses.

$$v_e = 1380 \exp(-0.00081 * v_c)$$

Figure 29. Equation. Revised exponential model based on single-lane data from Carmel, IN.

$$v_e = 1270 - 0.64 * v_c$$

Figure 30. Equation. Revised linear model based on single-lane data from Carmel, IN.

Table 18. Regression analysis of the Carmel-based model.

Revised Model	Figure Number	Data Set	Model Method	RMSE for Carmel Data Only	RMSE for All Data
$v_e = 1380 \exp(-0.00081 * v_c)$	Figure 29	Best fit to Carmel sites only	Exponential	153	212
$v_e = 1270 - 0.64 * v_c$	Figure 30	Best fit to Carmel sites only	Linear	152	219

As can be seen from table 18, the fit of the revised Carmel models improves considerably when applied only to the Carmel data, in effect matching the goodness of fit (RMSE) of the original NCHRP Report 572 model to its data.

Figure 31 shows these models plotted against the Carmel data subset, with the full dataset included in the background.

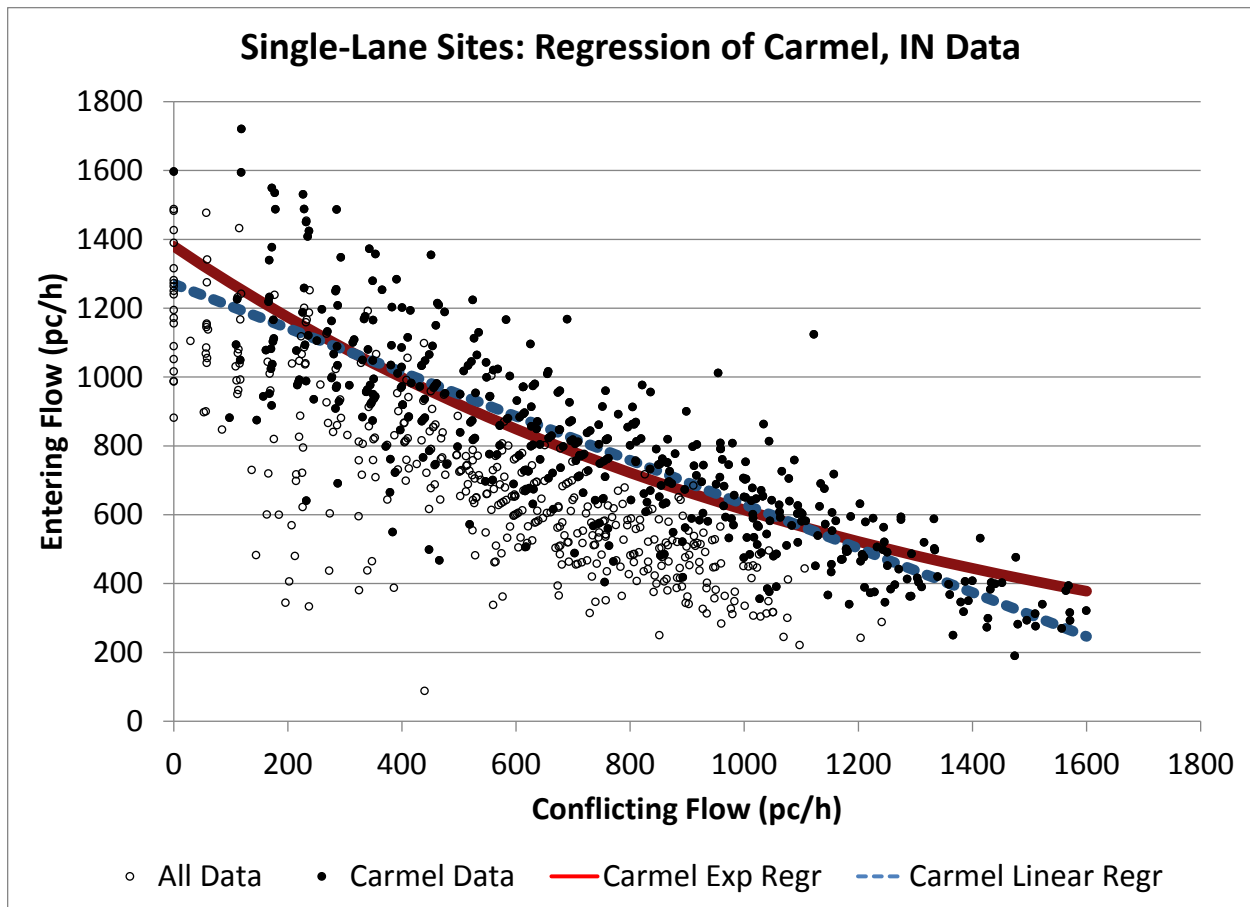


Figure 31. Scatter Plot. Regression models for Carmel, IN data.

When the Carmel model is applied to all sites, the goodness of fit degrades considerably. The intercept is considerably higher than for the regression to all data (for the exponential model, 1,380 for Carmel sites only versus 1,200 for all sites). The Carmel-specific model is clearly the best result for Carmel sites, but the generalized fit of the Carmel-specific model to national conditions is worse than other models explored.

Regression Model Form

The choice of model form—exponential or linear—has been of particular interest. To help clarify the choice of model, the data were sorted by conflicting flow, clustered into groups of 10 observations, and summarized by a series of group means of conflicting flow and entering flow for each cluster of 10 observations. The purpose for doing this is to reduce the variability inherent in one-minute observations and to see if a clear pattern emerges with respect to model form. These models of group means should not be used for actual predictions because they mask the variability of the data, but they are useful in providing indicators for model form.

Figure 32 presents the regression of group means for the entire set of single-lane data, and figure 33 and figure 34 present plots of predicted versus measured entering flow for the exponential and linear regression models, respectively. Both sets of regression model parameters were selected to minimize RMSE for their respective forms. The exponential group mean model has a RMSE of

72 and an R^2 of 0.95; the linear group mean model has a RMSE of 82 and a R^2 of 0.93. Visual inspection confirms what the RMSE and R^2 values indicate: the exponential model does a better job of matching the group mean data throughout the range, particularly with both low and high conflicting flows.

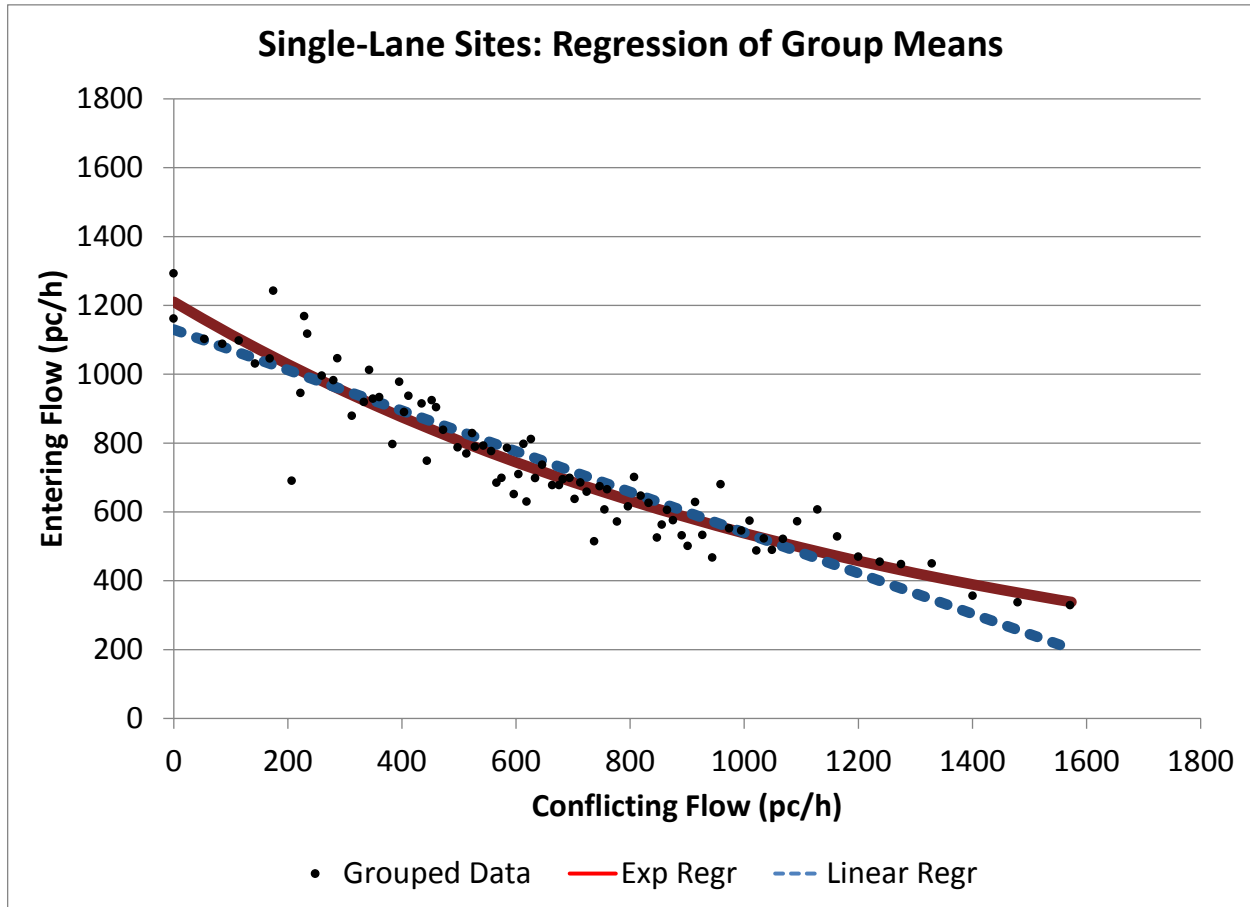


Figure 32. Scatter Plot. Regression of group means for single-lane sites.

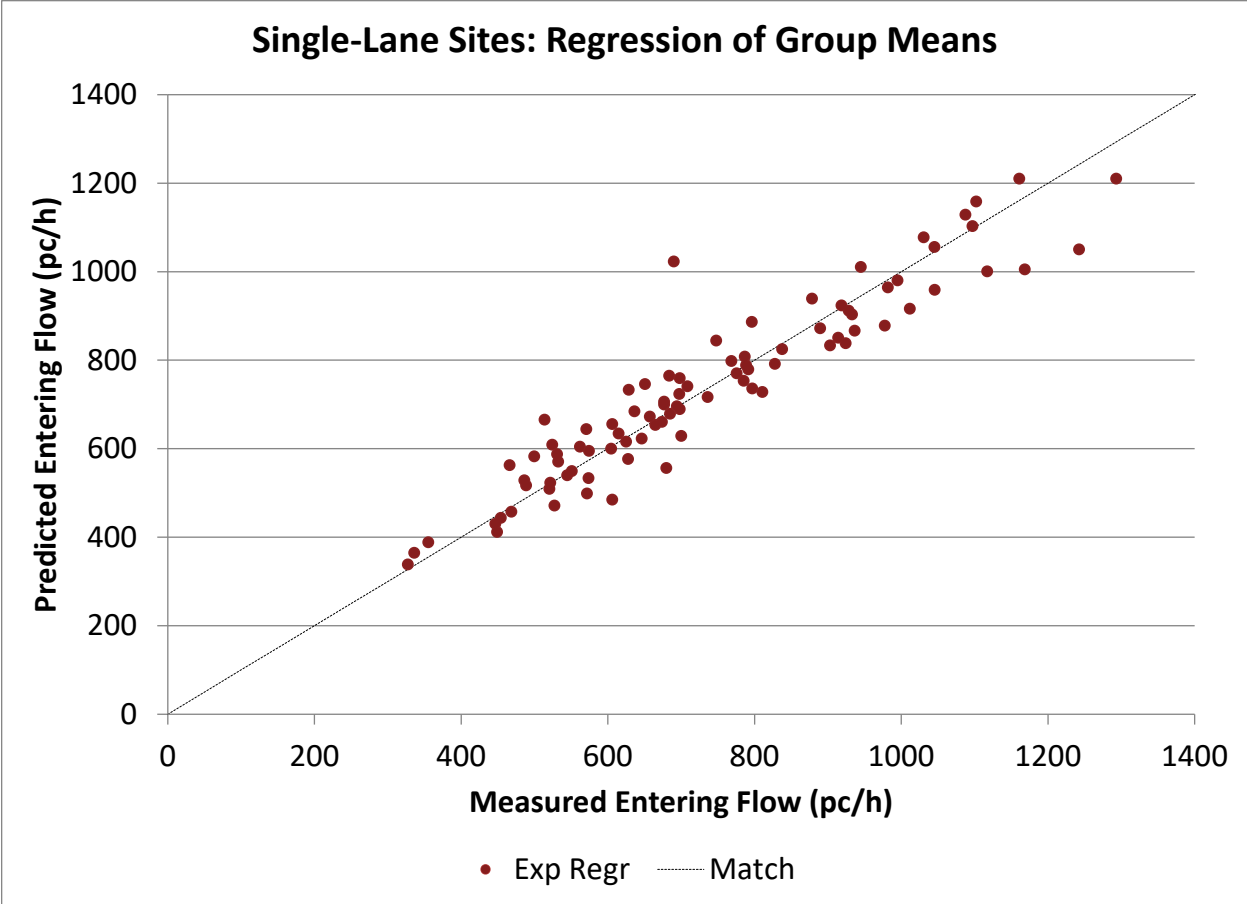


Figure 33. Scatter Plot. Exponential regression of group means, predicted vs. measured entering flow, for single-lane sites.

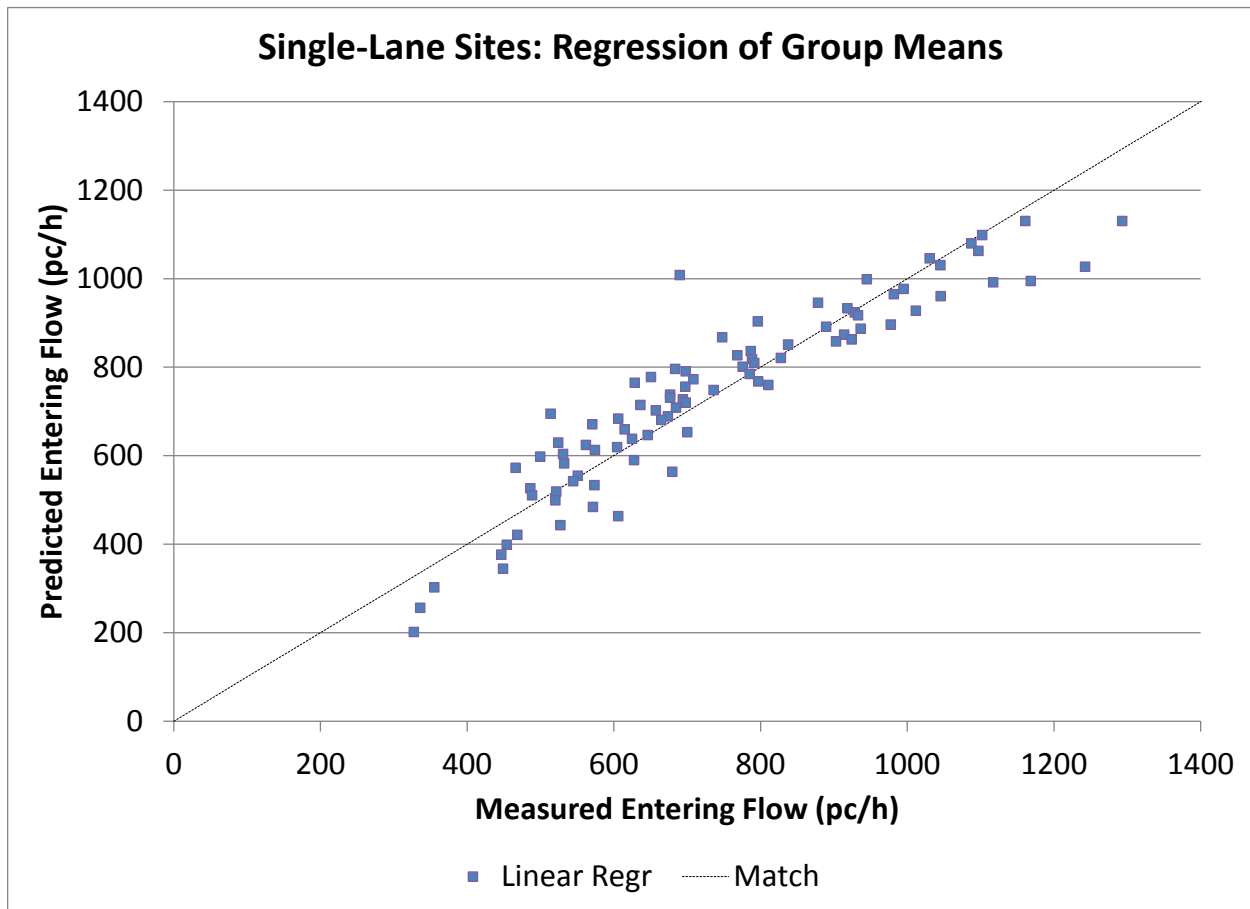


Figure 34. Scatter Plot. Linear regression of group means, predicted vs. measured entering flow for single-lane sites.

A slightly different set of observations emerge when one separates the single-lane sites into two groups—Carmel and non-Carmel, as shown in figure 35 and figure 36, respectively. For the Carmel sites, the exponential group mean model has a RMSE of 78 and an R^2 of 0.88; the linear group mean model has a RMSE of 67 and a R^2 of 0.91. For the non-Carmel sites, the exponential group mean model has a RMSE of 57 and an R^2 of 0.93; the linear group mean model has a RMSE of 61 and a R^2 of 0.92. Based on these observations, a linear regression model appears to fit the Carmel group mean data better than the exponential model, particularly at high conflicting flows. The exponential model performs slightly better for the non-Carmel group mean data.

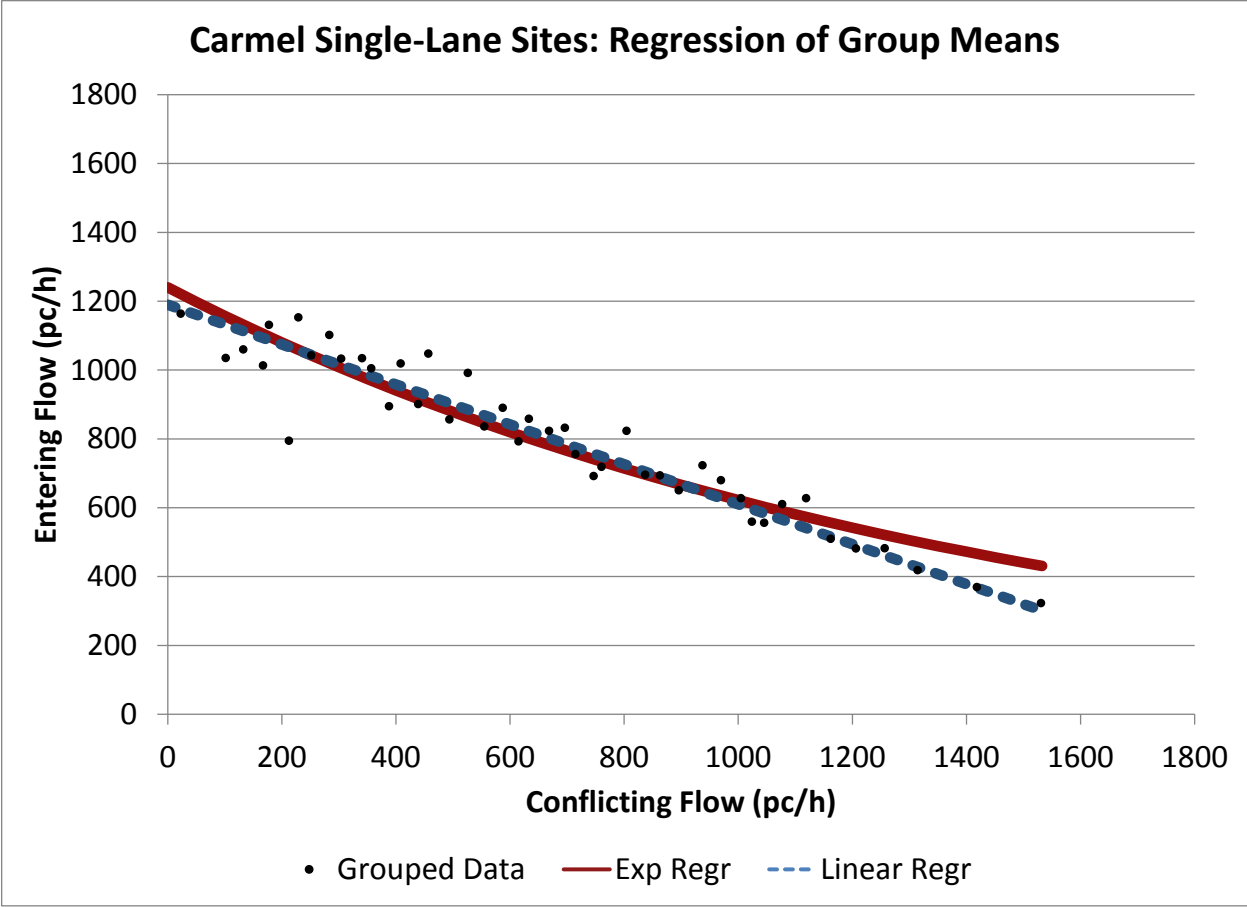


Figure 35. Scatter Plot. Regression of group means for Carmel-only single-lane roundabout sites.

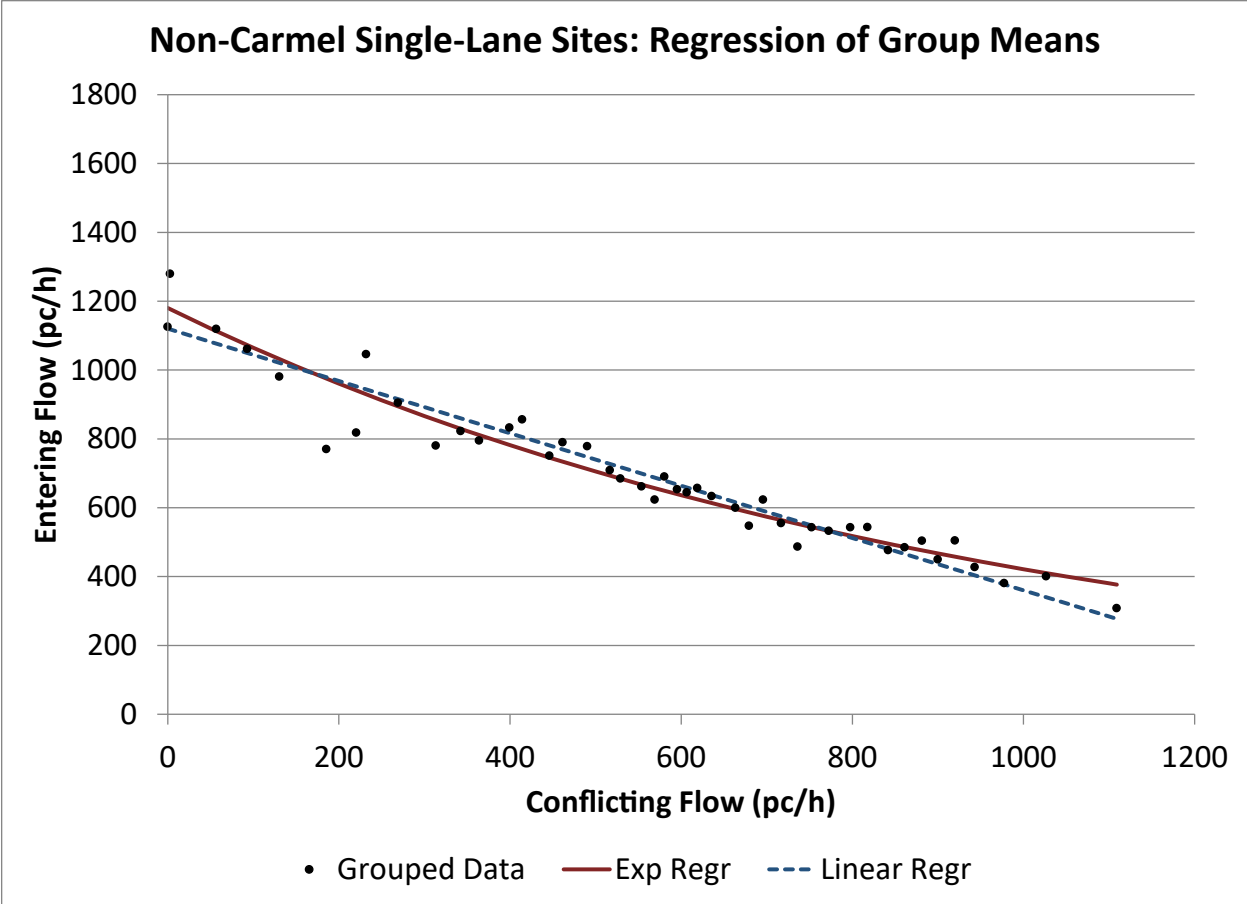


Figure 36. Scatter Plot. Regression of group means for non-Carmel single-lane roundabout sites.

A detailed look at two approaches of one roundabout in Carmel, IN10, (figure 37) provides an interesting illustration of the relationship between exponential and linear regression models. Two sites at the roundabout, IN10-N and IN10-W, have essentially identical geometric configurations but differ in flow patterns, with IN10-N experiencing low circulating flows and IN10-W experiencing high circulating flows, as shown in figure 37. Looked at individually, a linear regression model fits each site very well, with very high R^2 values. However, it is clear when plotting the two sites together on the same graph that the two linear regression models have different slopes, despite having the same geometric configuration. An exponential model visibly provides the best overall fit (RMSE of 99) by capturing the higher slope under low circulating flows and the lower slope under high circulating flows. By contrast, a linear regression model across both sites yields an RMSE of 117.

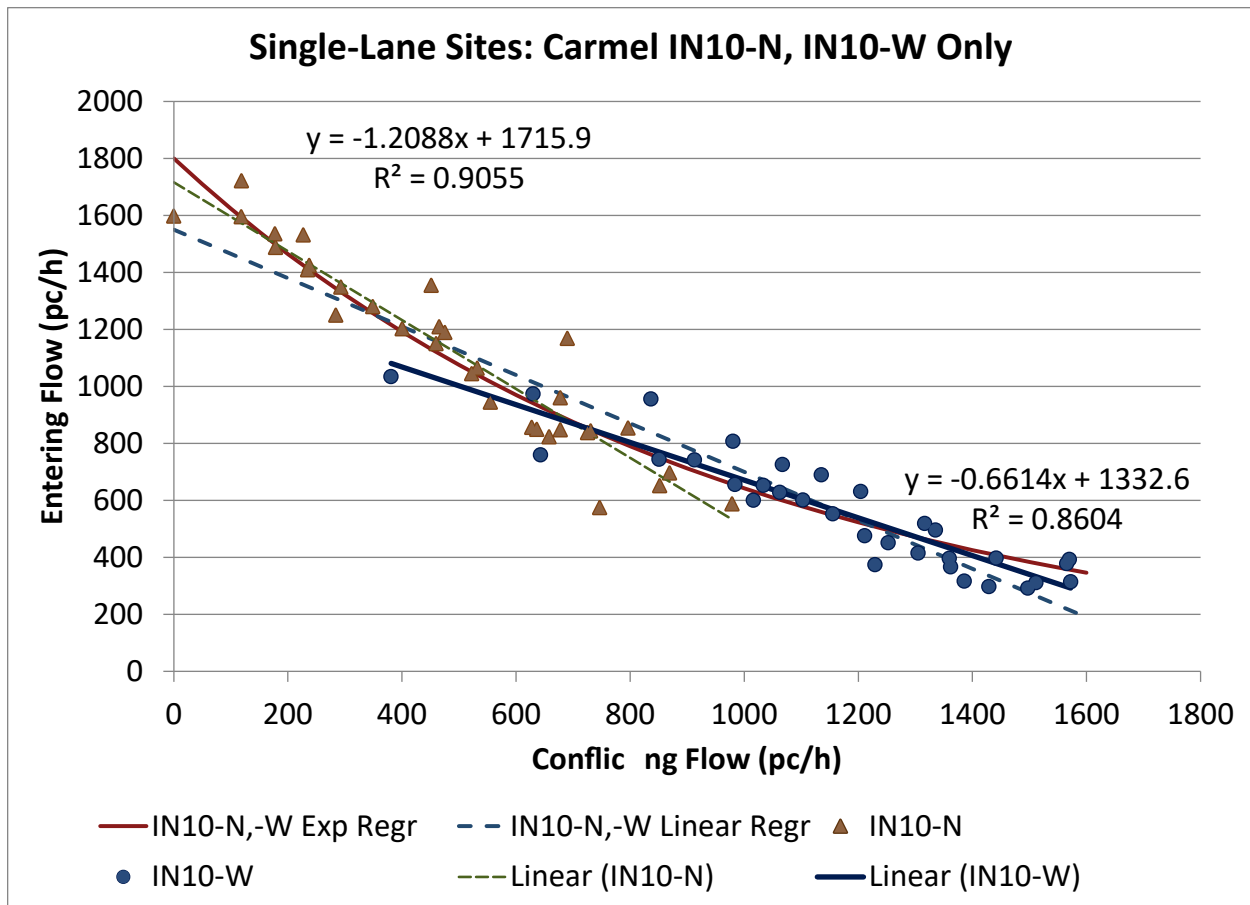


Figure 37. Scatter Plot. Regression models for two approaches at a single roundabout in Carmel, IN.

This analysis demonstrates two other important features. First, local calibration is important. The intercept that best fits the IN10 sites is higher than the best fitting intercept for the Carmel sites in general, and the intercept for the IN10 sites is much higher than experienced across the US. Second, both linear and exponential models appear to fit small data sets reasonably well. For analysis of existing roundabouts where one can calibrate to local conditions, either a linear or exponential model appears to work equivalently. However, when looking at larger data sets for prediction purposes, such as is necessary for proposed sites where local calibration is not possible, the exponential models appear to fit better than the linear models.

DEVELOPMENT OF MULTILANE MODELS

This section presents the development of models for each of the multilane cases: 2x2 sites (two entry lanes conflicting with two circulating lanes), 2x1 sites (two entry lanes conflicting with one circulating lane), and 1x2 sites (one entry lane conflicting with two circulating lanes). The section presents regression and calibration approaches, followed by a summary.

Regression

Linear and exponential regression models were developed using the data for each of the multilane cases. Figure 38 through figure 41 show these models plotted on the data for four different roundabout lane configurations and entry lanes.

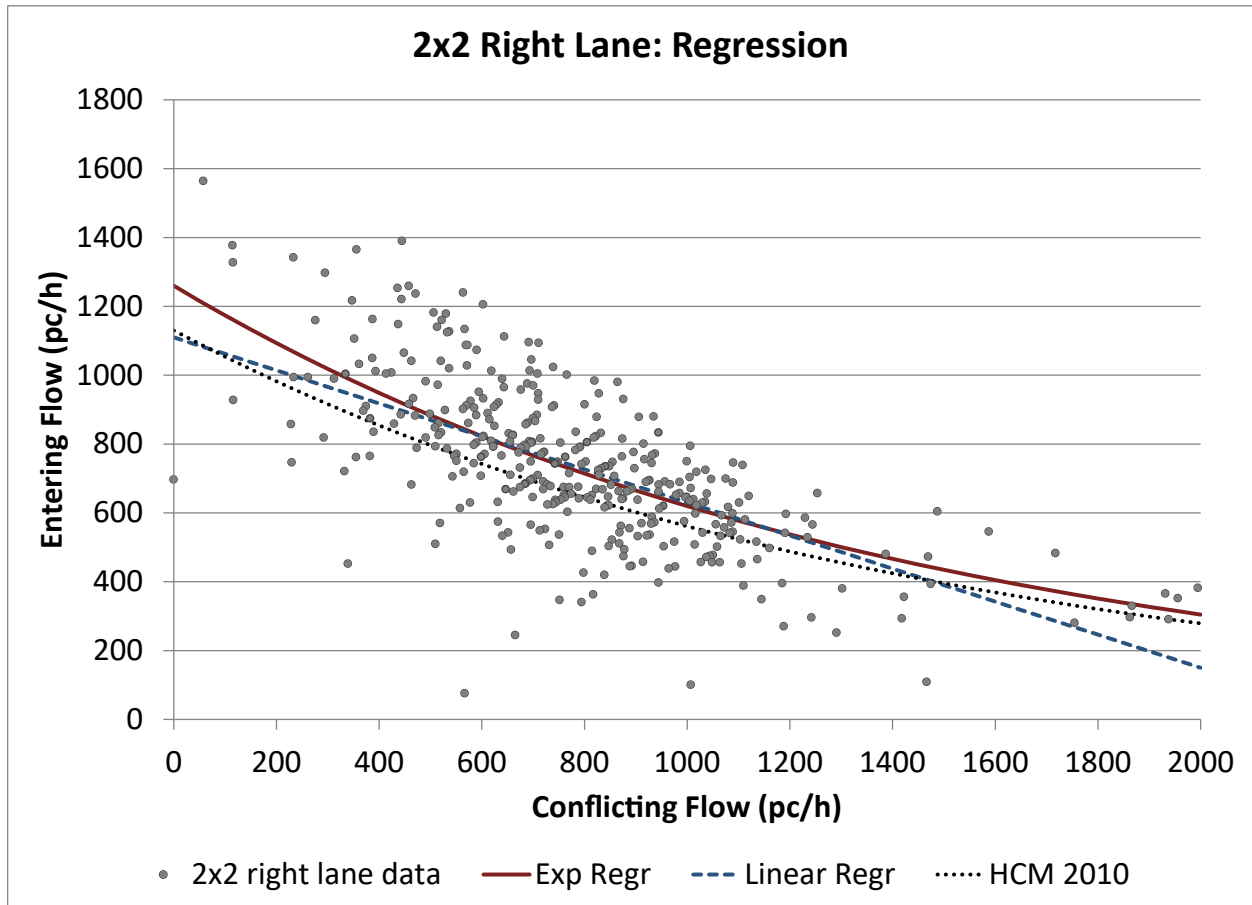


Figure 38. Scatter Plot. Regression models for multilane, 2x2 roundabout sites, right entry lane.



Figure 39. Scatter Plot. Regression models for multilane, 2x2 roundabout sites, left entry lane.

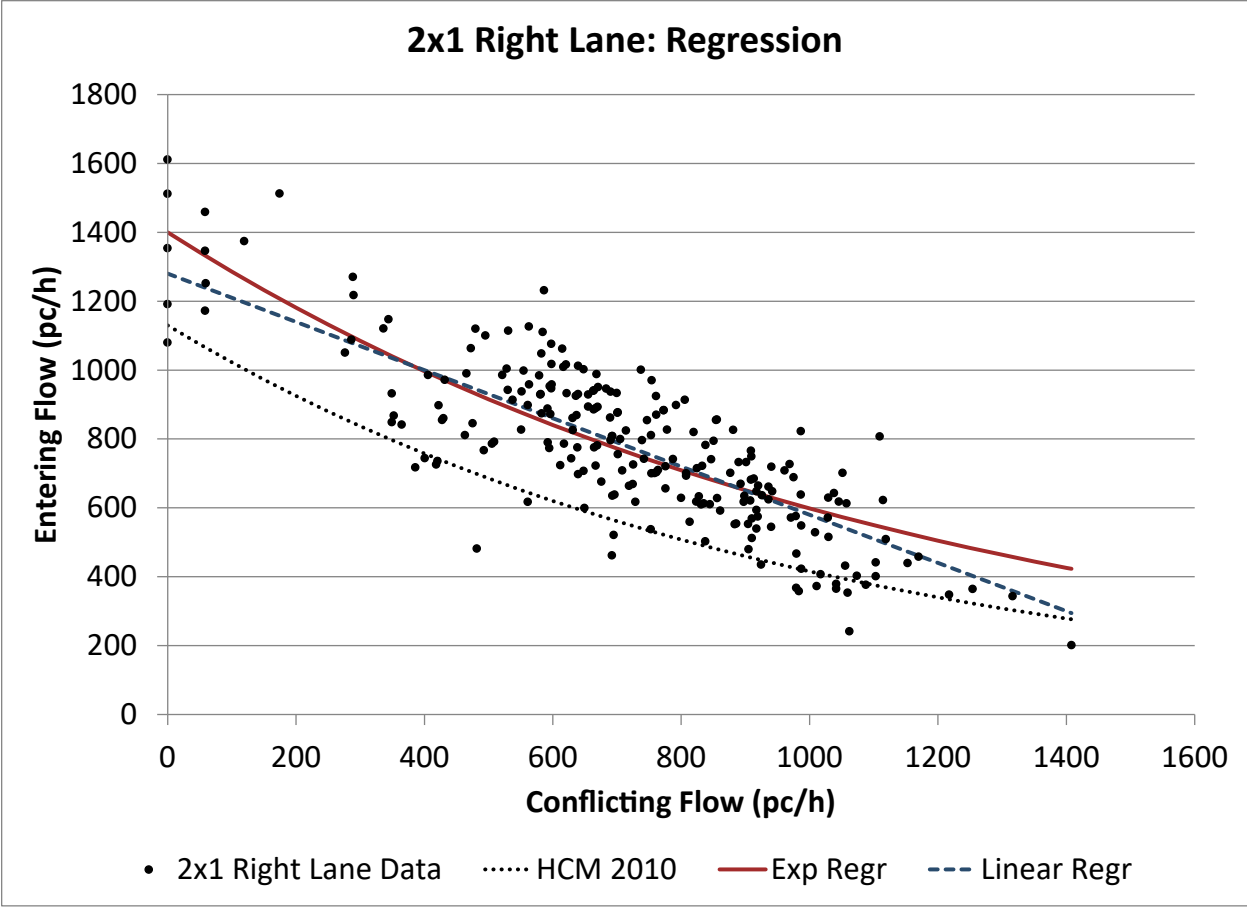


Figure 40. Scatter Plot. Regression models for multilane, 2x1 roundabout sites, right entry lane.

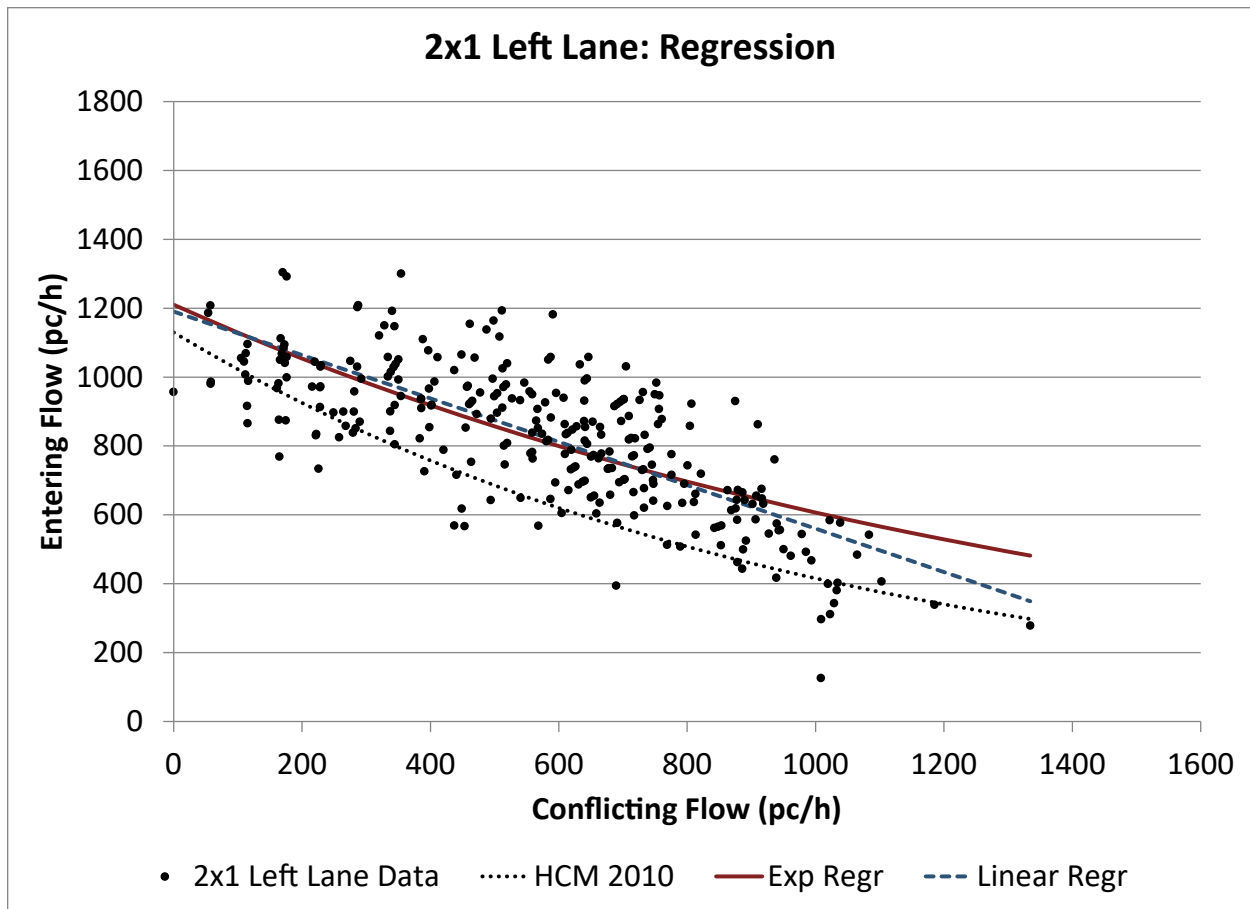


Figure 41. Scatter Plot. Regression models for multilane, 2x1 roundabout sites, left entry lane.

For the 2x2 right lane case, the regression analysis improves the fit from an RMSE of 183 for the HCM 2010 to 167 and 170 for the exponential and linear regression models, respectively. For the 2x2 left lane case, the regression analysis had little effect in improving the fit (RMSE of 218 for HCM 2010 versus 213 and 214 for exponential and linear regression, respectively). The regression for the 2x1 case had the greatest effect, reducing the RMSE by approximately 40 percent for both the right and left lanes. Each of the models and their associated RMSE values are summarized in a table at the end of this section.

Calibration

Similar to the model development process for single-lane sites, it is desirable to determine whether a field-observable parameter, particularly follow-up time, can be used to anchor the multilane regression models and thus enable their calibration to local conditions. Follow-up time is especially desirable as a calibration parameter for multilane sites due to it being considerably easier to collect than critical headway. The collection and estimation of critical headway is particularly challenging at multilane roundabouts, and for consistency with most modeling practices for critical headway, it requires the assumption that the circulating flow is a single

conflicting stream (i.e., without regard to lane use). Follow-up time, on the other hand, can be directly measured for each lane independently.

Using the data presented previously for follow-up time, a regression model was developed that fixes the y-intercept and allows the slope parameter to float to achieve the minimum RMSE. Figure 42 and figure 43 present the regression models anchored to follow-up time for the right and left lanes, respectively, for the 2x2 cases. In addition, two different anchoring values for the intercept were tested for the 2x1 case. Figure 44 presents a regression model for the combined 2x1 case anchored to the follow-up time for the 2x2 right lane case. Figure 45 presents a regression model for the combined 2x1 case anchored to a combined follow-up time for the 2x1 sites.

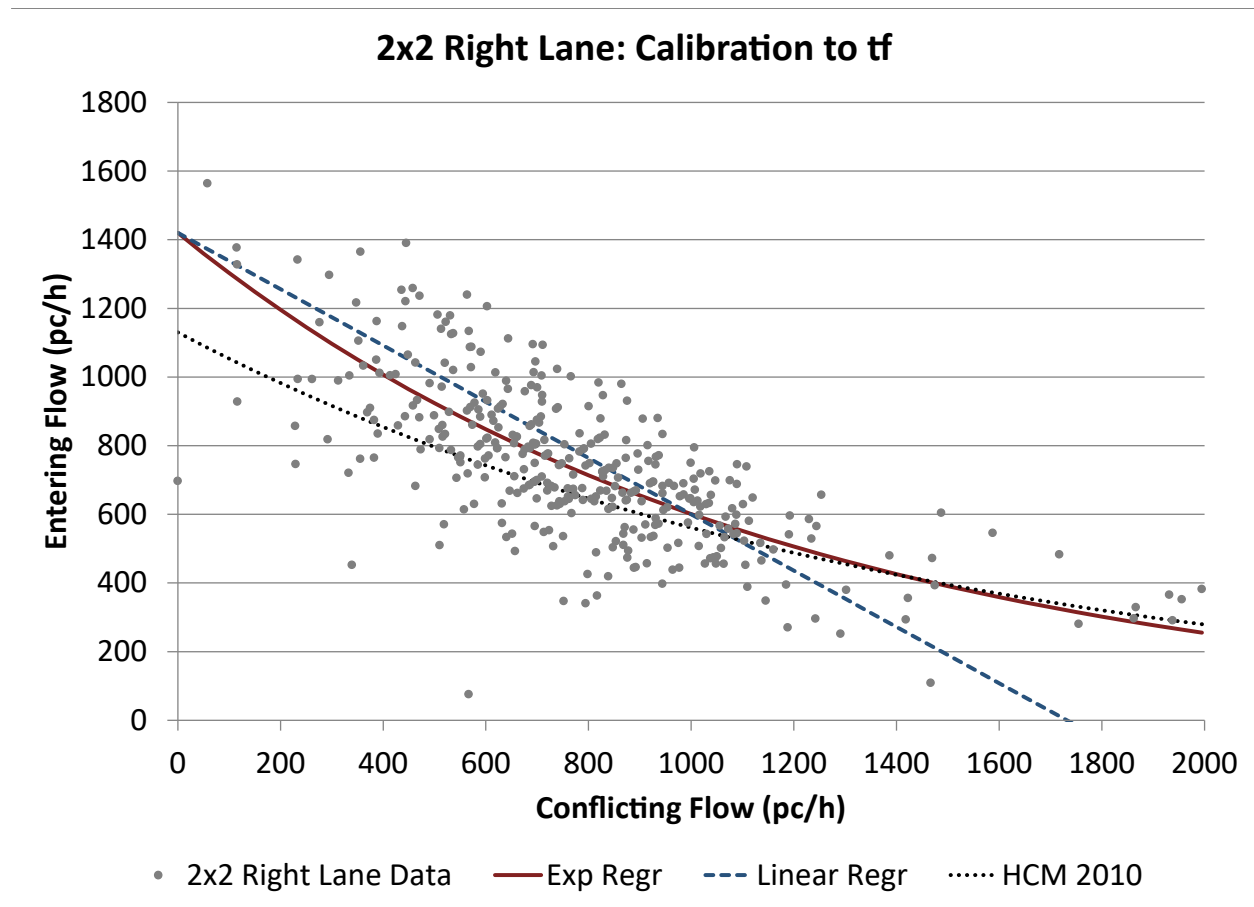


Figure 42. Scatter Plot. Regression models for multilane 2x2 roundabout sites, right entry lane with calibration to follow-up time.

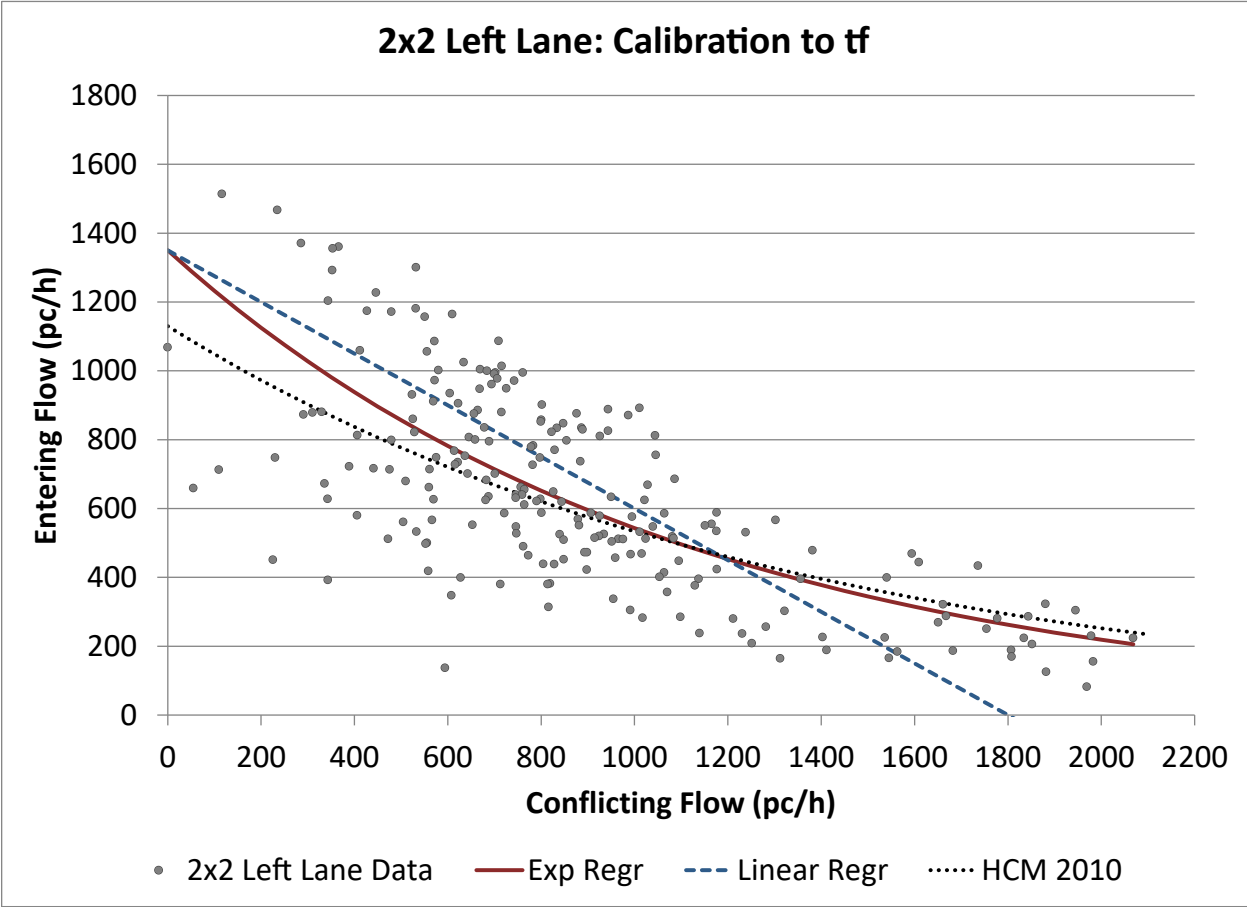


Figure 43. Scatter Plot. Regression models for multilane 2x2 roundabout sites, left entry lane with calibration to follow-up time.

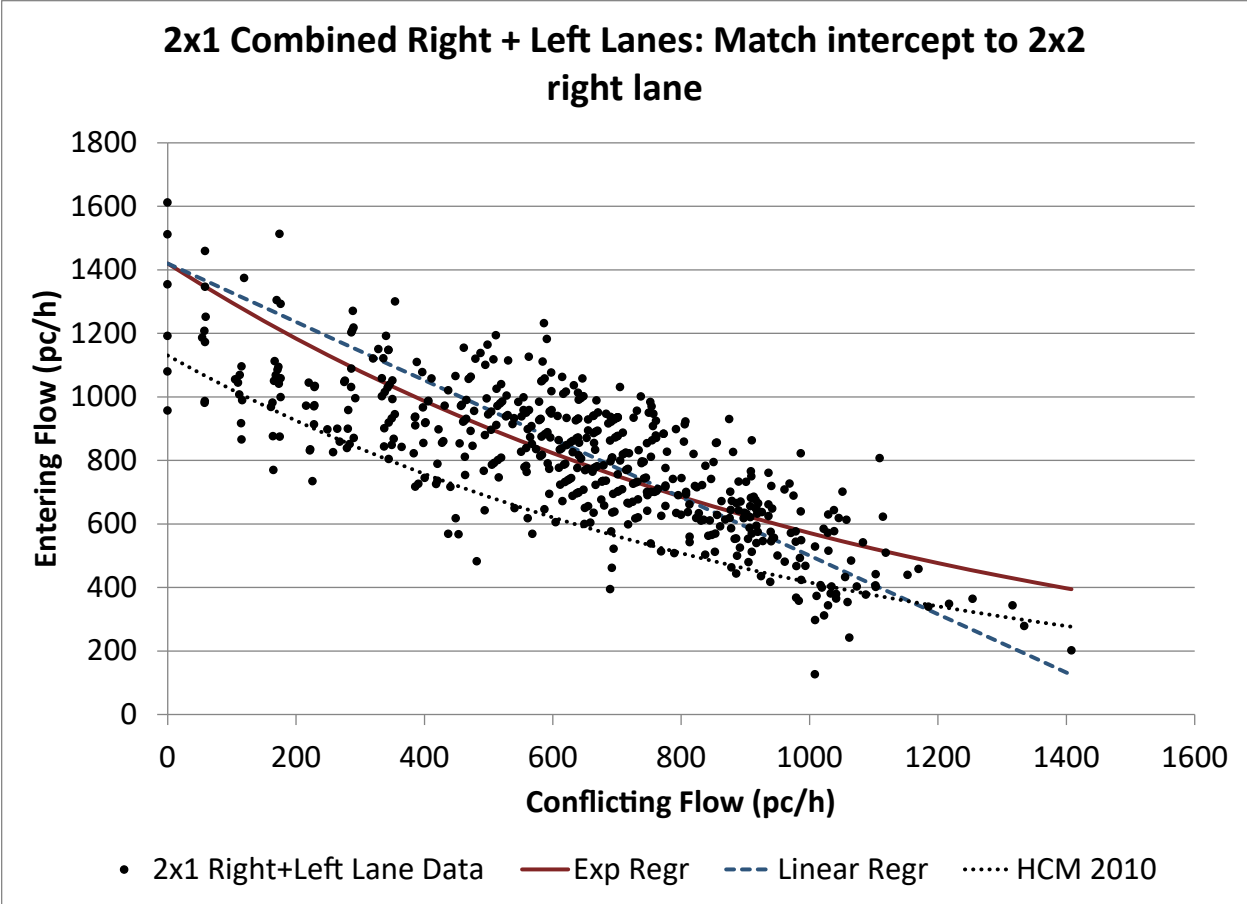


Figure 44. Scatter Plot. Regression models for multilane 2x1 roundabout sites with calibration matching the y-intercept to the 2x2 roundabout, right entry lane.

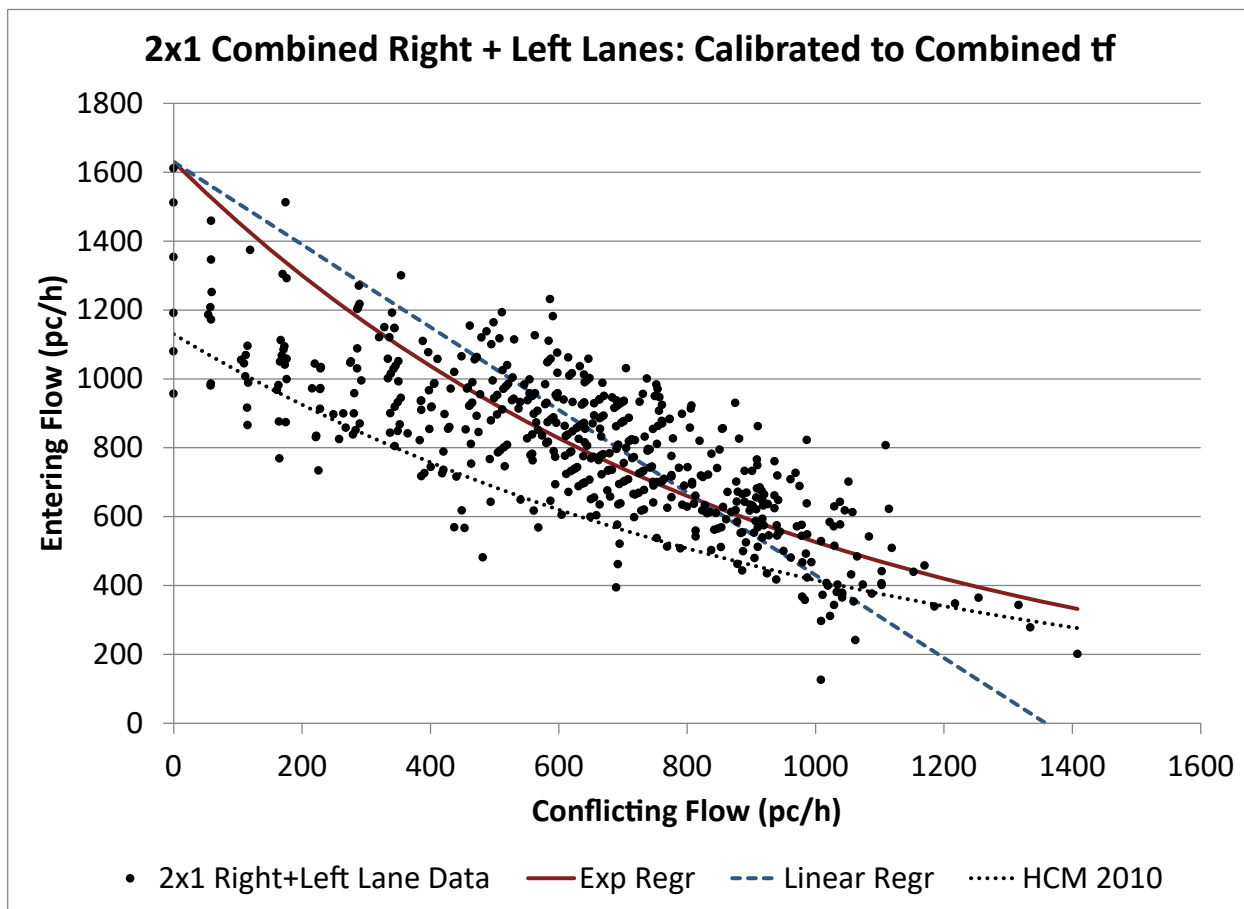


Figure 45. Scatter Plot. Regression models for multilane 2x1 roundabout sites, combined right and left entry lanes with calibration to combined follow-up time.

The calibrated models for the 2x2 cases demonstrate a good fit to the data with a field-measured anchor of follow-up time. For the 2x1 cases, the observed follow-up times in the left lane were higher than those in the right lane for reasons that the authors could not confirm, and the values were considerably higher than those observed for the 2x2 cases. The authors speculate a number of reasons for the observed follow-up times for the 2x1 cases: (1) sample sizes are smaller for the 2x1 cases than for the 2x2 cases. This may make the results more sensitive to individual site variations; (2) the 2x1 sites have a strong influence from Carmel, IN, where capacities appear higher than the national average; and (3) there may be other unique site attributes, such as sight distance or the influence of exiting vehicles, that the authors were unable to explore within this study. The use of the 2x2 right lane follow-up time data to anchor the intercept for the 2x1 model demonstrates a better overall fit to the regression model and appears to give more reasonable results.

INFLUENCE OF EXITING VEHICLES

As noted in previous sections, the effect of exiting vehicles has been demonstrated to affect entry capacity. A limited investigation was conducted as part of this study to see if the fit of the above

models could be improved through the inclusion of exiting vehicles. Two approaches were briefly explored with the single-lane data set, in which the researchers:

- Added a fixed percentage of exiting vehicles to the conflicting flow to create an effective conflicting flow.
- Added a variable percentage of exiting vehicles to the conflicting flow based on splitter island width.

A factor k_{ex} was introduced to represent the proportion of exiting vehicles that are added to the conflicting flow. The resulting flow, the effective conflicting flow, is calculated using the equation in figure 46.

$$v_{c,eff} = v_c + k_{ex}v_{ex}$$

Figure 46. Equation. Equation incorporating constant exiting vehicles flow to calculate effective conflicting flow.

Where $v_{c,eff}$ = *effective conflicting flow (pcu/h)*, v_c = *conflicting flow (pcu/h)*, k_{ex} = *proportion of contributing exiting flow*, and v_{ex} = *exiting flow (pcu/h)*.

In the first case, k_{ex} is assumed to be constant, and the regression model was developed by holding the intercept parameter fixed to follow-up time and allowing the slope parameter to vary to minimize RMSE. The value of k_{ex} that produced the lowest RMSE was found to be 0.33, meaning that one third of the exiting flow is added to the circulating flow. The resulting models are shown in figure 47. For the exponential model, the RMSE is 181 and R^2 is 0.56. For the linear model, the RMSE is 194 and R^2 is 0.49. When compared to the exponential model that only includes calibration to follow-up time (RMSE of 190, R^2 of 0.51 for exponential; RMSE of 223, R^2 of 0.33 for linear), little improvement can be seen due to the opposite directions of the two measures.

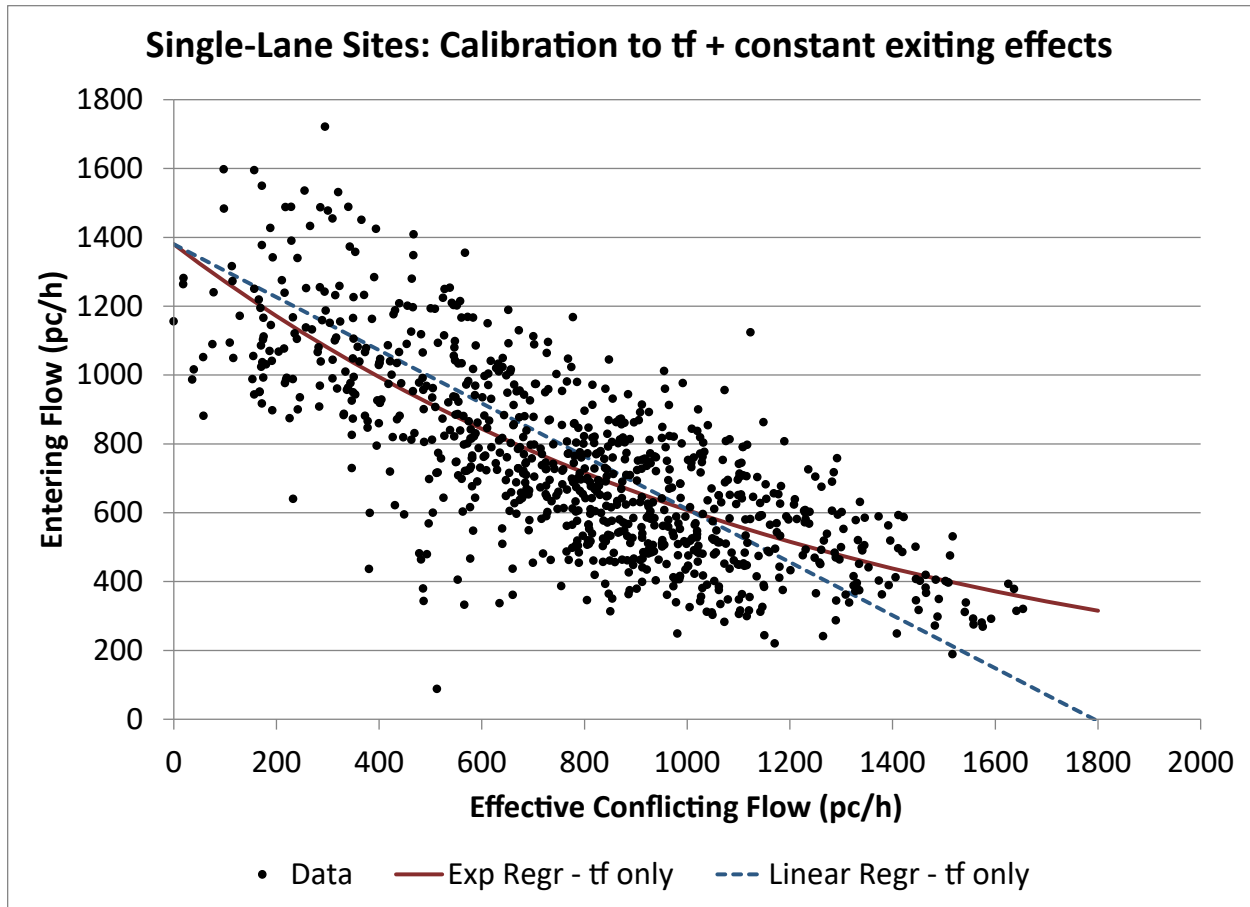


Figure 47. Scatter Plot. Regression models for single-lane sites with calibration to follow-up time and constant effects of exiting vehicles.

In the second case, k_{ex} is assumed to be a variable associated with splitter island width. Two logical boundary conditions are assumed for this model. First, for splitter island widths above an assumed maximum value of $w_{s,max}$, k_{ex} is assumed to be equal to zero. In other words, if the splitter island is large enough, drivers are assumed to be able to adequately distinguish exiting vehicles from circulating vehicles, allowing them to ignore exiting vehicles completely. Second, for splitter island widths below an assumed minimum value of $w_{s,min}$, k_{ex} is assumed to be equal to one. In other words, if the splitter island is small enough, drivers are assumed to be unable to distinguish exiting vehicles from circulating vehicles, thus treating all exiting vehicles as circulating vehicles.

The model form tested for these boundary conditions is assumed to be a simple linear model, formulated in the equation in figure 48.

$$k_{ex} = \begin{cases} 0 & w_s \geq w_{s,max} \\ \frac{w_{s,max} - w_s}{w_{s,max} - w_{s,min}} & w_{s,max} > w_s > w_{s,min} \\ 1 & w_s \leq w_{s,min} \end{cases}$$

Figure 48. Equation. Equation incorporating variable exiting vehicle flow to calculate effective conflicting flow.

Where k_{ex} = *proportion of contributing exiting flow*, w_s = *width of splitter island (ft)*, $w_{s,max}$ = *maximum contributing width of splitter island (ft)*, and $w_{s,min}$ = *minimum contributing width of splitter island (ft)*.

Values for $w_{s,max}$ and $w_{s,min}$ were tested in increments of 1.5 m (5 ft), holding the intercept parameter fixed to follow-up time and allowing the slope parameter to vary to minimize RMSE. The values of $w_{s,max}$ and $w_{s,min}$ that were found to minimize RMSE were 25 and 0, respectively.

Using this model for k_{ex} , the resulting models are shown in figure 49. For the exponential model, the RMSE is 187 and R^2 is 0.53. For the linear model, the RMSE is 203 and R^2 is 0.45. These values are not as strong as those for the models with constant exiting effects.

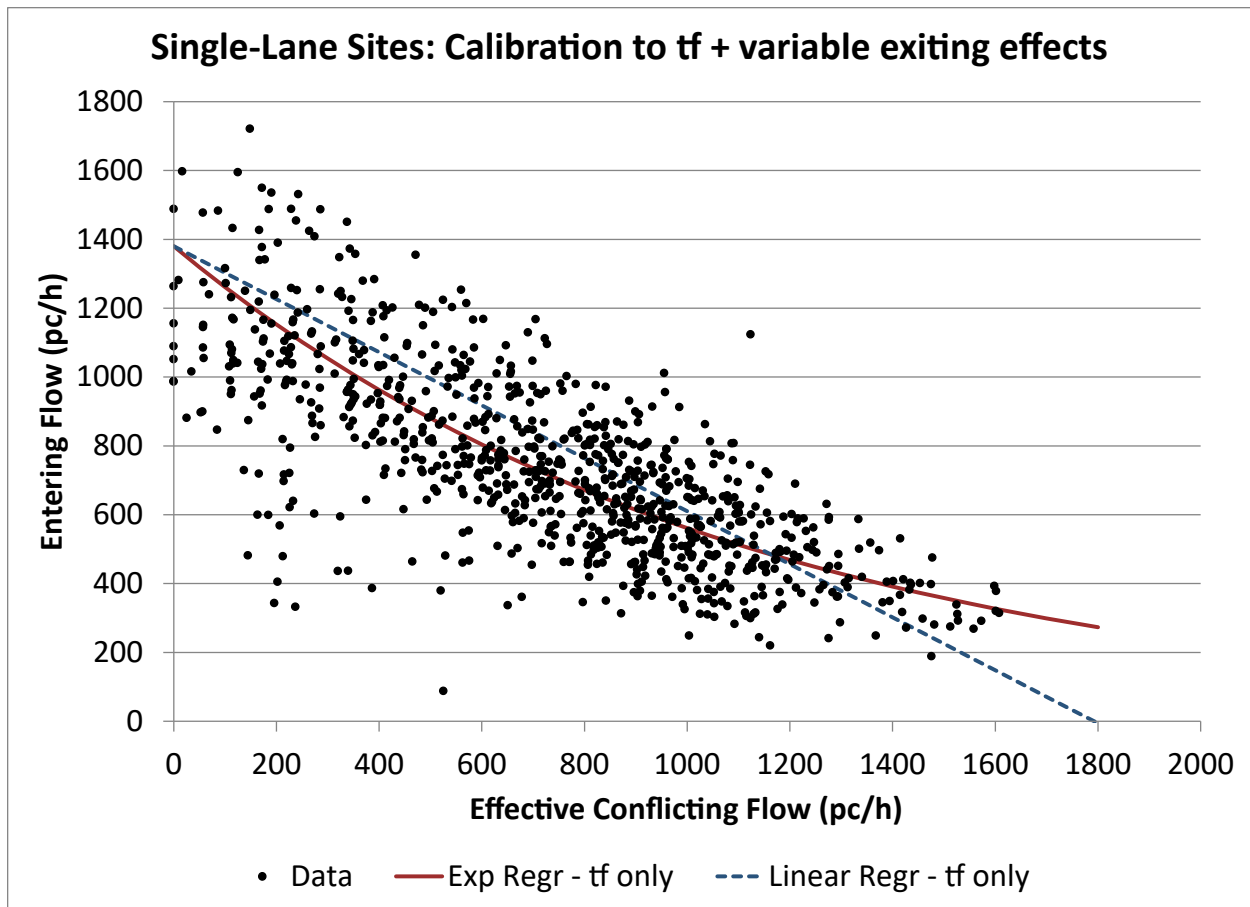


Figure 49. Scatter Plot. Regression models for single-lane sites with calibration to follow-up time and variable effects of exiting vehicles.

A similar exercise was conducted for the left lane of the 2x2 sites. The value of constant k_{ex} that produced the lowest RMSE was found to be 0.10, a value considerably less than that found for the single-lane sites. The resulting models are shown in figure 50. For the exponential model, the RMSE is 213 and R^2 is 0.46. For the linear model, the RMSE is 236 and R^2 is 0.34. When compared to the models with calibration to follow-up time (RMSE of 214, R^2 of 0.47 for exponential; RMSE of 243, R^2 of 0.32 for linear), neither of these models show any significant improvement.

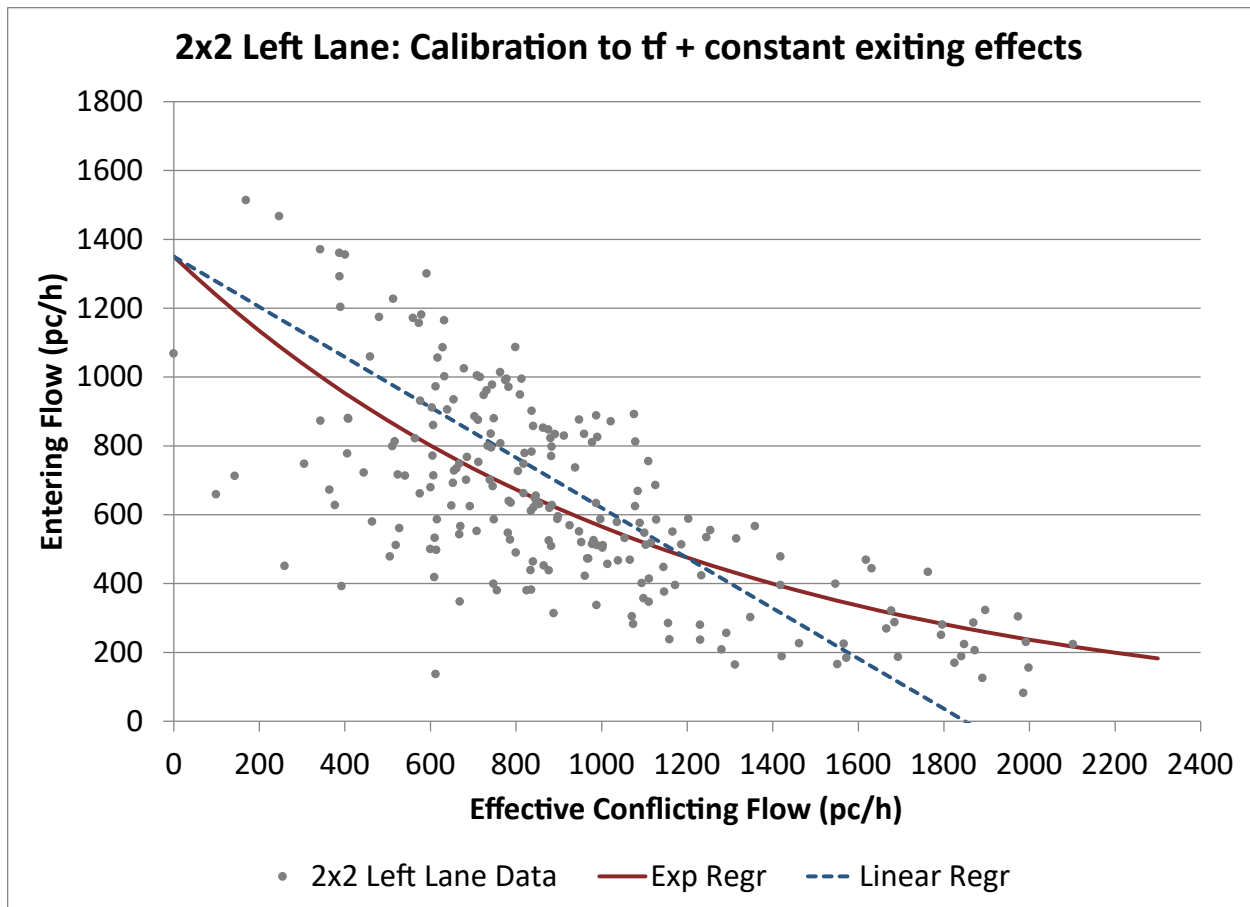


Figure 50. Scatter Plot. Regression models for 2x2 multilane roundabout sites and left entry lane with calibration to follow-up time and constant effects of exiting vehicles.

For the variable exiting effect model, the values of $w_{s,max}$ and $w_{s,min}$ that were found to minimize RMSE were 35 and 5, respectively. This outcome is consistent with the expectation that multilane roundabouts have somewhat higher circulating speeds than single-lane roundabouts. Using this model for k_{ex} , the resulting models are shown in figure 51. For the exponential model, the RMSE is 192 and R^2 is 0.56. For the linear model, the RMSE is 210 and R^2 is 0.47. When compared to the models with calibration to follow-up time (RMSE of 214, R^2 of 0.47 for exponential; RMSE of 243, R^2 of 0.32 for linear), both of these models show improvement.

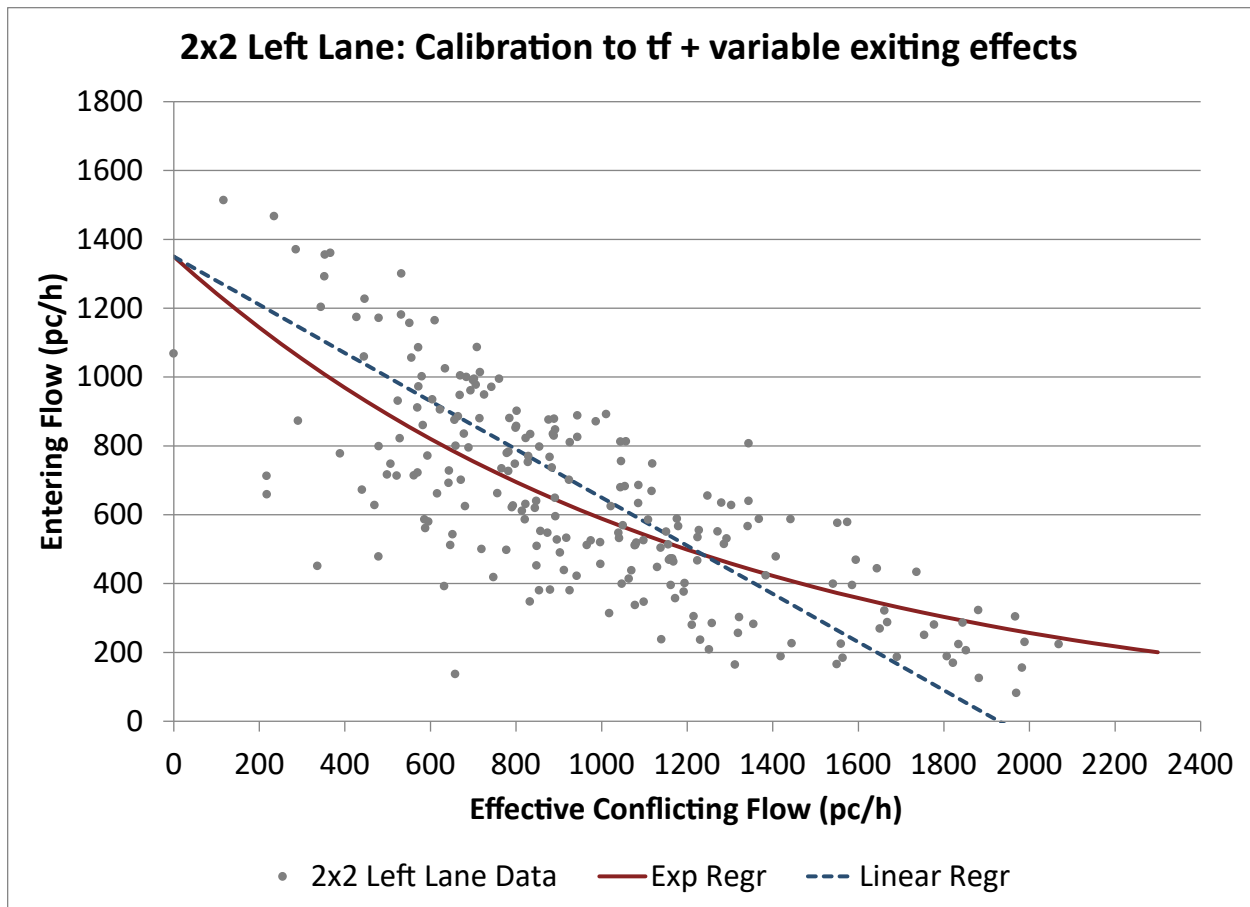


Figure 51. Scatter Plot. Regression models for 2x2 multilane roundabout sites and left entry lane with calibration to follow-up time and variable effects of exiting vehicles.

In summary, the investigation of the effect of exiting vehicles proved to be inconclusive. The modeling that includes exiting vehicles has some effect, but the modeling framework that appears to work best for multilane sites (variable geometric effects) does not transfer as well to the single-lane sites. Neither exiting vehicle model improves the fit of the model as well as the version that locally calibrates the model to local follow-up times. This suggests, at least within the confines of this limited investigation, that the inclusion of exiting vehicles adds complexity to the model without improving its fit as well as basic local calibration. Limitations of time and budget prevented further exploration in this area, and further research is recommended.

ANALYSIS OF CAPACITY TRENDS OVER TIME

One of the questions raised at the beginning of this study was whether the performance of roundabouts in the United States has changed over time, specifically whether capacities have increased. To examine this question, two roundabouts were selected that were used for data collection for this study and for NCHRP Report 572. These include a single-lane site, WA04 (SR 166/Mile Hill Drive/Bethel Avenue in Port Orchard, WA), and a multilane site, VT03 (SR 9/US 5 in Brattleboro, VT). The NCHRP Report 572 data was collected in the spring/summer of 2003 and the data for this study (TOPR 34) was collected in the spring/summer of 2012, thus enabling

a comparison of performance over a period of nine years. This section explores whether driver behavior has changed over time at these locations.

At the WA04 intersection, the north leg yielded the greatest amount of data for both this study and NCHRP Report 572. Figure 52 displays the 2012 data collected in this study with the data from 2003 for the north leg of WA04. As shown in the figure, the two data sources overlap considerably, with no visual evidence of change in driver behavior between 2003 and 2012. Significantly, the upper bounds of the two data groups are almost exactly coincident.

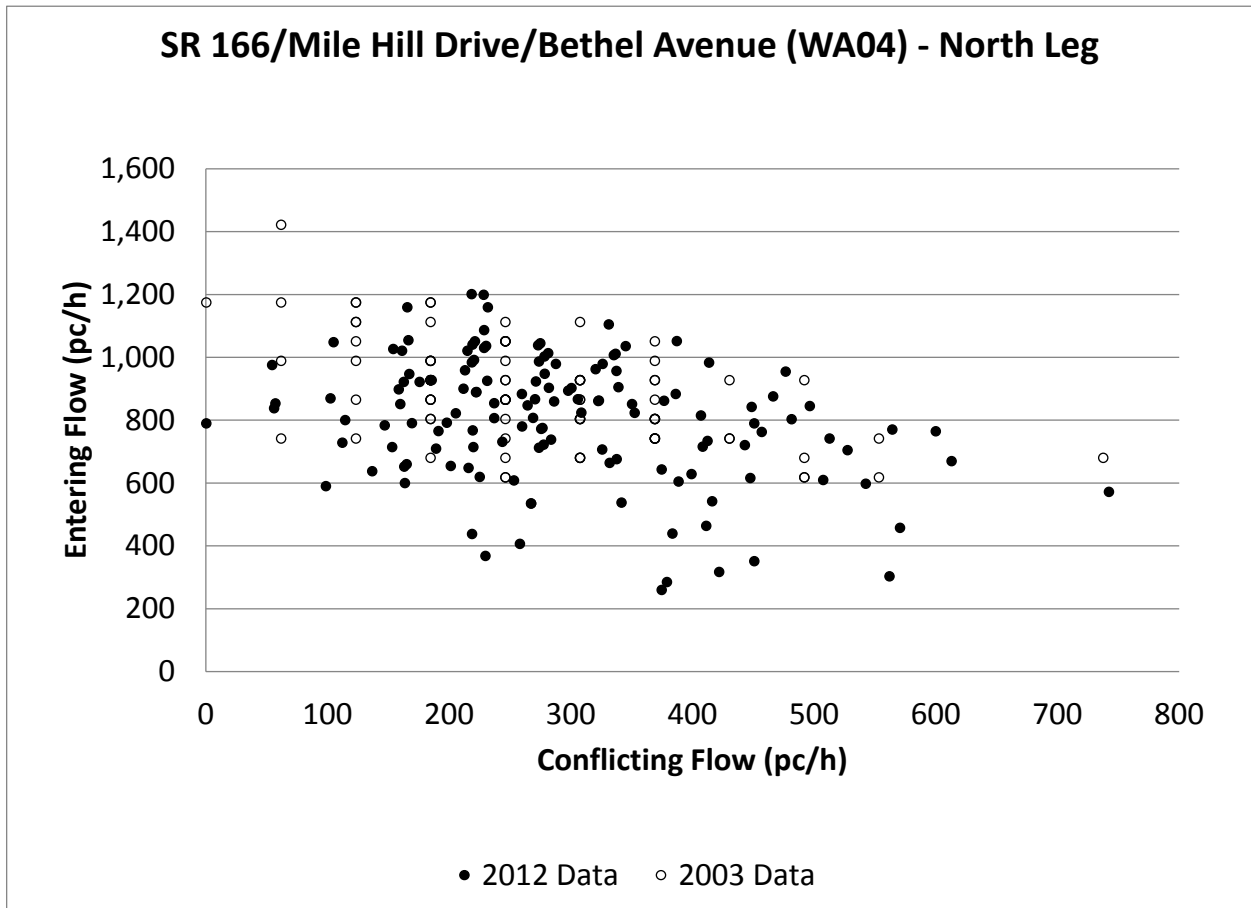


Figure 52. Scatter Plot. Comparison of 2003 and 2012 flow data for single-lane roundabout site (WA04 North Leg).

Figure 53, figure 54, and figure 55 display 2012 and 2003 data for the right lanes of the east, south, and west legs of VT03, respectively.

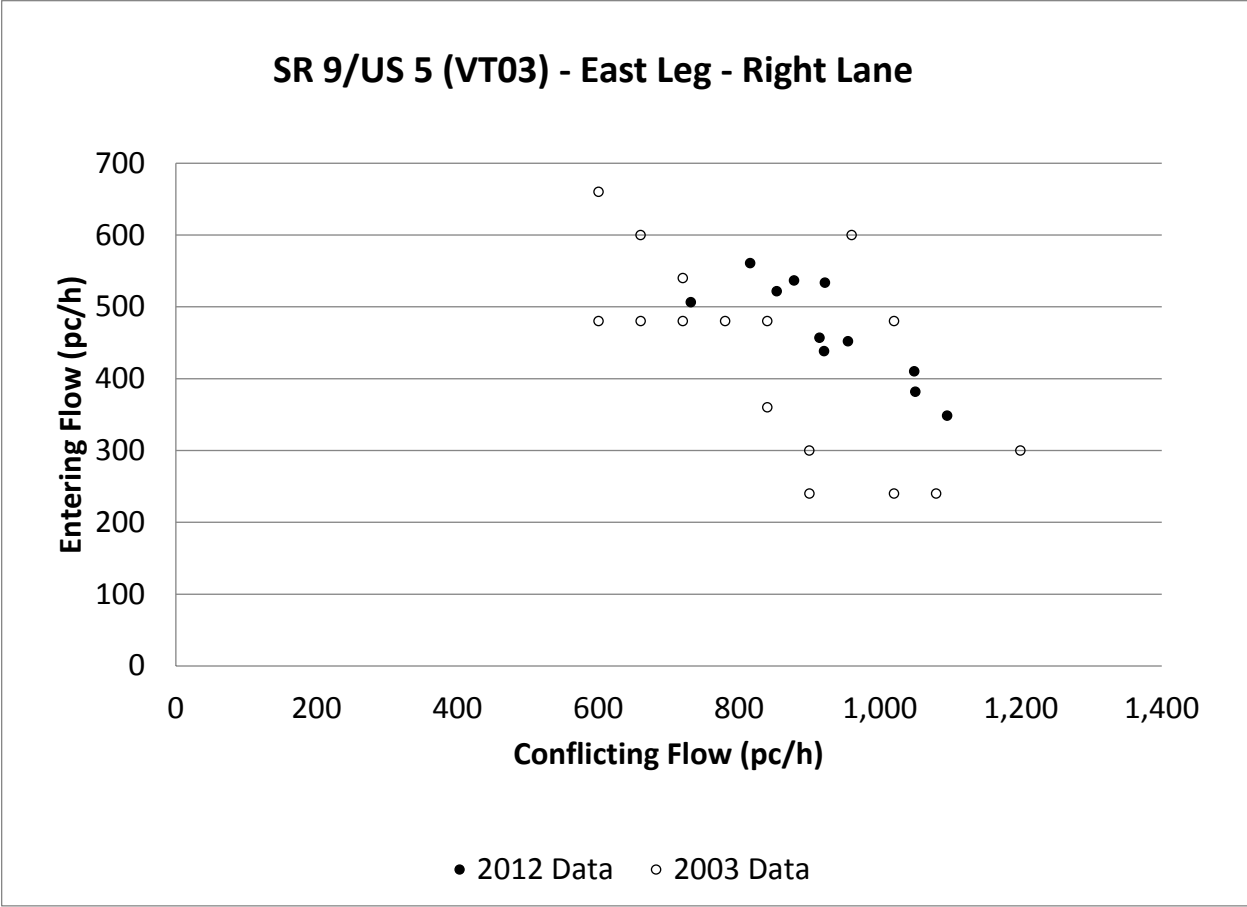


Figure 53. Scatter Plot. Comparison of 2003 and 2012 flow data for multilane roundabout site VT03 east leg, right lane.

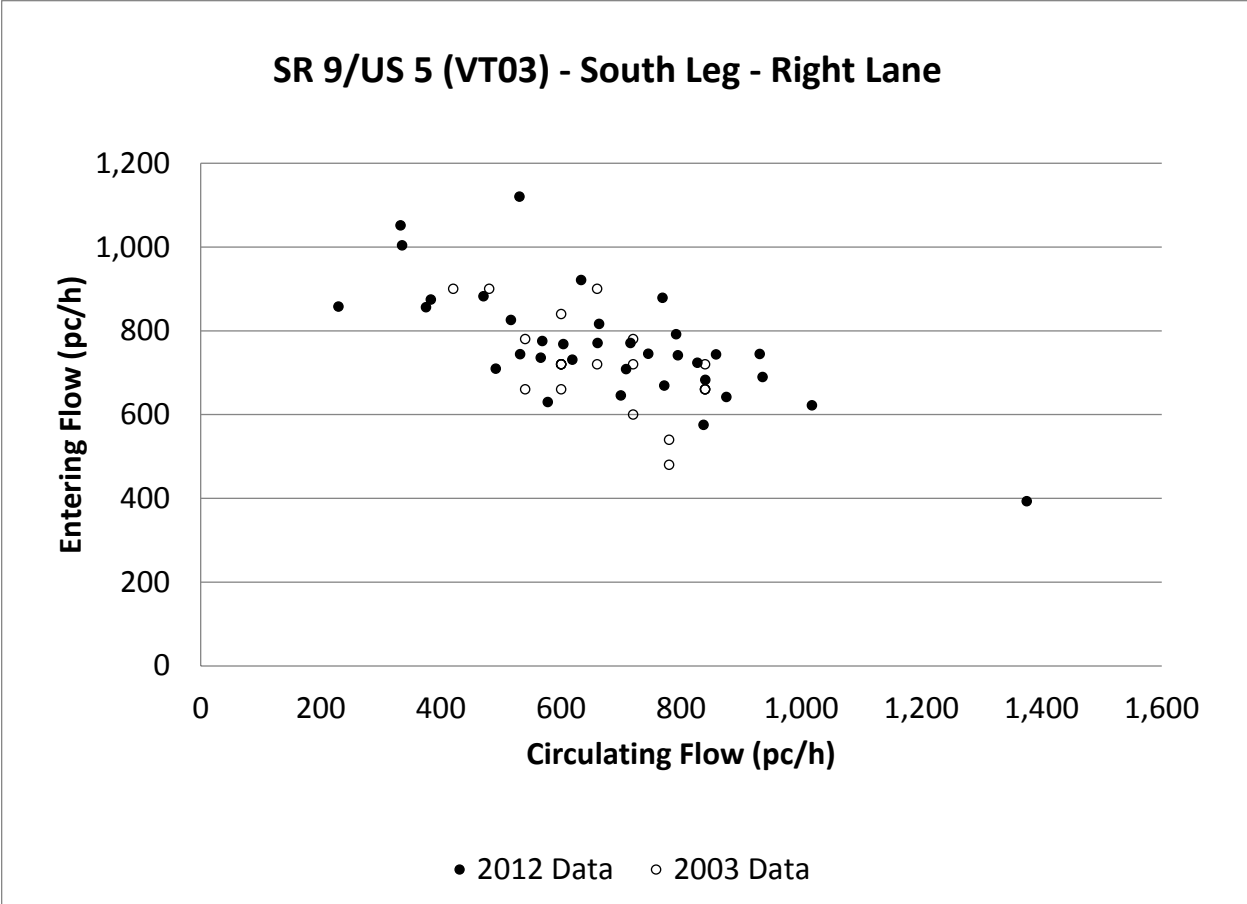


Figure 54. Scatter Plot. Comparison of 2003 and 2012 flow data for multilane roundabout site VT03 south leg, right lane.

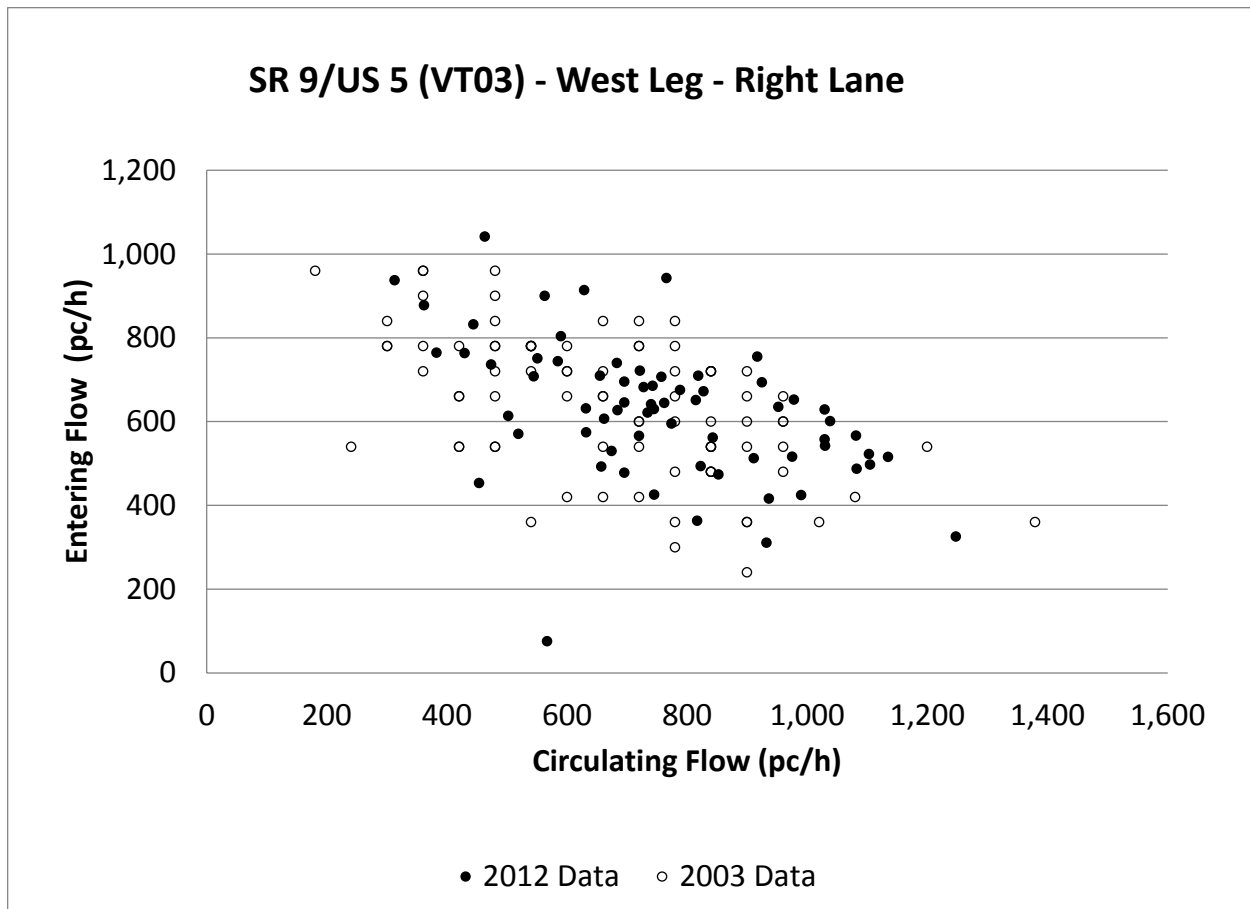


Figure 55. Scatter Plot. Comparison of 2003 and 2012 flow data for multilane roundabout site VT03 west leg, right lane.

As shown in these figures, the scatters for the two different years of data essentially overlap one another, with no visible evidence of a significant difference. The examination of these plots provides no evidence to support the hypothesis that capacities have increased over time. Given that WA04 was constructed in 1998 and VT03 was constructed in 1999, it may be possible that increases in capacity were attained in the initial years after construction, and before 2003.

SUMMARY OF MODEL DEVELOPMENT

Table 19 presents a summary of the results across the various modeling methods presented above. Of the models, the model that is locally calibrated with individual follow-up times for each site performs the best based on the lowest RMSE. For the models relying on global data, the pure regression models perform the best based on the lowest RMSE. However, the exponential model that is calibrated to a global follow-up time performs nearly as well and has the benefit of a field-verified anchor for the y-intercept. As discussed in subsequent sections, this method is also consistent with the modeling approach that produced the best fit for the multilane sites. To this end, the recommended model is an exponential model anchored to a global follow-up time, with localized calibration recommended if possible.

The models presented in Table 19 are in one of two forms, with the values of the parameters A and B provided in the table. The exponential model is of the form shown in figure 56, and the linear model is in the form shown in figure 57.

$$c_{e,pce} = A * \exp(-B * v_{c,pce})$$

Figure 56. Equation. Model Summary, Exponential Model Form

$$c_{e,pce} = A - B * v_{c,pce}$$

Figure 57. Equation. Model Summary, Linear Model Form

Where $c_{e,pce}$ = entry capacity (pc/h) and $v_{c,pce}$ = conflicting flow (pc/h).

Table 19. Comparison of single-lane roundabout models.

Row	Model Type	Model Method	Model Parameter A	Model Parameter B	RMSE Using All Data	R ²
1	HCM 2010	Exponential	1130	0.0010	217	0.37
2	Regression fit to all sites	Exponential	1200	0.00080	182	0.55
3	Regression fit to all sites	Linear	1120	0.58	186	0.54
4	Calibrated to global t_f ; slope set for best RMSE fit	Exponential	1380	0.00102	190	0.51
5	Calibrated to global t_f ; slope set for best RMSE fit	Linear	1380	0.89	223	0.33
6	HCM 2010 calibration method (calibrated to global t_f and t_c)	Exponential	1380	0.00094	193	0.5
7	Calibrated to local t_f ; slope set for best RMSE fit	Exponential	Variable	Variable	171	0.59
8	Best fit to Carmel sites only	Exponential	1380	0.00081	212	0.4
9	Best fit to Carmel sites only	Linear	1270	0.64	219	0.36

Table 20 presents a summary of the results across the various modeling methods presented above for the cases with 2x1 multilane roundabout, and the 2x2 left entry lane, and the 2x2 right entry lane, in that order. Of the models, the 2x2 left-lane and right-lane model with calibration to global follow-up time perform as well as pure regression models, and have the benefit of a field-measurable anchor.

Table 20. Comparison of multilane roundabout models.

Row	Model Type	Roundabout Configuration	Model Method	Model Parameter A	Model Parameter B	RMSE Using All Data	R ²
1	HCM 2010 2x2 Right	2x2, right lane	Exponential	1130	0.0007	183	0.38
2	Regression fit to all sites	2x2, right lane	Exponential	1260	0.00071	167	0.49
3	Regression fit to all sites	2x2, right lane	Linear	1110	0.48	170	0.47
4	Calibrated to global t_f ; slope set for best RMSE fit	2x2, right lane	Exponential	1420	0.00086	164	0.49
5	Calibrated to global t_f ; slope set for best RMSE fit	2x2, right lane	Linear	1420	0.82	192	0.3
6	HCM 2010 2x2 Left	2x2, left lane	Exponential	1130	0.00075	218	0.28
7	Regression fit to all sites	2x2, left lane	Exponential	1060	0.00076	213	0.31
8	Regression fit to all sites	2x2, left lane	Linear	960	0.45	214	0.31
9	Calibrated to global t_f ; slope set for best RMSE fit	2x2, left lane	Exponential	1350	0.00092	214	0.47
10	Calibrated to global t_f ; slope set for best RMSE fit	2x2, left lane	Linear	1350	0.75	243	0.32
11	HCM 2010 2x1, fit to right-lane data only	2x1	Exponential	1130	0.0010	255	-0.13
12	Regression fit to right-lane data only	2x1	Exponential	1400	0.00085	139	0.66
13	Regression fit to right-lane data only	2x1	Linear	1280	0.70	136	0.68
14	HCM 2010 2x1, fit to left-lane data only	2x1	Exponential	1130	0.0010	224	-0.18
15	Regression fit to left-lane data only	2x1	Exponential	1210	0.00069	145	0.51
16	Regression fit to left-lane data only	2x1	Linear	1190	0.63	139	0.55
17	Calibrated to global t_f combined lanes; slope set for best RMSE fit to all data	2x1	Exponential	1630	0.00113	180	0.35
18	Calibrated to global t_f combined lanes; slope set for best RMSE fit to all data	2x1	Linear	1630	1.20	213	0.09
19	Intercept set to match 2x2 right lane; slope set for best RMSE fit to all data	2x1	Exponential	1420	0.00091	153	0.53
20	Intercept set to match 2x2 right lane; slope set for best RMSE fit to all data	2x1	Linear	1420	0.92	161	0.48

The 2x1 model reflected some inconsistencies and proved more challenging to calibrate. The pure regression models fit much better than the ones anchored to a global follow-up time. The observed follow-up times would result in an intercept that is much higher than the observed capacities at low circulating flows. The use of the intercept from the 2x2 right-lane model produces a much better fit to the data than the use of the directly measured follow-up times.

CHAPTER 6. CONCLUSIONS AND RECOMMENDATIONS

This study resulted in a considerably larger set of usable data than was realized for NCHRP Report 572. This study included 24 single-lane sites (defined as an approach to a roundabout) and 37 multilane sites, versus 18 single-lane sites and 7 multilane sites in NCHRP Report 572. It also included 819 minutes of single-lane data and 1,230 minutes of lane-specific multilane data, versus 318 minutes of single-lane data and 473 minutes of lane-specific multilane data from NCHRP Report 572.

The HCM 2010 models generally underestimate capacities based on the new set of data. A new set of models is recommended for each case in the HCM. These have been developed using a consistent model form: an exponential regression model (figure 56) with an intercept anchored to national average follow-up times. Because their form and input parameters remain the same as in the HCM 2010, implementation is anticipated to be straightforward. The recommended models are shown in table 21.

Table 21. Recommended models for roundabout types, configuration, and entry lanes.

Roundabout Type	Roundabout Configuration	Entry Lane	Model Equation (Figure 56)	Parameters From
Single Lane	n/a	n/a	$v_e = 1380 \exp(-0.00102 * v_c)$	Table 19, Row 4
Multilane	1x2	n/a	2x2 right lane model	
Multilane	2x2	right	$v_e = 1420 \exp(-0.00085 * v_c)$	Table 20, Row 12
Multilane	2x2	left	$v_e = 1350 \exp(-0.00092 * v_c)$	Table 20, Row 9
Multilane	2x1	both	$v_e = 1420 \exp(-0.00091 * v_c)$	Table 20, Row 19

The exponential form fit generally the same or better than the linear form across the entire range of lane configurations and sites analyzed in this project. In some cases the linear form was a better regression fit, such as the Carmel single-lane sites. However, for generalized modeling purposes, the exponential model is recommended for three reasons. First, the anchor to follow-up time is notably stronger with the exponential form than with the linear form. Second, there is no evidence from this project that entering flows will reach zero under very high conflicting flows, as would be indicated with a linear model. No measurements of zero entering flow were found in the data for this project. Documentation of similar conditions for other unsignalized intersections appears to be limited, but anecdotal observation suggests that under heavily saturated conditions the two traffic streams tend to alternate rather than observe strict priority rules. This suggests that true zero entering flows typically are not realized in practice. Third, the exponential model form has an analogous analytical form, the Siegloch model, suggesting a basis for the model in established traffic flow theory.

The use of critical headway to further calibrate the single-lane model did not improve the overall fit. Calibration using follow-up time as a primary measure is recommended for the HCM 2010 major update. Calibration to site-specific follow-up times provides the best overall model fit, demonstrating that local calibration continues to be a recommended practice. This simplification of the calibration process should be easier for practitioners to implement in the field.

Effects of geometric parameters and exiting vehicles showed promise in some cases but proved inconclusive in a generalized model.

The benefit of local calibration is clear from the research presented in this paper. Models prepared that are specific to a region, such as those demonstrated with localized follow-up times collected in Carmel, IN or separate regression models (exponential or linear), provide better predictive power for sites in that area, even though the Carmel-specific models do not fit as well to the full national data set. While calibration to individual sites provides even better accuracy, such a level of localized calibration is impractical for developing a model for predictive purposes for sites not yet built. Local data collection of follow-up time is anticipated to be a reasonable and cost-effective way to calibrate the national model to a region without the need to also collect critical headway as specified in the HCM 2010.

Further research is recommended in a few areas. The effect of geometric parameters showed trends that are consistent with international findings but could not be developed sufficiently to improve the predictive power of the model. Entry angle was the most significant of the geometric parameters studied but did not have a strong enough correlation to pursue further. Sight distance was not evaluated as a geometric parameter but may be significant. The effect of exiting vehicles also showed some promise in specific cases but could not be generalized into a model. More samples are needed for the 1x2 case, as well as for sites with three-lane entries and sites with bypass lanes. Sites with these characteristics were included in the video data collection effort but were not used due to the small sample size and prioritization of study resources.

REFERENCES

1. Rodegerdts, L., M. Blogg, E. Wemple, E. Myers, M. Kyte, M. P. Dixon, G. F. List, A. Flannery, R. Troutbeck, W. Brilon, N. Wu, B. N. Persaud, C. Lyon, D. L. Harkey, and D. Carter. *NCHRP Report 572: Roundabouts in the United States*. Transportation Research Board of the National Academies, Washington, D.C., 2007.
2. Transportation Research Board. *Highway Capacity Manual 2010*. Transportation Research Board of the National Academies, Washington, D.C., 2010.
3. Siegloch, W. (1973). *Die Leistungsermittlung an Knotenpunkten Ohne Lichtsignalsteuerung (Capacity Calculations for Unsignalized Intersections)*. Schriftenreihe Strassenbau und Strassenverkehrstechnik, Vol. 154.
4. Troutbeck, R. J. and W. Brilon. "Chapter 8: Unsignalized Intersection Theory." In *Revised Monograph on Traffic Flow Theory*. Federal Highway Administration. <http://www.fhwa.dot.gov/publications/research/operations/tft/>. Accessed October 2, 2014.
5. Kittelson & Associates, Inc. *Roundabout Evaluation and Design Guidelines*. City of Bend, Oregon, April 2010.
6. Tian, Z. Z., F. Xu, L. A. Rodegerdts, W. E. Scarbrough, B. L. Ray, W. E. Bishop, T. C. Ferrara, and S. Mam. *Roundabout Geometric Design Guidance*. Report No. F/CA/RI-2006/13. Division of Research and Innovation, California Department of Transportation, Sacramento, Calif., June 2007.
7. Wei, T., J. L. Grenard, and H. R. Shah. Developing Capacity Models for Local Roundabouts: Streamlined Process. In *Transportation Research Record: Journal of the Transportation Research Board, No. 2257*. Transportation Research Board of the National Academies, Washington, D.C., 2011.
8. Zheng, D., M. Chitturi, A. Bill, and D. A. Noyce. *Comprehensive Evaluation of Wisconsin Roundabouts, Volume 1: Traffic Operations*. Traffic Operations and Safety Laboratory, University of Wisconsin. Wisconsin Department of Transportation, September 2011.
9. Mensah, S., S. Eshragh, and A. Faghri. "Critical Gap Analysis for Modern Roundabouts." Presented at the 89th Annual Meeting of the Transportation Research Board, Washington, D.C., January 10-14, 2010.
10. Kittelson & Associates, Inc. "Calibration of HCM Capacity Models for Kansas Roundabouts", Unpublished Draft Memorandum, March 28, 2012.

11. Mereszczak, Y., M. Dixon, M. Kyte, L. Rodegerdts, and M. Blogg. "Incorporating Exiting Vehicles in Capacity Estimation at Single-Lane U.S. Roundabouts." Paper presented at the Transportation Research Board National Roundabout Conference, Vail, Colorado, 2005.
12. Hagrings, O., Derivation of Capacity Equation for Roundabout Entry with Mixed and Circulating and Exiting Flows", Transportation Research Record 1776, Transportation Research Board, Washington, D.C., 2001, pp. 91-99.
13. Kimber, R. M. The Traffic Capacity of Roundabouts. TRRL Laboratory Report LR 942. Transport and Road Research Laboratory, Crowthorne, Berkshire, England, 1980.
14. Akçelik, R. "An Assessment of the Highway Capacity Manual 2010 roundabout capacity model." Paper presented at the International Roundabout Conference, Transportation Research Board, Carmel, Indiana, 2011.
15. Brilon, W., and N. Wu. "Unsignalized Intersections – A Third Method for Analysis." Proceedings of the 15th International Symposium on Transportation and Traffic Theory, Pergamon-Elsevier Publications, Adelaide, Australia, pp. 157 –178, 2002.
16. Schmotz, M., and R. Maier. "Capacity of Mini-Roundabouts." Presented at International Roundabout Conference, Transportation Research Board, Carmel, Indiana, 2011.

